FATIGUE BEHAVIOR OF SPOT WELDS

by

Ahmet Hanifi Ertaş

B.S. in M.E., Atatürk University, 1997

Submitted to the Institute for Graduate Studies in
Science and Engineering in partial fulfillment of
the requirements for the degree of
Master of Science

Graduate Program in Mechanical Engineering
Boğaziçi University

2004

To my family

ACKNOWLEDGMENTS

I would like to express the very most thanks to my thesis supervisor, Prof. Öktem Vardar, who has always been more sensitive than anyone for the preparation of this thesis.

My extreme thanks are also to Assoc. Prof. Vahan Kalenderoğlu for his suggestions and cooperation for extended experimental studies from the beginning to the end of this study. I would also like to thank to Assoc. Prof. Fazıl Önder Sönmez, Teaching Assistant (in Atatürk University) Hakan Ertaş, Research Assistant Mehmet Gökhan Gökçen, Research Assistant Abdullah Korkut Üstün and Research Assistant Osman Kaya for their suggestions.

The supply of material from Mercedes-Benz Türk A.Ş. is gratefully acknowledged.

Finally I would like to thank my family for their invaluable support and encouragement.

ABSTRACT

FATIGUE BEHAVIOR OF SPOT WELDS

The resistance spot welding process is widely used in industry, especially in automotive industry. This type of joining method is used widely because of its simplicity, cheapness and of course reliability which are significant aspects of manufacturing processes. Because the spot welded specimens are used widely in industry, the spot weld fatigue life predictions are very important. So, intense scientific studies have been carried out on this subject for years, especially for the last 30 years. In this dissertation, firstly the spot weld fatigue life prediction methods were reviewed. Secondly, using Material Testing System (MTS) test machine that has closed loop servo-hydraulic control system, the suitable lives for modified tensile shear specimen under different pure tension loads (changing from 210 N to 350 N) were determined experimentally. All experiments were conducted at 1-3 Hz. loading frequency; no effect of frequency is expected in this range. For every load condition, the numbers of cycles to failure were obtained. These experimental studies were carried out for different loads in order to obtain sufficient data to predict the S-N curve behavior. Hence, it can be said that fatigue life predictions of spot welded constructions, which is modified tensile shear specimen in this study, is the main objective of this study.

In addition to the experimental study a numerical study has been carried out. Finite element model of the tensile shear specimen was generated using ANSYS and the resulting stress distribution discussed.

ÖZET

PUNTA KAYNAKLARININ YORULMA DAVRANIŞI

Direnç punta kaynağı işlemi özellikle otomobil olmak üzere sanayide yaygın bir şekilde kullanılmaktadır. Bu tip birleştirme yöntemi, aynı zamanda üretim yöntemlerinin öncelikli beklentileri olan basitliği, ucuzluğu ve tabiki güvenilirliği şartlarınıda yerine getirmesinden dolayı yaygın bir şekilde kullanılmaktadır. Punta kaynağı ile yapılmış makina komponentleri sanayide yaygın bir şekilde kullanılmasından dolayı, punta kaynağının yorulma ömrünün tahmini çok önemlidir. Sonuç olarak son otuz yılda çok daha yoğun olmak üzere son yıllarda bu konu üzerindeki çalışmalar oldukça yoğundur. Bu çalışmada, ilk olarak punta kaynağı yorulma tahmin metotları incelendi. İkinci olarak, kapalı döngülü hidrolik sisteme sahip MTS (Malzeme Test Sistemi) test cihazı kullanılarak farklı gerilme yükleri altında (210 N ile 350 N arasında değişiyor) kayma gerilmesine dayanıklı yanlardan güçlendirilmiş numune için uygun kullanım zamanları deneysel olarak tesbit edildi. Bu çalışmada, deneysel çalışmalar farklı frekanslar için tekrar edilmedi. Çünkü daha önce yapılan çalışmalardan biliniyorki, özellikle küçük frekanslar (1, 2 yada 3 Hz. gibi) arasındaki değişmelerden dolayı deneysel çalışmaların sonuçlarında önemli bir farklılık oluşmamaktadır. Sonuç olarak, herbir yük durumu için, hasar oluşması için gerekli olan devir sayısı elde edildi. Bu deneysel çalışmalar, sözkonusu numunenin güvenilir ömrünü tesbit edebilmek için yeteri kadar veri elde etmek için, farklı yüklerde tekrar edildi. Sonuç olarak punta kaynağı ile elde edilmiş numuneler için uygun ömür tayini (yani kayma gerilmesine dayanıklı güçlendirilmiş numune için) bu tezin öncelikli amacıdır.

Deneysel çalışmaya ilave olarak, ayrıca sözkonusu bu numune için sonlu elemanlar yöntemi kullanılarak modeller geliştirildi ve yapılan gerilme analizi ile punta etrafındaki gerilme dağılımı ve yığılması saptandı.

TABLE OF CONTENTS

LIST OF FIGURES

LIST OF TABLES

LIST OF SYMBOLS/ABBREVIATIONS

a	Crack length
a_f	Crack length at failure
a_i	Crack length at initiation
a_o	Crack length at which initiation ends and crack propagation begins
$\underline{a}$	Material constant
A_2	Material constant
b	Material constant used in Basquin relation
C	Material constant (spot weld fatigue life coefficient) used in Paris-Erdogan power law, also dependent on the load ratio, R
D	Spot weld diameter, assuming a circular weld
E	Modulus of elasticity
ΔE	The drawing force for fatigue crack growth
$Factor_F$	Correction factor in Henrysson's structural stress equation
$Factor_M$	Correction factor in Henrysson's structural stress equation
$Factor_V$	Correction factor in Henrysson's structural stress equation
F'	"Running through" tensile force
F_x	Force on the "x" Cartesian coordinate system
F_y	Force on the "y" Cartesian coordinate system
F_z	Force on the "z" Cartesian coordinate system
K	Stress intensity factor and also empirical stress correction factor in Rupp's equation
K'	Cyclic strength coefficient
K_f	Fatigue notch factor appropriate for the notch geometry
K_f^{max}	Maximum fatigue notch factor appropriate for the notch geometry
K_j	Empirical stress correction factor in Henrysson's structural stress equation
K_t	Elastic stress concentration factor
K_C	Fracture toughness
K_{IC}	Fracture toughness
K_I	Mode-I (opening) type stress intensity factor
K_{II}	Mode-II (sliding) type stress intensity factor

K_{III}	Mode-III (shearing) type stress intensity factor
ΔK	Range of stress intensity factor in general
ΔK_I	Range of opening mode stress intensity factor
ΔK_{II}	Range of sliding mode stress intensity factor
m	Material constant (spot weld fatigue life exponent) used in Paris-Erdogan power law
M_{ij}	Membrane bending moment
M_x	Moment on the "yz" plane
M_y	Moment on the "xz" plane
M_b'	"Running through" bending moment
ΔM_{ij}^*	Bending moment range at the edge of the nugget
n	Material constant
n'	Cyclic strain hardening exponent
N	Specimen life in terms of number of cycle in general
N_f	Cyclic life of specimen to some degree of failure
N_i	Initiation part of total life of the specimen
N_p	Propagation part of total life of the specimen, in other words portion of life devoted to creating a crack of length a_f-a_i
N_I	Fatigue life of the specimen for the first stage, the number of cycles to crack initiation
N_{II}	Fatigue life of the specimen for the second stage, the number of cycles to crack propagation
N_{III}	Fatigue life of the specimen for the third stage, the number of cycles to crack fracture
P	Applied load per spot weld
P_{ij}	Membrane load
ΔP	Range of tensile shear loading (fatigue load range)
ΔP_{Ai}	Axial load range in the nugget
ΔP_{ij}	Membrane load range at the edge of the nugget
r	Weld radius
R	Load ratio, also used as stress intensity factors ratio
s	Fatigue strength exponent that must be determined experimentally
max $S_{ij\ peak}$	Maximum structural stress value at the peak load af a loading cycle

ΔS	Remote applied stress
ΔS_{ij}	Range of structural stress
ΔS_{max}	Maximum structural stress range
ΔS_B	Bending stress range
ΔS_T	Nominal membrane stress range
t	Thickness of sheet metal
t_i	Thickness of sheet metal
V_i	Force components of structural stress equation in Henrysson's equation
w	Effective width of the sheet metal
α	Material constant
β	Material constant that must be determined from tests
β_s	Width of the metal sheet
γ	Material constant
ρ_f	Fictitious notch radius
θ_0	Angle of crack growth
θ_N	The nugget rotation angle of spot welded specimen
$\Delta\theta_N$	Range of nugget rotation angle of spot welded specimen
$\Delta\theta_S$	Range of angular (resultant sheet) rotation angle of spot welded specimen
σ	Nominal structural tensile stress
σ_{max}	Maximum local tensile stress
σ_a	Local stress amplitude
σ_f'	Material constant used in Basquin relation
σ_m	Mean stress (stress amplitude)
σ_{ns}	Nominal structural stress
σ_r	Tensile structural stress in Rupp's equation
σ_{rs}	Tensile residual stress
$\sigma_{r,\,max}$	Maximum tensile structural stress in Rupp's equation
$\Delta\sigma$	Range of stress locally
τ	Nominal structural shearing stress
ε_{max}	Maximum local strain
$\Delta\varepsilon$	Range of strain locally

BM	Base metal
CP	Coach peel specimen
CT	Cross tension specimen
CTOD	Crack tip opening displacement
FEA	Finite element analysis
FKN	Stiffness factor of contact element in finite element analysis
HAZ	Heat affected zone in the spot welded specimen
MCP	Modified coach peel specimen
MTS	Material testing system, also Modified tensile shear specimen
RSW	Resistance spot welding
TS	Tensile shear specimen
WM	Weld metal

1. INTRODUCTION

1.1. Motivation

Resistance spot weld fatigue is of great importance to manufacturing industry. Resistance spot welding (RSW) is important because it is a commonly used method of joining thin-sheet components of metals. For example, a car body contains approximately 5000 spot weld and this spot weld numbers reach to 15000 in a bus or coach body according to contraction engineers. Hence the integrity of the resistance spot welds determines the overall structural rigidity and integrity of the vehicle. Thus, it is important to understand the mechanical behavior of spot welds under representative types of loading conditions (for example in this study under cyclic loading conditions).

RSW is important because it is a much more convenient joining technique than the other type of joining techniques (for example bolted joint, riveted joint, adhesive bonded joint etc.) especially in terms of automation (in other words in terms of mass production) in industry, especially in automotive industry. In addition to adaptability of RSW to the automation, it is also an inexpensive and effective way to join especially thin sheet components of metals.

Although resistance spot-welding has been used for many years (especially for last 30 years) and in different industrial sectors, predicting exactly what occurs in and around the weld is very difficult and has not been understood exactly by previous researchers. Complex geometries, a non-homogeneous metallurgical structure, and residual stresses make analysis extremely difficult.

As a result, it is the purpose of this study to try to understand fatigue behavior of modified tensile shear specimens (MTS) (experimentally and also numerically using ANSYS package program) and then to obtain a suitable life for these specimens, because understanding fatigue behavior and performance of spot-welds and obtaining reliable life for these specimens are important when designing a spot welded structure.

1.2. Project Details

In general, specimens, that are used to predict fatigue life of structures, can be divided into two categories. The simplest specimens are called coupons; consisting of two strips of steel connected by a single spot weld. Some coupons have multiple welds, but still connect only two pieces of sheet metal. The second category of specimen is a structure which consists of more than two pieces of sheet steel connected by multiple welds [1, 2]. Multiple welds introduce greater difficulty in analysis because the stress distribution around welds may interact. The most common coupon specimen has a lap-shear geometry. Two strips of metal are laid such that the ends overlap and one or more welds connect these strips. The specimen is loaded such that a shear condition occurs across the weld. Other geometries (like modified tensile shear (MTS), coach peel (CP), modified coach peel (MCP), cross tension (CT), and T-joint) exist, which create a variety of loading conditions, but the lap-shear geometries, especially tensile shear (TS) and modified tensile shear (MTS) specimens, are two of the strongest and most common geometries used. Figure 1.1 shows different and most used specimen design types that are frequently referenced by spot weld related literature.

In this study modified tensile shear specimens were used that were provided from Mercedes-Benz Türk A.Ş. Specimens are prepared using St-12 type of steel.

This dissertation reviews the spot weld fatigue life prediction methods in general and discusses the fatigue behavior of modified tensile shear specimens both experimentally and computationally using ANSYS package program.

The existing spot weld fatigue life prediction methods are reviewed in Chapter 2 in detail. The experimental study is described in Chapter 3 and results of the experimental study are mentioned in Chapter 4. An alternative study -ANSYS package program- in order to check the results, that are found using experimental study, is also described in Chapter 5 using same specimens and characteristics. The effectiveness and future enhancement possibilities of these techniques are discussed in Chapters 6.

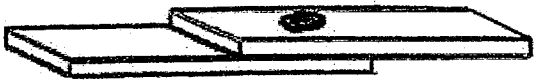

(a) Tensile shear (TS)

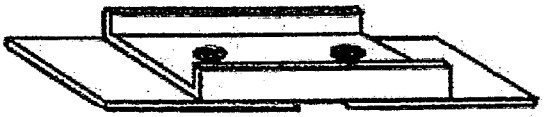

(b) Modified tensile shear (MTS)

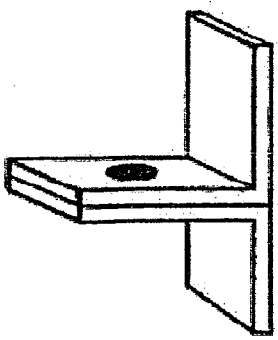

(c) Coach peel (CP)

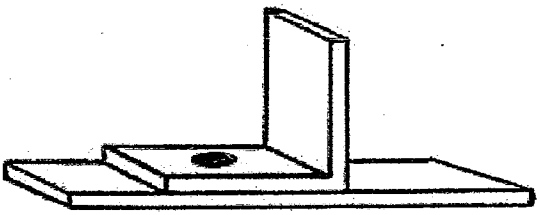

(d) Modified coach peel (MCP)

(e) Cross tension (CT)

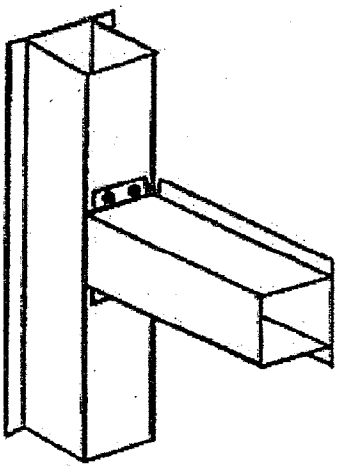

(f) T-joint

Figure 1.1. Typical spot-welded specimens [3]

1.3. The Welding Process

The resistance spot welding process was first introduced by Thomson in the 1880s. Figure 1.2 shows the resistance spot welding process schematically.

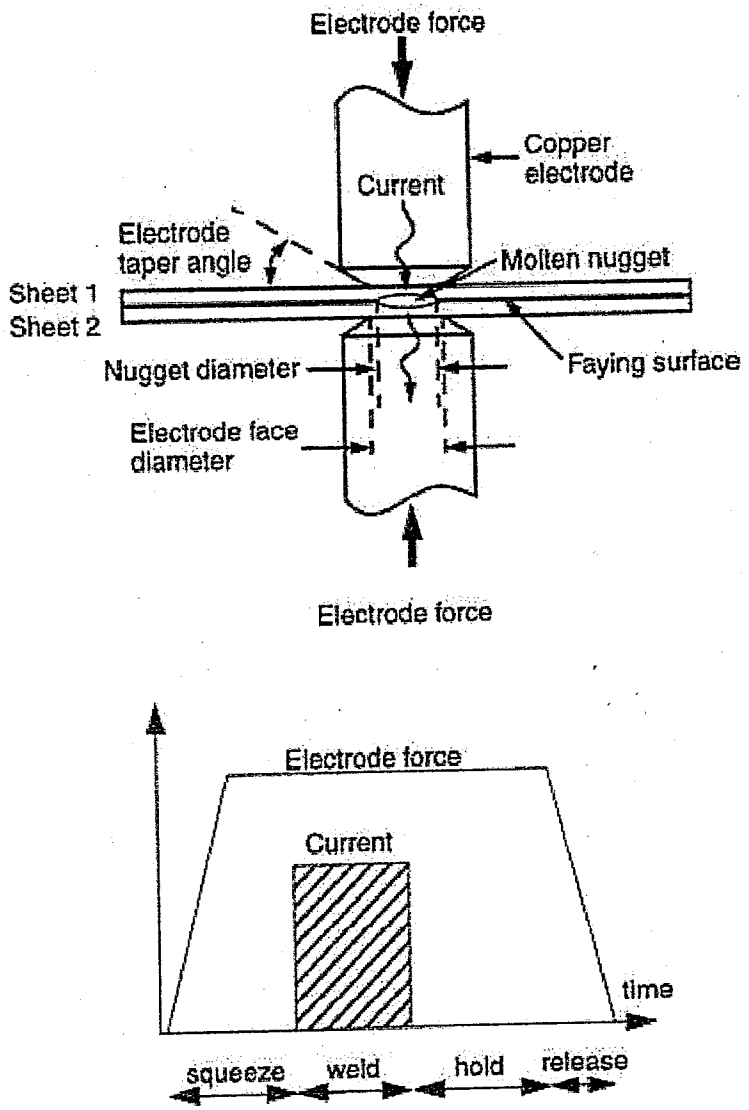

Figure 1.2. The resistance spot welding process [4]

The welding sequence is simply as follows; Firstly the two sheets that are wanted to joint are situated together between the top and bottom electrodes and then the force which is determined using some data such as sheet thickness, spot weld diameter, type of material that are used to manufacture the sheets, etc. is applied to the electrodes either to both of them or top electrode in order to ensure the contact between the sheets and electrodes to

ensure a passing current. Then a voltage is applied that results in a current passing through the sheets clamped between the top and bottom electrodes to make the weld. Finally the welding current is terminated and then the electrodes released. The electrical contact resistance between the contacting sheets generates enough heat at the faying surface and eventually a nugget develops. The nugget solidifies after termination of the welding current as it is cooled by the surrounding materials. As a result, the solidified nugget joins the two sheets (Figure 1.2).

In the welding processes, the variables involved, electrode force, current, hold time, and cycles of current allowed into the weld, etc., to produce a sound spot-weld are known but not universally accepted as to their specific values. Much work has been performed to investigate the effects of these variables on weld performance for static, fatigue, and impact cases. Most of the concern about the welding process deals with producing a sufficiently large weld diameter and the effects of welding heat on the metal surrounding the weld.

2. LITERATURE REVIEW

2.1. Introduction

Spot-welding is a widely-used method of manufacture for thin-sheet components, especially in mass-production industries such as the car industry. In the car industry, spot welds make up a large percentage of the joints that hold an automobile together. In fact, the typical car body contains about 5000 spot welds joining a mixture of sheet metal material types and thicknesses [5]. Although spot-welds are common, studying and predicting their behavior is complicated by residual stresses created from the welding process, complex stresses around the weld, and, in some cases, large deflections around welds.

Spot welding is the most common method of joining two strips of metal and has been studied for many years. In the industry's never-ending goal to reduce weight and increase performance, the spot welded joint has seen many changes. Manufacturers are using thinner, higher strength steels for weight reduction. While these metals may exhibit higher strength properties under static conditions, the effects of the higher strength steels on high-cycle fatigue lives are negligible [6, 7]. This has drawn attention to the behavior of spot welds under fatigue loading. It would not be unreasonable to assume that spot welds with few or no flaws or defects would exhibit higher fatigue lives than spot welds found to have defects.

Fatigue is a frequent cause of failure in sheet steel and aluminum joined by spot welds [8]. There are two primary schools of thought on how the fatigue of a spot weld should be modeled in general. Cooper and Smith support the theory that the spot weld is a sharp notch and fatigue of the spot weld consists of two stages – initiation and propagation [10, 11]. The other school of thought is supported Lawrence and others who believe that fatigue of spot welds is a three stage process [10, 11]. Stage I is devoted to initiating a crack of arbitrarily small length (~ 0.25 mm). Stage II is a crack propagation through the Heat Affected Zone (HAZ) to the exterior surface of the base metal as shown in Figure 2.1; and in Stage III the crack propagates around the circumference of the weld then out into the base metal perpendicular to the loading until it ruptures [6, 9, 12].

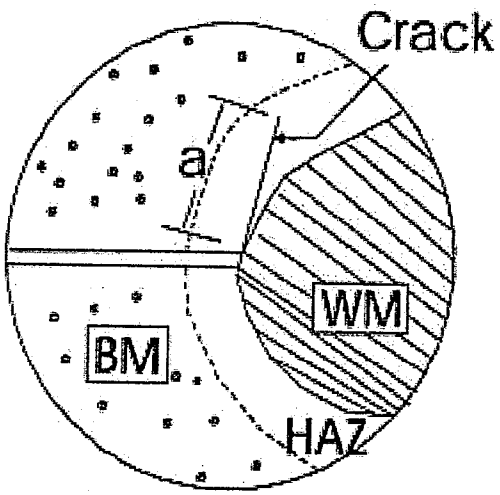

Figure 2.1. Crack initiation and propagation in the HAZ of Stage II [6]

It has been suggested that as much as 50 % of the fatigue life can be spent developing Stage I. Figure 2.2 may help to visualize the formation and propagation of a crack in a tensile shear spot weld. Figure 2.2(a) shows the crack in its early stage where it is internal. Figure 2.2(b) shows the crack as it has propagated through the thickness and is prepared to break through the surface causing a dimple-like feature on the surface. Figure 2.2(c) shows the crack through the surface and propagating along the circumference of the weld nugget in an eyebrow shape.

The majority of spot welds fail in fatigue due to through-thickness cracks. At the beginning, it was said that these cracks initiate from the notch root at the faying surface and propagate in the thickness direction, as shown in Figure 2.3. Interface failures with a crack parallel to the sheets are rarely observed when the weld nugget diameter is much larger than the sheet thickness, which is the case for the spot welds in automobiles. Therefore, fatigue failure in this study refers to the failure due to through-thickness cracks, as shown in Figure 2.3. The fatigue life is usually defined as the number of loading cycles it takes for the first crack in the joint to initiate and propagate through thickness of the sheet and becomes visible from the outer side of the sheet.

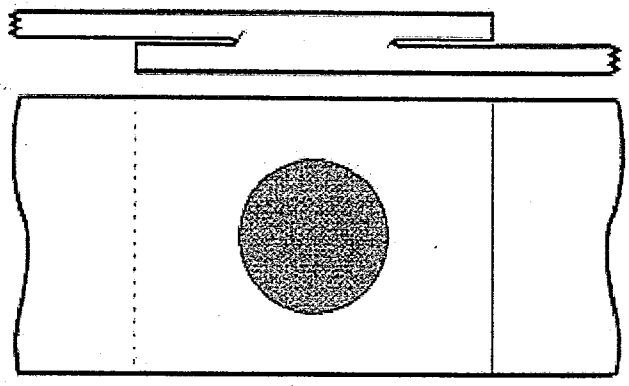

a). Early stages

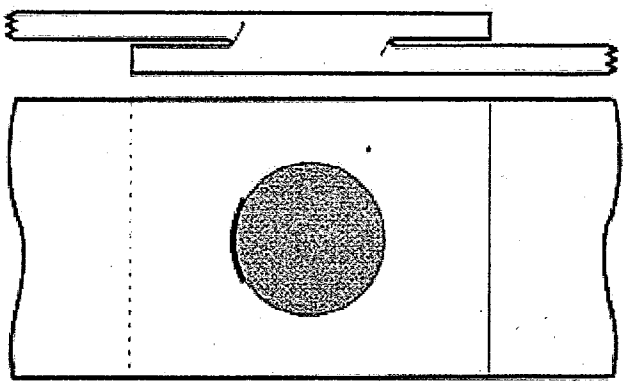

b). Propagating through the thickness to exterior surface

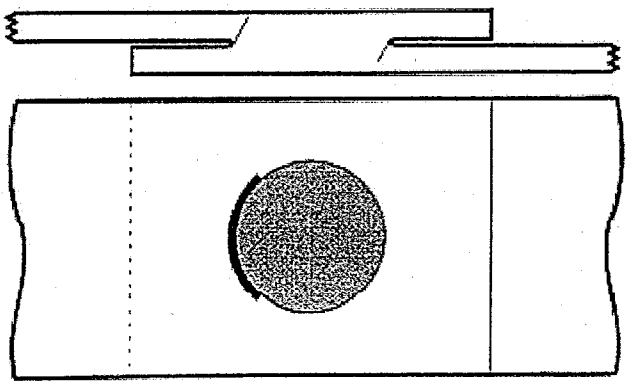

c). Propagating around the circumference of the weld

Figure 2.2 Depiction of a crack formation in a tensile shear spot welded specimen [6]

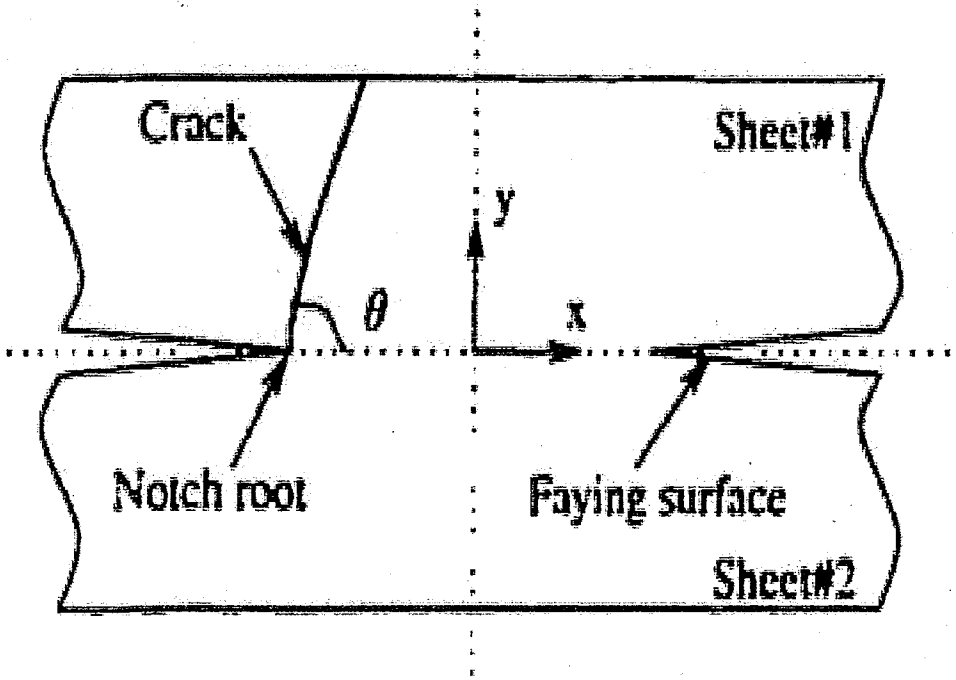

Figure 2.3. Typical fatigue failure mode of spot welds [3]

2.2. Fatigue Life Prediction Methods for Spot Welds

Over the past thirty years, many fatigue life prediction methods have been proposed. Several of the most commonly referenced methods are briefly reviewed in this section.

Failure in a spot-weld occurs in the heat affected zone (HAZ) of unmelted metal between the base metal and the weld metal. The HAZ is caused by the extreme heat of welding changing metallurgical properties on the microscopic level. The HAZ is subjected to higher stresses than the surrounding base metal and is the location of failure in most cases. Microscopic properties of the base metal, such as grain size, have been found to have no effect on high cycle fatigue of its HAZ [13]. Residual stresses, which are associated with the HAZ, can significantly alter fatigue lives [14]. For this reason alone, the HAZ should be considered as a distinct region separate from the surrounding base metal.

A well made spot-weld should not fail across its weld metal. Failure of the weld metal seems to be associated with yielding by shear. If the weld does not fail by yielding, fatigue crack growth in this region does not occur [15]. The weld metal seems to have material and fatigue properties superior to the surrounding base metal. A weld is very nearly circular and is characterized with a diameter, D. According to past studies that were done especially by Davidson, in order to produce welds that won't fail by gross yielding of weld metal, the relation between a spot-weld diameter and thickness of the welded specimen must be satisfied. This so called equation can be written as the following type [7].

$$D \geq \sqrt{t} \quad (D \text{ and } t \text{ in inches}) \tag{2.1-a}$$

$$D \geq 5\sqrt{t} \quad (D \text{ and } t \text{ in mm}) \tag{2.1-b}$$

where;

t = Sheet thickness,

D = Spot weld diameter.

Failure of spot welds can be placed into several categories. First of all, if a weld nugget is too small, or if too little current was used during welding, failure by yielding across the nugget may occur [16]. Such a failure would be considered to be caused by poor welding. In most cases, however, cracks would lead to failure where the stress intensity factors are greatest [17]. This crack propagates from the edge of the weld metal into the HAZ. Once a crack develops, one of two things may happen. If the load is sufficiently small, the crack will propagate far from the weld into the base metal before plastic instability ruptures the specimen. However, if the load sufficiently high, the crack is not allowed to grow far before plastic effects tear the crack around the weld [18]. This makes the crack appear to have an eyebrow (curved) shape. The greater the loads, the more the crack curves around the weld. Sometimes the weld may pull out of one of the sheets [7].

In general, the edges of spot-welds, where fatigue crack occur, are considered to be geometric notches with some notch radius at the root [7]. Researchers, who consider the spot-weld connection to behave as a notch, divide the life (of a spot-weld) into three distinct stages. The first stage is spent initiating a crack from a notch-like connection. The second stage is governed by fatigue crack growth from the connection at the interface of the two sheets completely through one steel sheet to the outside. In the third stage of life, the crack propagates away from the spot-weld, grows into the surrounding base metal, and ends when the specimen is in two or more separate pieces. The number of cycles for the first stage is N_I, while the life for the second and third stages are N_{II} and N_{III} respectively. Thus, the total life of the specimen N is the sum of the lives of the three stages [1, 7, and 24].

2.2.1. Local Strain-Based Approach

In general, each stage of spot-weld life is modeled separately because each stage is governed by a different mechanism of damage accumulation. In local strain-based method, only first stage, that is crack initiation stage, is considered and after initiation of specimen, it is accepted that the specimen is deformed. Hence the first stage is important and considered in this method. In this method, the first stage is typically analyzed by a strain based approach and because of this the method is called as "Local Strain-Based Approach" [6].

Some experimental studies has been conducted using strain gages on the outer faces of specimens and relating that strains to the strains at the notches [2, 19]. The remote stress is related to the local stress and local strain found at the notch by [7, 20, 21].

$$\Delta\sigma.\Delta\varepsilon = \frac{(K_f\,\Delta S)^2}{E} \tag{2.2}$$

where;

E = elastic modulus,

ΔS = Remote applied stress,

$\Delta\sigma$ = Local stress at the notch,

$\Delta\varepsilon$ = Local strain at the notch,

K_f = Fatigue notch factor appropriate for the notch geometry.

Fatigue notch factor appropriate for the notch geometry is usually estimated using Peterson's equation,

$$K_f = 1 + \frac{K_t - 1}{1 + \frac{a}{r}} \tag{2.3}$$

where;

r = Notch radius,

a = Material constant,

K_t = Elastic stress concentration factor.

In equation (2.3), elastic stress concentration factor can be obtained by a finite element scheme. For tensile-shear spot-weld geometry, it is given by,

$$K_t = 1 + \alpha\left(\frac{t}{r}\right)^{1/2} \tag{2.4}$$

where;

t = thickness of sheet metal,

α = Material constant.

The actual notch radius of a spot-weld connection is not very well defined. It is assumed that the radius has no specific value, so the worst possible value for a notch radius

is used. Extreme for K_f can be found by finding where its derivative with respect to notch radius, *r*, goes to zero. This is a maximum and is given as K_f^{max} [20].

$$K_f^{max} = 1 + \frac{\alpha}{2}\left(\frac{t}{a}\right)^{1/2} \tag{2.5}$$

The initiation life is estimated by modifying the empirical Basquin relationship with the Morrow mean stress correction, which is given as follows [1].

$$\sigma_a = (\sigma_f' - \sigma_m)[2N_I]^b \tag{2.6}$$

where;

N_I = The number of cycles to crack initiation,

σ_a = Local stress amplitude,

σ_m = Mean stress,

σ_f' = Material constant,

b = Material constant.

The Basquin relationship is modified by expressing the stress amplitude in terms of applied stress and the fatigue notch factor. Hence the modified Basquin relationship is; [1].

$$\frac{\Delta S}{2} K_f = (\sigma_f' - \sigma_m)[2N_I]^b \tag{2.7}$$

Hence life of specimen can be written as;

$$N_I = \frac{1}{2}\sqrt[b]{\frac{\Delta S.K_f}{2(\sigma_f' - \sigma_m)}} \tag{2.8}$$

Choosing the constants for this empirical equation may be troublesome. Some effort should be made to obtain the constants for the heat affected zone (HAZ), which is where cracks are found. Furthermore, Peterson's equation (Equation 2.4) may not be valid for an arbitrarily small notch radius [22]. Peterson himself warned that his equation was only intended for machined notches with a finite radius whose depth was not much greater that the notch radius [23]. As a notch becomes smaller, the fatigue notch factor, K_f, should increase because the notch is approaching the geometry of a sharp crack. It seems unreasonable to expect a vanishingly small notch radius to produce a longer life than a larger notch radius for the same loading conditions [7].

2.2.2. Linear Fracture Mechanics Method

In 1985, Cooper and Smith developed a direct current electric potential difference (PD) method to measure crack growth. They monitored the crack growth in mild steel spot welded joints and concluded that the predominant fatigue mechanism in spot welds is crack propagation [10]. Because of this, this method is sometimes named as "Fatigue Crack Growth Approach".

As previously stated, all researchers agree that fatigue crack growth is responsible for at least a portion of the life of spot-welded joints. The majority believe that a crack-like defect exists at the spot-weld connection initially and crack growth begins on the first cycle. In this case the initiation life, N_I, would not exist or at least represent a negligible portion of the total life.

On the other hand, exactly what happens at the vicinity of the spot, that is heat affected zone (HAZ), is somewhat of a mystery because the spot-weld connection is not accessible for observation [7]. Destructive tests performed on specimens interrupted before failure support the claims of a crack present an early stage in the weld life [25, 26]. Nondestructive tests, such as the electric potential drop method, also tend to indicate that early crack growth is a reality [3, 27]. The electric potential drop method, for example, detects the presence of a crack by passing a direct electrical current through a region in

which a crack is expected to form. The presence of the crack increases the electrical resistance, which in turn decreases the voltage (potential), measured across the weld [9].

The linear fracture mechanics approach, that was introduced firstly by Pook in 1975 and then used by Cooper and Smith in 1986, assumes that the notch root is a sharp crack, and the crack propagation process starts immediately from the existing crack. Most scientists that try to quantify crack extension use a form of the Paris power law to estimate the fatigue life of spot welds, which is of the following form [17, 28, 29, 30, 31, 32, 33].

$$\frac{da}{dN} = C(\Delta K)^n \tag{2.9}$$

where;

a = Crack length,
N = Specimen life in terms of number of cycle,
ΔK = Range of stress intensity factor,
C = Material constant (Also dependent on the load ratio, R),
n = Material constant.

The stress intensity factors, which is approximate opening mode, K_I, and edge sliding mode, K_{II}, stress intensity factors of point A in Figure 2.4, of the notch cracks for tensile shear (TS) specimens, for example, were given by Pook (1975) [17]. Pook conducted a study using the configurations, seen in Figure 2.4, and at the end of his studies, he proposed the following formulas [17].

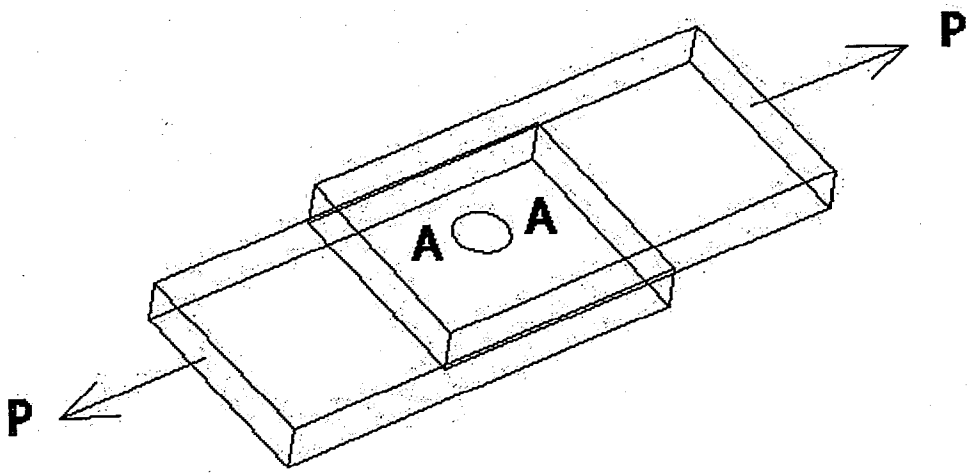

Single spot welded specimen

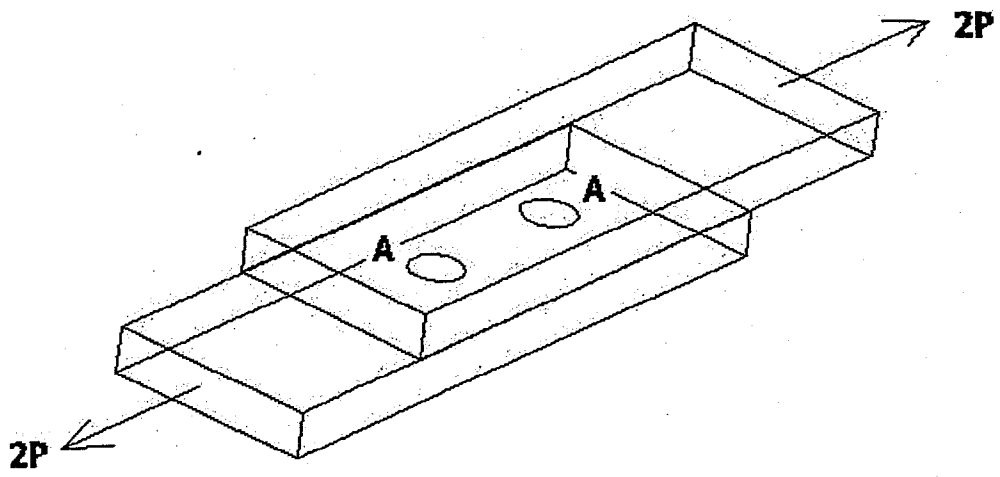

Two spot welds in line

Figure 2.4. Single spot welded and two spot welded (in line) specimens [17]

For a single spot weld with $r/t \leq 10$;

$$K_I = \left[P / r^{3/2} \right] \left[0.341 \left(\frac{r}{t} \right)^{0.397} \right] \tag{2.10}$$

and

$$K_{II} = \left[P / r^{3/2} \right] \left[0.282 + 0.162 \left(\frac{r}{t} \right)^{0.710} \right] \tag{2.11}$$

For two spot welds in line with centers at least three spot diameter apart and $1.92 \leq r/t \leq 10$;

$$K_I = \left[P / r^{3/2} \right] \left[0.282 \left(r/t \right)^{0.397} + 0.846 \left(t/r \right) \right] \tag{2.12}$$

and

$$K_{II} = \left[P / r^{3/2} \right] \left[0.282 + 0.162 \left(\frac{r}{t} \right)^{0.710} \right] \tag{2.13}$$

where;

K_I = Mode I (opening) type stress intensity factor,
K_{II} = Mode II (sliding) type stress intensity factor,
P = Applied load per spot weld,
r = weld radius,
t = thickness of sheet metal.

The edge of a spot weld must be at least one spot diameter apart from a plate edge [24].

It is assumed that a crack in a spot-weld, at the failure location, can be modeled as a planar crack. This approximation becomes valid as the ratio t/r is decreased [33]. For the typical welds, cracks grow from the interface of the two steel sheets at the edge of the weld, in a shape similar to a semi-ellipse, but curved slightly out of plane to give it a "thumbnail shape" (Figure 2.5) [33]. If the weld radius is large compared to the sheet thickness, this thumbnail cracks is nearly planar. Although not truly two-dimensional, this crack can be described by a single degree of freedom. Thus Equations (2.10) and (2.11) are used for this single-degree-of-freedom model for a single spot weld, for example [33].

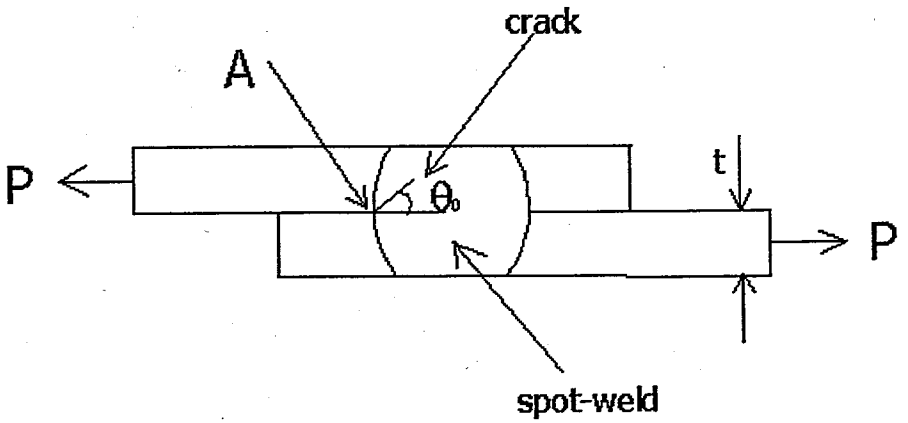

a) Side view (centerline).

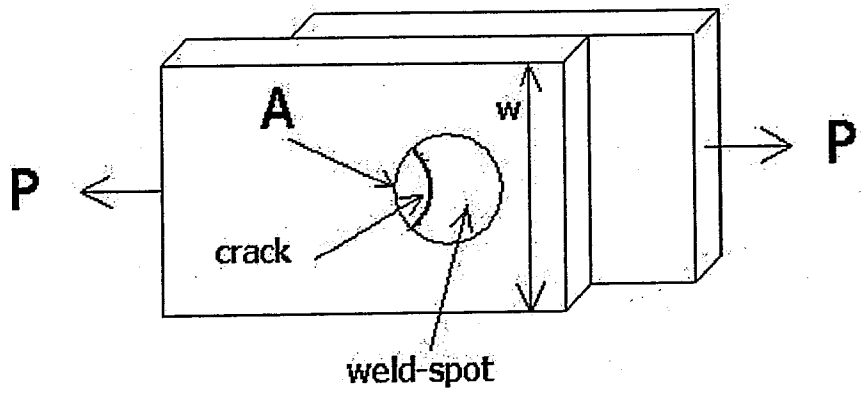

b) Front view (outer surface).

Figure 2.5. Failure location in a typical spot-welded TS specimen [33]

Now that this spot-weld model has been reduced to a single degree of freedom, fatigue life is modeled as starting from a two-dimensional crack, which exists initially under both Mode-I and Mode-II loading. If we assume that the crack propagates perpendicular to the direction of the maximum normal stress at the crack tip, it will initially grow at an angle, θ_0, as shown in Figure 2.5.a. This angle satisfies Equation (2.14), where K_I and K_{II} are the stress intensity factors initially acting at point A in Figure 2.5 before crack growth occurs [33]. This equation is obtained by combining well-known crack-tip singularity stress field equations for Mode-I and Mode-II stress intensity factors, and

finding the principal stress directions. Note that Equation (2.14) is valid only in the case where tearing mode stress intensity factor, K_{III}, is zero [33].

$$K_I \sin\theta_0 = K_{II}\left(3\cos\theta_0 - 1\right) \tag{2.14}$$

where;

θ_0 = Angle of crack growth.

It has been noted in the literature that the crack growth rate in spot-welds remains nearly constant as the test proceeds for constant amplitude loading and for a small ratio of t/r [10]. This suggests that the stress intensity factor also remains nearly constant. On the other hand, these assumptions are not valid for thick sheets and for small welds [34, 36].

Since the stress intensity factor is assumed to be constant according to Newman and Dowling, crack growth angle, θ_0 also remains constant through the test [33]. After solving for θ_0, an effective Mode-I stress intensity factor needs to be calculated in order to calculate fatigue life of desired specimen. This was obtained using equations for stress around large two-dimensional cracks subject to Mode-I and Mode-II loading with an infinitesimally small kinked crack growing from the original crack tip at an angle [7, 35]. The infinitesimal kink is assumed not to disturb the original stress field. The small kink grows in principal stress directions, so no local Mode-II loading exists at the kinked crack tip. The local Mode-I stress intensity factor, acting on the infinitesimal kinked crack, is given in Equation (2.15), and is obtained by examining the principal normal stresses acting on this new kinked crack tip. This is the formulation for effective Mode-I stress intensity factor used for tensile shear (TS) specimen, for example.

$$\Delta K = \frac{\Delta K_I}{4}\left[3\cos\frac{\theta_0}{2} + \cos\frac{3\theta_0}{2}\right] - \frac{\Delta K_{II}}{4}\left[3\sin\frac{\theta_0}{2} + 3\sin\frac{3\theta_0}{2}\right] \tag{2.15}$$

where;

ΔK = Range of stress intensity factors,

ΔK_I = Range of opening mode stress intensity factors,

ΔK_{II} = Range of sliding mode stress intensity factors.

In addition to this formula, a Paris-Erdogan crack growth relation, with an adjustment for the R-ratio effect as suggested by Walker [37], is assumed to describe crack growth, as in Equation (2.16). Hence, this so called equation is intended only for pure Mode-I loading.

$$\frac{da}{dN}=C\left[\frac{\Delta K}{(1-R)^{(1-\gamma)}}\right]^{m} \tag{2.16}$$

where;

C = Material constant,

m = Material constant,

γ = Material constant,

R = Load ratio, also used as stress intensity ratio.

Because both Mode-II and Mode-III loading is not present at the small kinked crack of length a, Equation (2.17) can be used in tensile shear (TS) and modified tensile shear (MTS) models. Using Figure 2.5, the so called crack grows a distance $a_f = t/\sin\theta_0$ before penetrating the outer surface of the plate, which is considered failure in this study. If we consider the crack growth as constant, then Equation (2.16) can be integrated to obtain an equation for fatigue life for this model, Equation (2.17) [33].

$$N_f=\frac{t}{C\sin\theta_0}\left[\frac{\Delta K}{(1-R)^{(1-\gamma)}}\right]^{-m} \tag{2.17}$$

where;

a_f = Crack length at failure,

N_f = Cyclic life of specimen to some degree of failure (here to propagate degree)

Finally, using Equations (2.15) and (2.17) together, Newman and Dowling expressed fatigue life explicitly for any known crack growth angle, θ_0. In these formulas, it is not forgotten that the so called crack growth angle must be known. Hence in order to calculate a proper angle, Equation (2.14) must first be solved for θ_0 using Equations (2.12) and (2.13) for calculating opening and sliding stress intensity factors respectively. As a result, the desired single-degree-of-freedom approximation for fatigue life in this method can be given by Equation (2.18) [33].

$$N_f = \frac{t}{C \sin\theta_0}\left[\frac{\Delta K_I\left[3\cos\frac{\theta_0}{2}+\cos\frac{3\theta_0}{2}\right]-\Delta K_{II}\left[3\sin\frac{\theta_0}{2}+3\sin\frac{3\theta_0}{2}\right]}{4(1-R)^{(1-\gamma)}}\right]^{-m} \quad (2.18)$$

2.2.3. Nugget Deformation Method

Scientists that work in this field focus on a better understanding of spot-weld fatigue behavior because of changes in automotive designs. In other words, the changes in automotive designs make the fatigue behavior of spot welds one of the primary parameters that governs the safety and reliability of automobiles. Fatigue behavior of spot welds under both constant amplitude load and variable-amplitude load fluctuations is essential to the development of accurate prediction methods of fatigue lives for automobile components [37].

Some scientists have used "Nugget Deformation Method" in order to find the fatigue lives of spot welded specimens. According to Davidson, Imhof, and Barsom , the life of spot weld connections depend on the stiffness of the spot-welded joint [37], in addition to the load level which are applied to the sheets, the metal thicknesses that are used manufacturing steel sheets, the nugget type and diameter, etc. Hence it can be said that the

stiffer joints exhibit longer fatigue lives according to these investigators. In "Nugget Deformation Method", using with simple relations in a design environment, load level or sheet metal thickness for a required fatigue life of specimen can also be found in addition to fatigue life of specimen for a required load level or sheet metal thickness. The less separation (angular rotation, $\Delta\theta_S$) that occurs between the overlapped portions of spot-welded sheets during tensile-shear loading (due to eccentric loading) is dependent on the stiffness of the joint. The angular-rotation parameter, $\Delta\theta_S$, shown in Figure 2.6, describes the fatigue life of specimens that loaded tensely, regardless of joint characteristics, because the angular-rotation parameter, $\Delta\theta_S$, is related to the stress-intensity range, ΔK, a fracture-mechanics parameter that is used to describe fatigue crack-growth as shown in Figure 2.6.

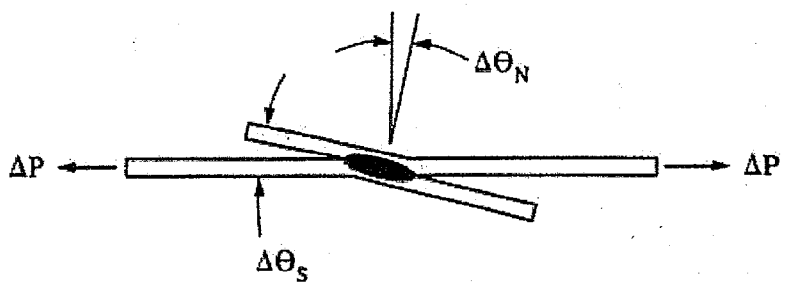

Figure 2.6. Side view of a spot-weld connection under tensile-shear loading [38]

The angular rotation, $\Delta\theta_S$ which occurs during fatigue loading of spot-welded connections, is related to the crack-tip opening displacement (CTOD) at the edge of the spot weld. Naturally for a spot-welded specimen and known elastic modulus, the CTOD dependent mostly on the angular rotation, $\Delta\theta_S$ [38]. However, measuring displacement near the edge of the spot weld in order to calculate the angular rotation is extremely difficult. Because of this difficulty, instead of the angular rotation, the nugget rotation, $\Delta\theta_N$, shown in Figure 2.6, is measured and used because the nugget rotation is a more convenient variable to measure. The nugget rotation can be used using with finite element analysis [28, 38].After this step, using the nugget rotation, the angular rotation can be found easily because there is a relation between these two variables [38].

In 1985, Barsom and Imhof demonstrated that the driving force for fatigue crack growth of spot-welded sheet is given as the following type [28].

$$\Delta E = \frac{\Delta P \, \Delta \theta_N^{1/2}}{t} \tag{2.19}$$

where;

ΔE = The driving force for fatigue crack growth,

ΔP = Fatigue load range,

θ_N = The nugget rotation of spot-welded specimen,

t = Thickness of sheet metal.

In this formula, the driving force for fatigue crack growth of as-welded sheet, ΔE, is a measure of the cyclic energy and generally this formula is valid for tensile shear (TS) specimens [3]. Finally, it was shown that the fatigue life in cycles to failure can be related to the driving force for fatigue crack growth, ΔE, by the simple power function as the following type [38].

$$N_f = C(\Delta E)^m \tag{2.20}$$

where;

m = Material constant (spot-weld fatigue life exponent),

C = Material constant (spot-weld fatigue life coefficient),

N_f = Life of specimen.

2.2.4. Combined Initiation and Propagation Method

In previous methods, we saw that sometimes crack initiation was accepted as the most important part of the life and the lives of the spot-welded specimens were calculated

only using data related to the initiation periods of the processes; and sometimes crack propagation was accepted as the most important part of the life and the lives of the spot-welded specimens were calculated only using data related to the propagation periods of the processes that time. In "Local Strain-Based Approach", for example, only crack initiation is thought the most important step of the processes and the formulas in order to calculate the fatigue lives of spot-welded specimens were obtained only thinking the initiation step of the processes; on the other hand, in "Linear Fracture Mechanics Method", this time only crack propagation is thought the most important part of the processes and the formulas for calculating fatigue lives of spot-welded specimens were obtained only using the propagation step of the process.

In this method, both crack initiation and crack propagation were taken into consideration and related equations were obtained. For example, McMachon and Lawrence proposed a combined initiation and propagation approach that took into consideration the initiation and propagation stages of the fatigue behavior of spot welded specimen together in 1985. Hence, the fatigue life of spot welds was treated as the sum of crack initiation life and propagation life [3].

The first part of the life estimation, that is the crack initiation life estimation, according to "Combined Initiation and Propagation Method" was similar to "Local Notch Strain Method", that is;

$$N_i = N_I = \frac{1}{2}\sqrt[b]{\frac{\Delta S.K_f}{2\left(\sigma_f' - \sigma_m\right)}} \tag{2.21}$$

where;

N_i = Initiation part of the total life, initiation life

In calculation of fatigue notch factor appropriate for the notch geometry, K_f, we used elastic stress concentration factor, K_t, in "Local Notch Strain Method" and some

formulas for both fatigue notch factor and elastic stress concentration factor were proposed in that method, but in 1984, Wang proposed a different elastic stress concentration factor for simplicity for tensile shear (TS) specimen used in McMahon and Lawrence's work, that is "Combined Initiation and Propagation Method". This stress concentration factor is given as follows;

$$K_t = \frac{W t}{(\pi r)^{1/2} D^{3/2}} \left[1.61 \left(\frac{D}{t} \right)^{0.397} + 0.593 + 0.34 \left(\frac{D}{t} \right)^{0.710} \right] \tag{2.22}$$

where;

W = Width of the plate,

D = Diameter of the spot weld.

In addition to Equation (2.21), McMachon and Lawrence by using Basquin's equation derived a different equation for the initiation life of spot-welded tensile shear specimens as follows [3];

$$\int_1^{2N_I} \left[\left(\frac{\sigma'_f}{\frac{\Delta\sigma}{2}} \right) \left(1 - \sigma_0 \frac{(2N)^k}{\sigma'_f} \right) \right]^{1/b} dN = 1 \tag{2.23}$$

where;

N_I = Cycles to crack initiation used in the Basquin relation, portion of life devoted to creating a crack of length a_i

σ'_f = Material constant used in Basquin relation,

$\Delta\sigma$ = Range of stress locally,

b = Material constant used in the Basquin relation,

k = Mean stress relaxation exponent,

σ_0 = Mean stress.

The second part of the life estimation, that is the crack propagation life estimation, was derived by integration of the well-known Paris-Erdogan law, that is;

$$N_P = \frac{1}{C}\int_{a_i}^{a_f} \Delta K^{-m}\, da \tag{2.24}$$

where;

a_i = Initial crack length,

a_f = Final crack length,

C = Constant used in Paris-Erdogan power law,

ΔK = Range of stress intensity factors,

m = Material constant used in Paris-Erdogan power law,

N_P = Portion of life devoted to creating a crack of length $a_f - a_i$, the propagation (second part) life of the specimen.

In Equation (2.24), the stress intensity factor is an equivalent parameter given as;

$$K = \sqrt{K_I^2 + \beta K_{II}^2} \tag{2.25}$$

where;

β = A constant that must be determined from tests.

As a result, the fatigue life of spot-welded specimen in this method can be obtained by adding these two steps results to each other, that is;

$$N_f = N_i + N_P \tag{2.26}$$

$$N_f = \frac{1}{2}\sqrt[b]{\frac{\Delta S.K_f}{2\left(\sigma_f^{'} - \sigma_m\right)}} + \frac{1}{C}\int_{a_i}^{a_f} \Delta K^{-m}\, da \qquad (2.27)$$

where;

N_f = Life of specimen.

2.2.5. Structural Stress Method

The structural or hot-spot stress approach, sometimes also called geometric stress approach, considers the stress increase due to the structural configuration or in other words, the macro-geometry [39]. In other words, structural stress method proposes that fatigue behavior can be described by the nominal stress in the sheet in the radial direction (with respect to the spot), and then calculated from the overall loadings at the spot itself [8]. For example for a spot welded specimen, because of the geometric complexity and hence difficulty of stress distribution in spot welds, the structural (nominal) stress at a distance of half the diameter of the weld nugget from the center of the weld is taken into consideration and is accepted that the structural stress is related to the fatigue life of the spot welds. As a result, the stresses (membrane type and bending type) at that point are calculated using some constants and formulas and considered for the life of the specimen.

Structural Stress Method was used firstly in the late 1980s and early 1990s [3]. The leading researchers that dealt with this approach are Sheppard, Radaj, Rupp and Henrysson. There are, of course, similarities and differences between the different models of structural stress that proposed by different scientists [3].

Sheppard's Structural Stress method: According to Sheppard's Structural Stress Approach, for fatigue life estimation the structural stress at a distance of half the diameter of the weld nugget from the center of a weld is related to the fatigue life of spot welds. Hence, as shown in Figure 2.7, the fatigue failure in this method can be defined as crack initiation and growth through the sheet thickness. Sheppard and Strange developed a general equation for structural stress in 1992 as the following type [3];

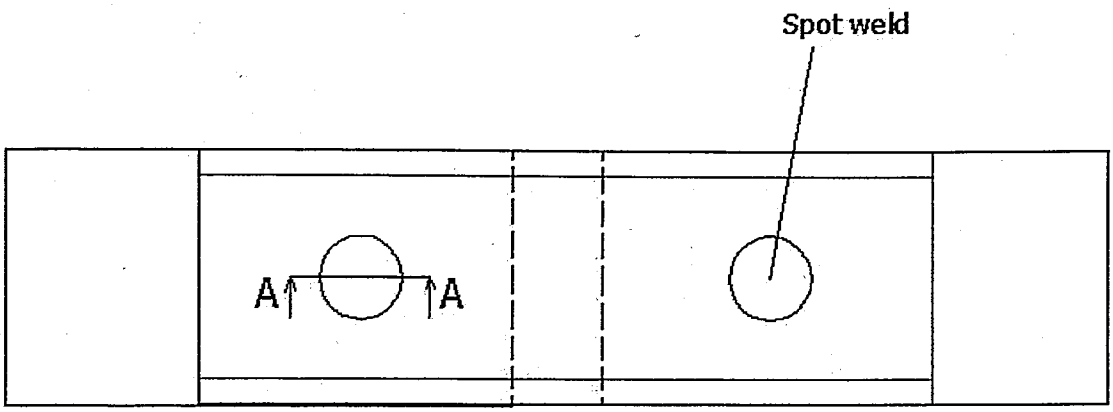

a) Technical drawing of MTS

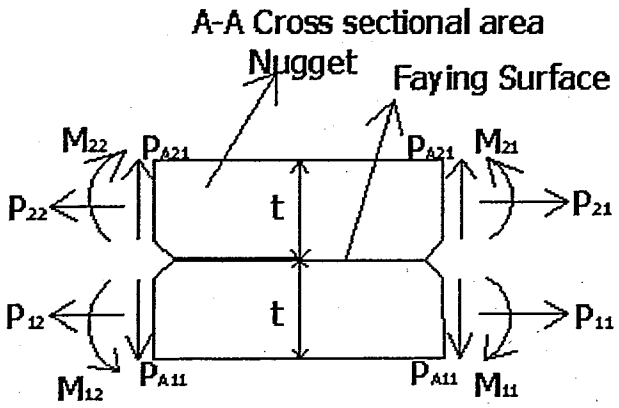

b) Nomenclature of local load for structural stress calculation

Figure 2.7. Fatigue failure in Sheppard's structural stress calculation [3]

$$\Delta S_{ij} = \frac{\Delta P_{ij}}{w t_i} + \frac{6\Delta M_{ij}^*}{t_i^2 \beta_s} \quad i, j = 1,2 \tag{2.28}$$

where;

ΔP_{ij} = Membrane load range at the edge of the nugget,

ΔM_{ij}^* = Bending moment range as defined in Table 2.1,

w = Effective width [defined as $\frac{\pi D}{3}$ (based on the work by Wang)],

t_i = Thickness of the sheet,

D = Diameter of the weld,

β_s = Width of the sheet,

ΔS_{ij} = Structural stress,

i = This subscript refers to the sheet (first and second) as shown in Figure 2.7,

j = This subscript refers to the side of the nugget edge as shown in Figure 2.7.

Table 2.1. Definition of ΔM_{ij}^{*} in Equations 2.28 and 2.29 [3]

Case No.	ΔP_{Ai}	ΔM_{i1}^{*}	ΔM_{i2}^{*}
1. $\Delta P_{Ai} > 0$			
1a. $\Delta M_{i1} > \Delta M_{i2} > 0$	ΔP_{Ai}	$\Delta M_{i1} - \Delta M_{i2}$	0
1b. $0 < \Delta M_{i1} < \Delta M_{i2}$	ΔP_{Ai}	0	$\Delta M_{i2} - \Delta M_{i1}$
1c. $\Delta M_{i1} > 0, \Delta M_{i2} < 0$	0	0	ΔM_{i2}
1d. $\Delta M_{i1} < 0, \Delta M_{i2} < 0$	tbd	tbd	tbd
2. $\Delta P_{Ai} < 0$			
2a. $\Delta M_{i1} > \Delta M_{i2} > 0$	0	$\Delta M_{i1} - \Delta M_{i2}$	0
1b. $0 < \Delta M_{i1} < \Delta M_{i2}$	0	0	$\Delta M_{i2} - \Delta M_{i1}$
1c. $\Delta M_{i1} > 0, \Delta M_{i2} < 0$	0	ΔM_{i1}	0
1d. $\Delta M_{i1} < 0, \Delta M_{i2} > 0$	0	0	ΔM_{i2}
1e. $\Delta M_{i1} < 0, \Delta M_{i2} < 0$	0	tbd	tbd

tbd: to be determined. This particular case has never been exhibited by any of the specimens studied to date.

A refinement of Equation 2.28 was given by Sheppard, in which the effect of a "cupping" deformation mode that results from a transverse load applied to the sheet was included as being following Equation 2.29 [3];

$$\Delta S_{ij} = \frac{\Delta P_{ij}}{wt_i} + \frac{6\Delta M_{ij}^{*}}{t_i^2 \beta_s} + \frac{\Delta P_{Ai}}{t_i^2} \quad i, j = 1,2 \tag{2.29}$$

where;

ΔP_{Ai} = Axial load range in the nugget.

The deformations resulting from the three loading modes in Equation 2.29 are shown in Figure 2.8.

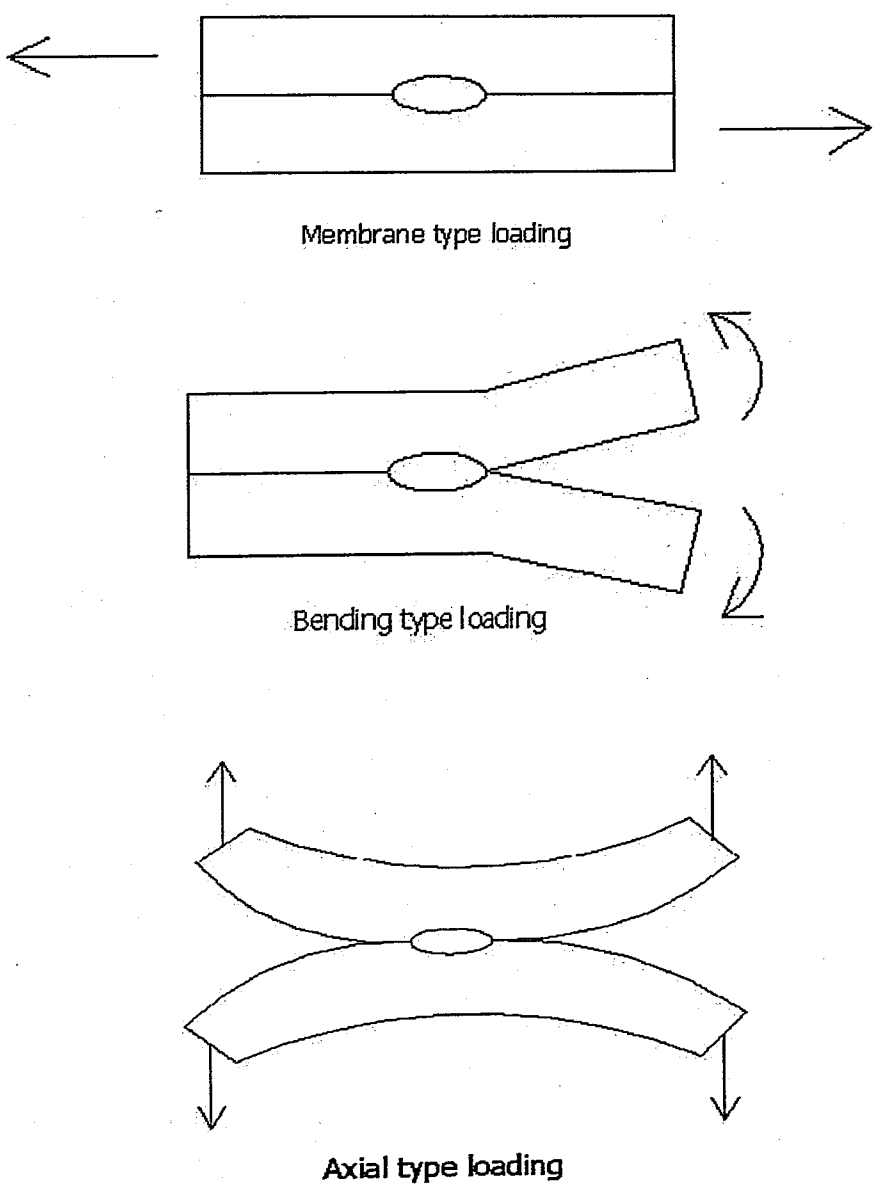

Figure 2.8. Structural stress from the three loading modes [3]

The subject of whether or not there is an initiation and early crack growth stage has been debated in the past and remains unsettled. For example, using electrical-potential drop

method in order to measure the crack growth, Cooper and Smith showed that fatigue in a spot weld joint is a pure crack propagation process, as we mentioned in Linear Fracture Mechanics Method, which means that there was no crack initiation stage observed at all. In addition to this, Cooper and Smith also observed that the crack propagation rate of the spot weld fatigue crack remains constant during the crack propagation process. Using the same electrical-potential drop method, however, Swellam and Lawrence found that there was a finite amount of fatigue life that was attributed to the crack initiation in 1992 [3].

Nevertheless, Sheppard and Strange argued that the early crack growth period is not described by linear elastic fracture mechanics method (LEFM), because according to Sheppard and Strange, LEFM typically breaks down when the crack is less than 5-10 times the grain size (the average size of a grain in HAZ was 20 μm). As a result, using the structural stress idea, Sheppard and Strange developed a specimen independent model in order to predict the fatigue life of a crack initiation and early crack growth to a crack length of 0.25 mm in resistance spot weld. Sheppard and Strange using Neuber's rule and cyclic Ramberg-Osgood materials law, in order to find the maximum local stress, σ_{max} [3];

$$\frac{\left(K_f \left|\max S_{ij_{peak}}\right| + \sigma_{rs}\right)^2}{E} = \sigma_{\max}\varepsilon_{\max} \tag{2.30}$$

$$\varepsilon_{\max} = \frac{\sigma_{\max}}{E} + 2\left(\frac{\sigma_{\max}}{2K'}\right)^{1/n'} \tag{2.31}$$

where;

$\max S_{ij_{peak}}$ = Maximum structural stress value at the peak load of a loading cycle,

σ_{max} = Maximum local stress,

ε_{max} = Maximum local strain,

K_f = Fatigue notch factor,

K' = Cyclic strength coefficient,

n' = Cyclic strain hardening exponent,

σ_{rs} = Residual stress.

Using these formulas, Sheppard and Strange estimated the fatigue life for a crack to initiate and grow to a length of 0.25 mm in HSLA spot weld joints. The equation was given as [3]

$$2N_i = \left(\frac{0.5\Delta\sigma_{\max}}{\sigma'_f - \sigma_m} \right)^{1/s} \tag{2.32}$$

where;

N_i = Fatigue life of crack initiation and early growth,

s = Fatigue strength exponent that must be determined experimentally,

σ_m = Stress amplitude ($\sigma_m = \sigma_{\max} - 0.5\Delta\sigma_{\max}$),

σ'_f = Material property that must be determined experimentally.

Here the most important point is that the early crack growth considered by Sheppard and Strange represents the crack growth to a length of approximately 0.25 mm.

In addition to this formula, that is the formula of fatigue life of crack initiation and early growth, Sheppard, in 1993, extended the early crack growth work and developed a model to use the structural stress to estimate fatigue life solely in terms of propagation. And the resulting formula was proposed by her as the following type [3];

$$N_p = A_2 \left(\Delta S_T + \Delta S_B \right)^{-s} \tag{2.33}$$

where;

$$A_2 = \frac{2 a_0^{(-s+2)/2}}{(s-1) C \pi^{s/2}},$$

C = Material constant as in Equation 2.9,

a_0 = Crack length at which initiation ends and crack propagation begins,

N_p = Total life spent propagation the crack through the sheet thickness, t,

ΔS_T = Nominal membrane stress range and is equal to the $\frac{\Delta P}{wt}$ term in Equation 2.29,

ΔS_B = The bending stress range and is equal to the $\frac{6\Delta M}{\beta t^2}$ term in Equation 2.29

Sheppard further refined the structural stress method for fatigue life prediction in order to include the stress ratio effect as the following type;

$$\frac{N_p}{1-R} = A_2 \left(\Delta S_{\max}\right)^{-s} \tag{2.34}$$

where;

A_2 = Material constant and is the same as defined in Equation 2.33,

$\Delta S_{\max}$ = The structural stress range that is defined as

$$\Delta S_{\max} = \max\left\{\Delta S_{11}, \Delta S_{12}, \Delta S_{21}, \Delta S_{22}\right\} \tag{2.35}$$

Finally, the total life, N_t, in Sheppard's work defines as the sum of the number of cycles for a crack to initiate, N_i, and grow through the sheet thickness, N_p.

Radaj's Structural Stress Method: In 1989, Radaj defined the meaning of structural stress term. According to him, there are three important parameters at the region around a spot weld nugget and these are structural stress, notch stress and stress intensity factor. Radaj explained these three terms as the following expressions [3].

- Structural stress is the stress linearly distributed over the sheet thickness with the singularity at the spot weld edge being completely suppressed.
- The notch stress is the stress at the slit edge of the spot weld with a fictitious radius of $\rho_f \approx 0.25$ mm. The slit is assumed to be an ideal slit (i.e. there is no gap between the two plates). The notch stress equals the product of the nominal structural stress and a stress concentration factor.
- The third important parameter according to Radaj is stress intensity factor. What is more is that the crack initiation and crack propagation at the weld spot edge are controlled not by the structural stress but by the stress intensity factor at the end of the slit.

Radaj showed that the stress intensity factors at the end of the slit of spot weld edge (not the crack in the through-thickness direction) are related to the structural stress by

$$K_I = 0.15(\sigma_{ti} - \sigma_{to} + \sigma_{bi} - \sigma_{bo})\sqrt{t} \tag{2.36}$$

$$K_{II} = 0.25(\sigma_{ti} - \sigma_{bi})\sqrt{t} \tag{2.37}$$

$$K_{III} = 0.71(\tau_{ti} - \tau_{bi})\sqrt{t} \tag{2.38}$$

where;

σ = Nominal structural stress (tensile stress),
τ = Nominal structural stress (shearing stress),
t = Thickness of the plate,
t = Subscript that means top plate,
b = Subscript that means bottom plate,
i = Subscript that means inner surface of the plate,
o = Subscript that means outer surface of the plate.

Radaj, in 1990 [3], gave expressions for structural stress in terms of "running-through" tensile force, F', and "running-through" bending moment, M_b'. F' and M_b' are the element forces at the spot weld nodal point of the considered plate. Hence;

- The structural stress for the case with "running-through" tensile force is:

$$\sigma_{ns} = 1.54\frac{F'}{wt} \tag{2.39}$$

where;

σ_{ns} = Nominal structural stress,
w = Width of the plate,
t = Thickness of the plate.

- The structural stress for the case with "running-through" bending moment is:

$$\sigma_{ns} = 9.244\frac{M'}{wt^2} \tag{2.40}$$

The "running through" tensile force, F', and "running through" bending moment, M_b', in Radaj's equations are equivalent to the membrane load at the edge of the nugget, P_{ij}, and bending moment, M_{ij}, in Sheppard's work (Figure 2.7).

In conclusion, the major differences between the Radaj's and Sheppard's approaches can be summarized as follows:

- Sheppard assumed that the crack is the through-thickness crack while Radaj assumed that the crack is the edge slit.
- Although the conceptual definitions of structural stress in these two different approaches are the same, the mathematical representations between the various loads are different, as shown in Equations 2.29 and 2.40 respectively.

Rupp's Structural Stress Method: In 1995, Rupp and Grubisic also proposed a structural stress formula that is similar to Equation 2.29. In Rupp's equations, an empirical stress correction factor, $K = 0.6\sqrt{t}$, is multiplied by the bending and tension terms. Hence, Rupp's structural stress equations are

$$\sigma_{r,\max} = \frac{F_{x,y}}{\pi D t_j} \tag{2.41}$$

$$\sigma_r = K\,1.744\frac{F_z}{t^2} \tag{2.42}$$

$$\sigma_{r,\max} = K1.872\frac{M_{x,y}}{Dt^2} \tag{2.43}$$

where;

t = Thickness of the sheet,

D = Diameter of the spot weld,

$F_{x,y}, F_z, M_{x,y}$ = Force and moment terms, as shown in Figure 2.9

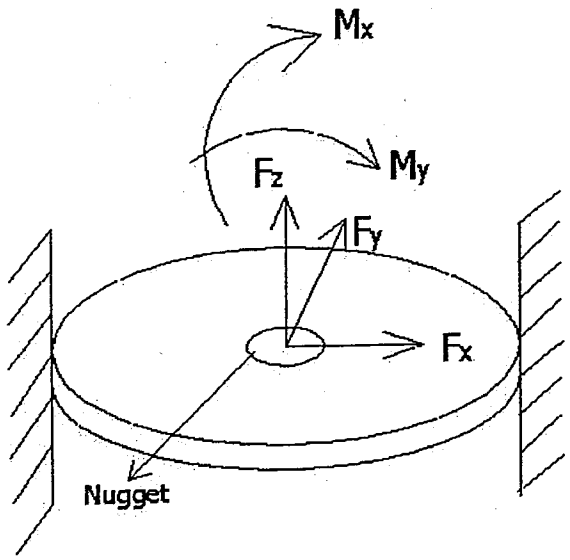

Figure 2.9. Force and moments for Rupp's formula [3]

Henrysson's Structural Stress Method: Henrysson and Akerson, in 1996, used Rupp's structure stress formula in order to predict the fatigue life of spot welds specifically for H-shape and tensile shear specimens. At the end of his studies, Henrysson showed that Rupp's equations need to be modified by a set of modification factors:

$$\sigma_{\max}(V_i) = \frac{V_i}{\pi D t_j} Factor_V \tag{2.44}$$

$$\sigma(F_z) = K_j 1.744 \frac{F_z}{t^2} Factor_F \tag{2.45}$$

$$\sigma(M_{ij}) = K_j 1.872 \frac{M_{ij}}{Dt^2} Factor_M \tag{2.46}$$

where;

$Factor_V, Factor_F, Factor_M$ = Correction factors,

t = Thickness of the sheet,

D = Diameter of the spot weld,

K_j = Empirical stress correction factor.

The correction factors $Factor_V$=2, $Factor_F$=0.5 and $Factor_M$=1 were obtained from fatigue tests. In addition to these values, the definition of V_i in Henrysson's work is the same as $F_{x,y}$ in Rupp's equation. Here, there is an interesting point that the stress results for the H-shape specimens and tensile shear specimens from equations 2.44, 2.45, and 2.46 that were proposed by Henrsson and Akerson are similar to those obtained by using Equation 2.29 that was proposed by Sheppard [3].

3. EXPERIMENTAL STUDY

3.1. Introduction

This section will describe the method used to perform the fatigue testing. This chapter will first give an overview of fatigue and then the current tests. The specimen designs, testing materials, testing fixtures and testing procedures will then be discussed in the later sections.

3.2. Fatigue

Until about the middle of the nineteenth century engineers treated fluctuating or repeated loading the same as static loading, except for the use of larger safety factors. Use of term "fatigue" in these situations appears to have been introduced by Poncelet of France in a book published in 1839. Modern authorities suggest that the term "progressive fracture" would perhaps have been more appropriate [41].

"Fatigue" fractures begin with a minute (usually microscopic) crack at a critical area of high local stress. This is almost always at a geometric stress raiser. Additionally, minute material flaws or preexisting cracks are commonly involved [41].

Machine members are often found to have failed under the action of repeated or fluctuating stresses, and yet the most careful analysis reveals that the actual maximum stresses were below the ultimate strength of the material and quite frequently even below the yield strength. [40]. If a specimen subjected to a cyclic load, a fatigue crack nucleus can be initiated on a microscopically small scale, followed by crack growth to a macroscopic size, and finally specimen failure in the last cycle of the fatigue life [42]. The most distinguishing characteristic of these failures has been that the stresses have been repeated a very large number of times. Hence, the failure is called a "fatigue failure" [40].

A fatigue failure begins with a small crack. The initial crack is so minute that it cannot be detected by the naked eye and is even quite difficult to locate in X-ray

inspection. The crack will develop at a point of discontinuity in the material, such as a change in cross section, a keyway, or a hole. Less obvious points at which fatigue failures are likely to begin are inspection or stamp marks, internal cracks, or even irregularities caused by machining. Once a crack has developed, the stress-concentration effect becomes greater and the crack progresses more rapidly. As the stress area decrease in size, the stress increases in magnitude until, finally, the remaining area fails suddenly. A fatigue failure, therefore, is characterized by two distinct areas of failure. The first of these is that due to the progressive development of the crack, while the second is due to the sudden fracture. The zone of the sudden fracture is very similar in appearance to the fracture of a brittle material, such as cast iron, which has failed in tension [40].

When machine parts fail statically, they usually develop a very large deflection, because the stress has exceeded the yield strength, and the part is replaced before fracture actually occurs. Thus, many static failures are visible ones and give warning in advance. But a fatigue failure gives no warning; it is sudden and total, and hence dangerous. It is a relatively simple matter to design against a static failure because, except for brittle materials, our knowledge is quite complete. But fatigue is a much more complicated phenomenon, only partially understood [40].

The fatigue life is usually split into a "crack initiation period" and a "crack growth period". The initiation period is supposed to include some microcrack growth, but the fatigue cracks are still too small to be visible by the unaided eye. In the second period, the crack is growing until complete failure. It is technically significant to consider the crack initiation and crack growth periods separately because several practical conditions have a large influence on the crack initiation period, but a limited influence or no influence at all on the crack growth period [42].

Microscopic investigations in the beginning of the twentieth century have shown that fatigue crack nuclei starts as invisible cracks in slip bands. After more microscopic information on the growth of small cracks became available, it turned out that nucleation of microcracks generally occurs very early in the fatigue life. Indications have been obtained that it may take place almost immediately if a cyclic stress above the fatigue limit is applied (the fatigue limit is the cyclic stress level below which a fatigue failure does not

occur). In spite of early crack nucleation, microcracks remain invisible for a considerable part of the total fatigue life. Once cracks become visible, the remaining fatigue life of a laboratory specimen is usually small percentage of the total life. The latter percentage may be much larger for real structures such as ships, aircrafts, automobiles, etc [42].

After a microcrack has been nucleated, crack growth can still be a slow and erratic process, due to effects of the micro structure, e.g. grain boundaries. However, after some microcrack growth has occurred away from the nucleation site, a more regular growth is observed. This is the beginning of the real crack growth period. Various steps in the fatigue life are indicated in Figure 3.1. The important point is that the fatigue life until failure consists of two periods: the crack initiation period and the crack growth period. Differentiating between the two periods is of great importance because some conditions (e.g. surface conditions, surface roughness, corrosive environment, etc.) do affect the initiation period and the crack growth period, but in different way for the two periods. For example, several surface conditions do effect the initiation period, but have a negligible influence on the crack growth period. It were already noted that fatigue prediction methods different for the two periods. The stress concentration factor K_t is the important parameter for predictions on crack initiation. The stress intensity factor K is used for predictions on crack growth [42].

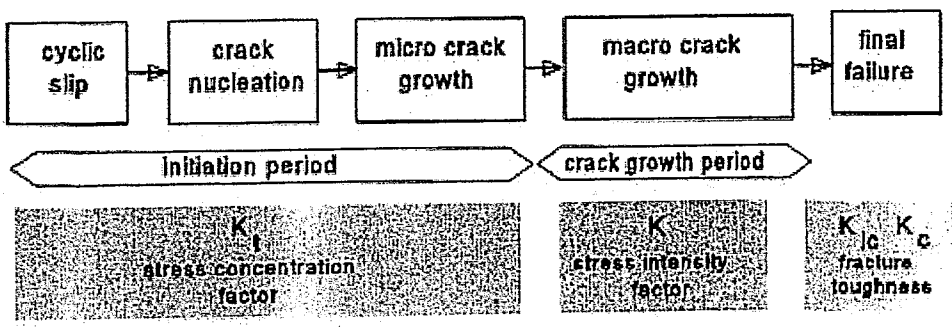

Figure 3.1. Different phases of the fatigue life and relevant factors [42]

Fatigue crack initiation and crack growth are consequence of cyclic slip in slip bands. It implies cyclic plastic deformation as a result of moving dislocations. Fatigue occurs at stress amplitudes below the yield stress. At such a low stress level, plastic deformation is limited to a small number of grains of the material. This micro-plasticity

can occur more easily in grains at the material surface because the surrounding material is present at one side only. The other side is the environment, usually a gaseous environment (e.g. air) or a liquid (e.g. sea water). As a consequence, plastic deformation in surface grains is less constraint than in surface grains; so it can occur at a lower stress level [42].

Because of an inhomogeneous stress distribution, a peak stress occurs at the surface (stress concentration). Furthermore, surface roughness also promotes crack initiation at the material surface. Other surface conditions with a similar effect are corrosion pits and fretting fatigue damage both occurring at the material surface. Hence, the most important conclusion for the crack initiation period, fatigue is a material surface phenomenon [42].

As long as the size of the microcrack is still in the order of a single grain, the microcrack is obviously present in an elastically anisotropic material with a crystalline structure and a number of different slip systems. The microcrack contributes to an inhomogeneous stress distribution on a micro level, with a stress concentration at the tip of the microcrack. As a result, more than one slip system may be activated. Moreover, if the crack is growing into the material in some adjacent grains, the constraint on slip displacements will increase due to the presence of the neighboring grains. Similarly, it will become increasingly difficult to accommodate the slip displacements by a single slip system only, e.g. on parallel crystallographic planes. It should occur on slip planes in difficult direction. In general, there is a tendency to grow perpendicular to the loading direction. Because the crack front must remain a coherent crack front, the crack can not grow in each grain in an arbitrary direction and at any growth rate independent of crack growth in the adjacent grains. This continuity prevents large gradients of the crack growth rate along the crack front. The crack front can be approximated by a continuous line, which could have a semi-elliptical shape. How fast the crack will grow depends on the crack growth resistance of the material. Two important surface aspects are no longer relevant. The lower restraint on cyclic slip at the surface is not applicable at the interior of the material. Secondly, surface roughness and other surface conditions do not affect crack growth. This leads to the second important conclusion, that is, crack growth resistance, when the crack penetrates into the material, depends on the material as a bulk property. It is no longer a surface phenomenon. As a result, the initiation period is supposed to be

completed when micro-crack growth is no longer depending on the free surface conditions [42].

At the end of these explanations, it is possible to show all these mentioned effects as conclusion in Figure 3.2 as the follows,

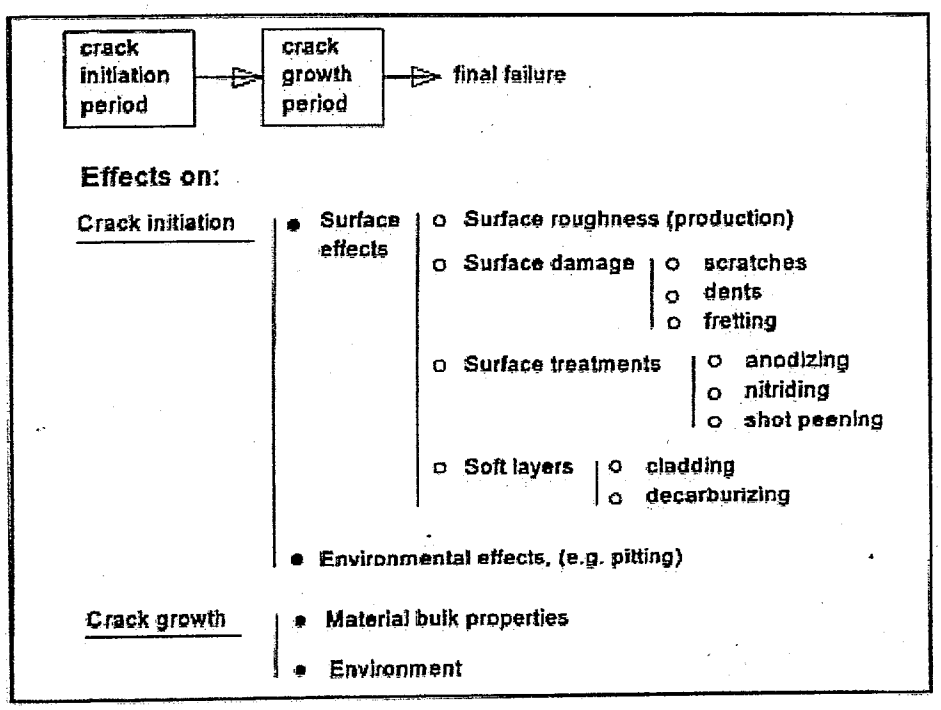

Figure 3.2. Effects on the crack initiation and crack growth period

3.3. Fatigue Testing

In order to determine the strength of materials and components, that planned to use in mechanical devices, under the action of fatigue loads, specimens are subjected to repeated or varying forces of specified magnitudes while the cycles or stress reversals are counted to destruction The most widely used fatigue-testing device for determining the strength of materials is high-speed rotating beam machine. This machine subjects the specimen to pure bending (no transverse shear) by means of weights. The specimen is very carefully machined and polished, with a final polishing in an axial direction to avoid circumferential scratches. In addition, other fatigue-testing machines are available for applying fluctuating or reversed axial stresses, torsional stresses, or combined stresses to the test specimens [40].

To establish the fatigue strength of a material, quite a number of tests are necessary because of the statistical nature of fatigue. In addition, it is always good engineering to conduct a testing program on the materials to be employed in design, and this is especially true in designing against the possibility of a fatigue failure. Since testing is not always feasible, methods of estimating the endurance limit or fatigue strength directly from published tensile properties are desirable [40].

A cyclic fatigue load in this study is assumed to be associated with so called constant amplitude loading which implies that the amplitude and the mean value of the load are both constant. In general, the load amplitude (or the stress amplitude) is considered to be characteristic for the cyclic load [42].

The current fatigue testing was performed on 812 22 kip (100 kN) model MTS (Material Testing System) testing machine that has closed loop servo-hydraulic testing system as shown in Figure 3.3.

Figure 3.3. Testing machine

The specimens were mounted in the grips 30 mm from both ends. All of the specimens were made by Mercedes-Benz Türk A.Ş. to be as close to identical as possible. Tensile tests were used in order to determine the fatigue lives cycles of modified tensile shear specimens as shown in Figures 3.4. and 3.5. In these experimental studies, an R-ratio of changing between 0.050 and 0.075 for both "Manual Spot" and "Nipper Spot" were used.

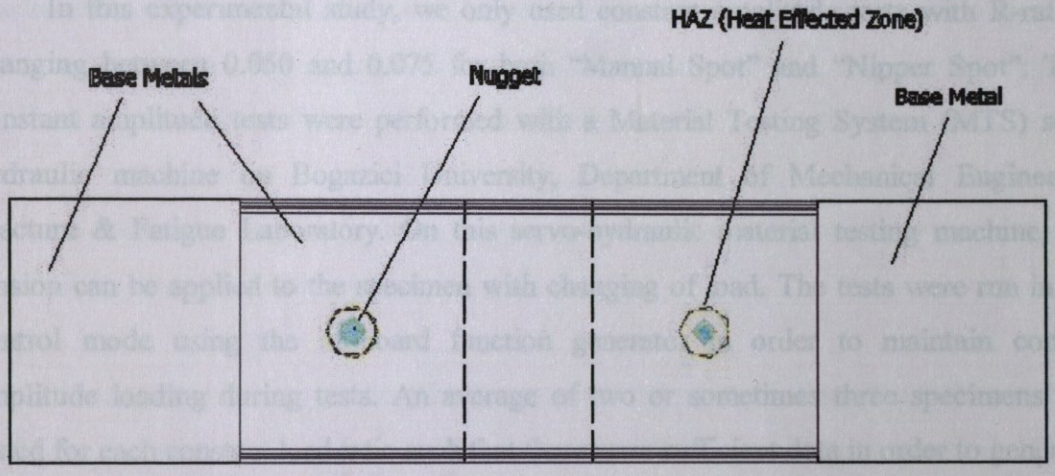

Figure 3.4. Technical drawing of MTS (modified tensile shear specimen)

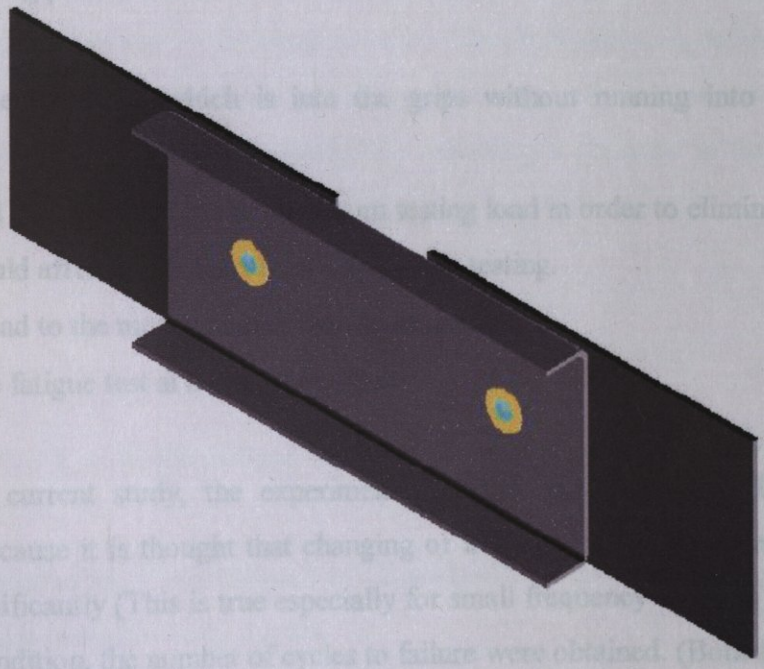

Figure 3.5. Three-dimensional appearance of MTS (modified tensile shear specimen)

One important goal of the current study is to further validate the using experimental studies with additional fatigue tests.

The fatigue tests in this current study were targeted to fatigue lives range from 10.000 to 100.000 cycles for "Manual Spot" and 15.000 to 300.000 cycles for "Nipper Spot".

In this experimental study, we only used constant amplitude tests with R-ratio of changing between 0.050 and 0.075 for both "Manual Spot" and "Nipper Spot". These constant amplitude tests were performed with a Material Testing System (MTS) servo-hydraulic machine on Bogazici University, Department of Mechanical Engineering, Fracture & Fatigue Laboratory. On this servo-hydraulic material testing machine, pure tension can be applied to the specimen with changing of load. The tests were run in load control mode using the on-board function generator in order to maintain constant amplitude loading during tests. An average of two or sometimes three specimens were tested for each constant load ratio such that there were sufficient data in order to generate a load versus life curve.

The testing procedures are:

- Load the specimen which is into the grips without running into any extraneous loading.
- Pre-load the specimen to the maximum testing load in order to eliminate any yielding that would affect load control stability during testing.
- Bring load to the mean value of the testing load.
- Start the fatigue test at a small amplitude.

In this current study, the experimental studies were not done for changing of frequency, because it is thought that changing of frequency does not effect the results of the study significantly (This is true especially for small frequency changes) As a result, for every load condition, the number of cycles to failure were obtained. (Both for initiation and

propagation point were considered and the cycles for these two points are obtained separately.).

Generally for a loading condition, we can accept that "failure" could mean total separation of the specimen parts, or it could the inability of the specimen to handle the applied load. But for this system, that is axially loading condition of spot-welded specimen, we were not assume failure neither total separation of the specimen parts nor the inability of the specimen to handle the applied load. Instead of these two types failure mechanisms we assumed that "failure" means any noticeable separation on the specimen. After any separation, we accepted that the so called specimen deformed and was not carry any load any more even if it could carry the applied load for some additional time.

All tests were performed using a sinusoidal wave form that was operating primarily at 1 or 2 Hz. in air at room temperature.

Testing of specimen was terminated when we detected a failure. The failure criterion in this study, as it was mentioned previously, was defined as the appearance of a fatigue crack of the surface of any sheet near the spot weld. In order to aid in the visual detection of a crack, a small amount of machine oil was deposited as much as possible between the specimen sheets before testing. When the crack grew through the sheet, it allowed the oil to seep through and appear on the outer surface of the sheet signaling failure. In addition to the oil technique, another indication of fatigue crack growth is apparent. The maximum deflection increases quickly as specimen fails indicating a decrease in the stiffness of the specimen.

3.4. Test Specimen

3.4.1. Modified Tensile Shear Specimen (MTS) Material

In this current study, we choused St 12 steel material because this kind of material is widely used in automotive body frames.

The St 12 steel used in this current study was received from Mercedes-Benz Türk A.Ş. The steel that received with a thickness of 1.00 mm was used for the MTS specimen. The chemistries for the St 12 in Table 3.1 were provided by Mercedes-Benz Türk A.Ş. In addition, tensile tests of the St 12 material used in this study were performed at again in Mercedes-Benz Türk A.Ş. The tensile test coupons were taken along the steel rolling direction. Table 3.2 lists the test results.

Table 3.1. Chemistries of St 12 steel material

Chemical material	% weight
C	0.003
Mn	0.21
P	0.08
S	0.008
Si	0.01
Al	0.06

Table 3.2. Tensile test results of St 12 steel material

Number of test done to determine strength characteristics of St 12	5
Average tensile strength of St-12 (MPa)	445
Average yield strength of St 12 (MPa)	329
Average % Elongation (50 mm)	37.5

3.4.2. Specimen Details

This section presents the design and fabrication procedures for the specimen, that is MTS (Modified Tensile Shear Specimen) specimen, used in this current study.

Before dealing the design and fabrication procedures of the so called MTS specimen, firstly it can be helpful if we explain why we choused MTS type specimen in this current study.

We choosed St 12 steel type modified tensile shear (MTS) specimen (Figures 3.4, 3.5, 3.6.) for this study. The reasons this specimen was selected are

- The specimen design is simple and therefore easy to fabricate.
- Modified tensile shear (MTS) type specimens are the most commonly used specimen designs for spot welds tests.
- In addition two important reasons, the third one is that the Tensile Shear (TS) type specimens cannot sustain high compressive loads (e.g. test with a load ratio of R= -1.0) because of possible buckling, hence in this current experimental studies, a new tensile shear type design, the modified tensile shear (MTS), was used instead of tensile shear (TS) type design.

Dimension of MTS Specimen: The MTS specimen design is given in Figure 3.5 detailed. The specimen width is designed to be 40.00 mm. in order to fit the grip size of the existing test fixtures. (This width is smaller than the "saturation width", a value beyond which an increase of the specimen width will not affect the fatigue life of the spot welds.) The quadrilateral shape flange is designed in order to improve the buckling resistance. (As it was mentioned before, the quadrilateral shape flange is the main difference between modified tensile shear specimen (MTS) and tensile shear specimen (TS). In addition, because of quadrilateral shape flange, MTS is more resistance to buckling than TS). The specimen thickness is designated as 1.00 mm. The shaded portions of the specimen (Figure 3.5) are clamped in testing fixture during the test.

Specimen Fabrication: All pre-assemblies of MTS test specimen was prepared at Mercedes-Benz Türk A.Ş. The specimens were welded (Two types weld techniques were used in the MTS specimens' weld processes. These are "Manual Spot" and "Nipper Spot") again at Mercedes-Benz Türk A.Ş. in Istanbul, Turkey.

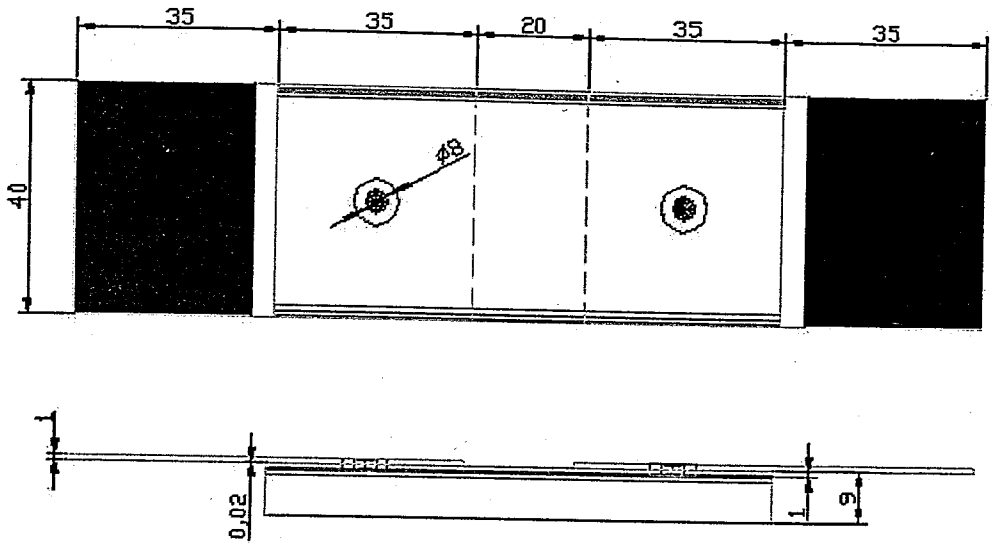

Figure 3.6. Geometry of modified tensile shear (MTS) specimen (top and side view)

The MTS specimens consist of three pieces. These are two end pieces and one centerpiece. The end pieces were attached to the centerpiece through two spot welds, as shown Figures 3.4, 3.5 and 3.6. The pre-assemblies of all three pieces were sheared from steel sheets. These blanks were cut in a way that the loading direction of the final specimen was parallel to the steel rolling direction.

Fabrication of Modified Tensile Shear (MTS) specimen involved three primary steps:

- The steel was cut using jump shear in Mercedes-Benz Türk A.Ş. During shearing the length of the cut piece was controlled by a manual stop adjusted for each length.
- Once the pieces were cut to size, the centerpieces were stamped with a set of V-shape dies through a manual press in order to form the two 90 degree angles of quadrilateral shape flanges.
- After the three pieces were machined, they were prepared for welding process. Each one of the three pieces was rinsed in methyl alcohol and then dried in order to remove the oil coating, because the oil coating causes negative effects (e.g. it causes not a good connection between the sheets) in spot-weld, that is nugget. A jig was attached to the welder to allow for convenient a consistent assembly. The separate steel strips then were aligned with dowel pins which are set into the weld fixture.

These pins aligned the strips so that each weld was in the center of the intended weld area. Once the free pieces were aligned, they finally were spot-welded.

The spot-weld nugget diameter is designed to be 8.00 mm. A reference welding schedule is given in Table 3.3. In this table; it must be noted that the welding parameters were the same for manual and nipper spots except apparatus that were used weld operations. Reel tests on steel strips were performed prior to the production of real specimens in order to tune the welding parameters and hence to give the desired nugget diameter. Several peel tests were also performed during specimen fabrication in order to ensure that the weld nugget size did not change due to tip wear.

Extra specimens were produced. This allowed us to choose the specimens that best fit specifications, and to replace specimens when testing errors such as accidental specimen overload occurred. Through the fabrication process, each specimen was measured in order to ensure that the critical dimensions conformed to the drawings.

Table 3.3. Average welding parameters for St 12 steel

Spot weld type	Manual Spot	Nipper Spot
Electrode force (kp)	-	150
Welding current (Amps)	14	10
Weld time (Cycles @ 60-80 Hz)	7.5	8.5
Electrode Diameter (mm)	4.45	4.45

3.4.3. Test Fixture

In general, R-ratio and variable amplitude tests require special test fixtures in order to ensure that the specimens can be loaded in both tension and compression. Therefore, the design of MTS specimen test fixture is more sophisticated.

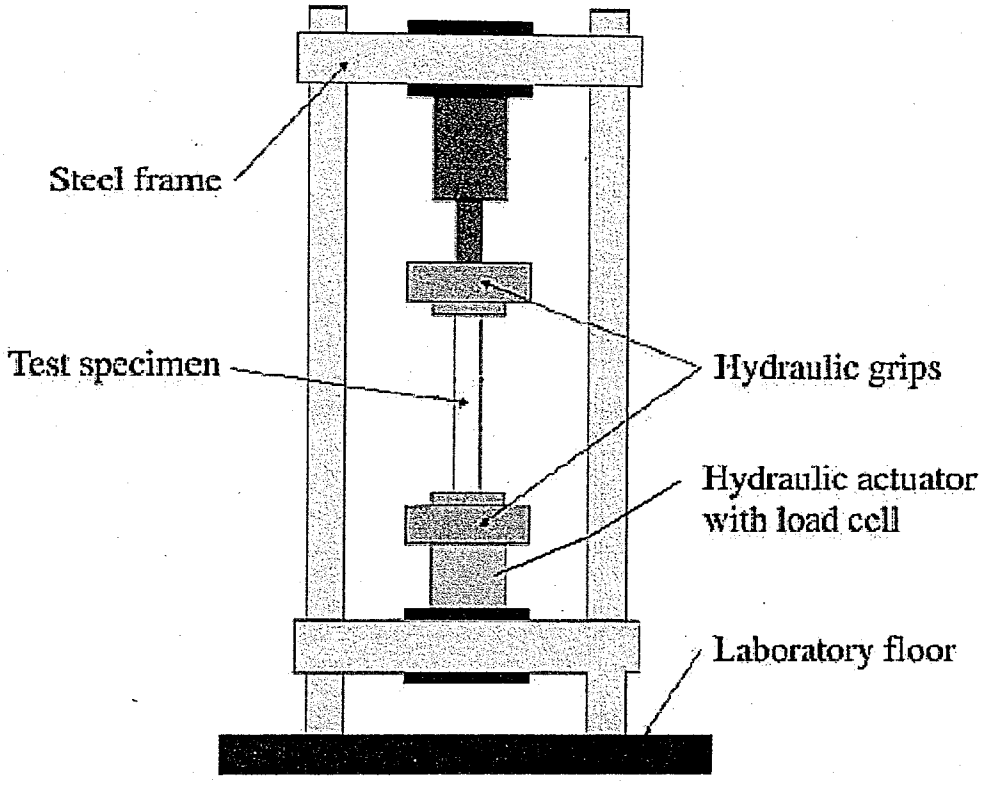

Figure 3.7. Test fixture for MTS specimen

The test fixture for MTS is shown in Figure 3.7. Both ends of the specimens are clamped in the fixture.

4. EXPERIMENTAL RESULTS

4.1. Introduction

This chapter presents the results of constant amplitude fatigue tests of modified tensile shear specimen, as outlined in Chapter 3. In all tests presented here, failure is defined as the state when a crack initiates and propagates through the thickness of the sheet. Specimen fabrication, testing procedures, and failure detection method have been discussed in Chapter 3.

MTS specimens of St-12 steel were tested with an R-ratio of essentially zero (0.050 and 0.075) for both "Manual Spot" and "Nipper Spot".

4.2. Failure Mode of MTS Specimens

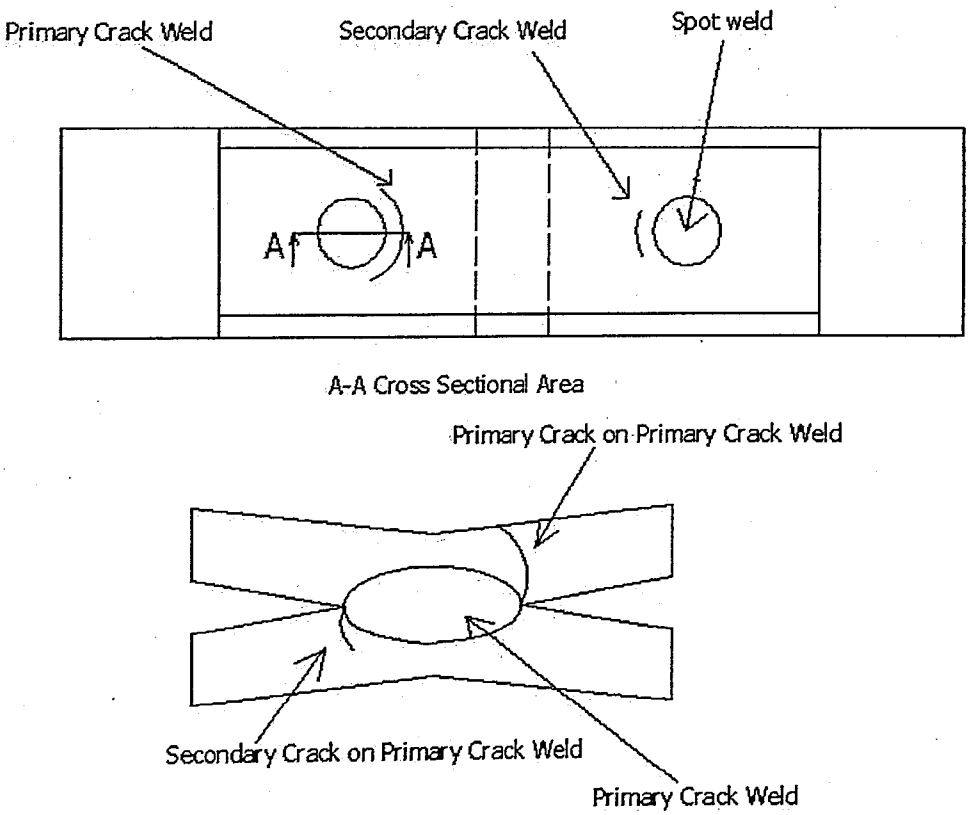

Figure 4.1. Typical failure mode for MTS specimens

MTS specimens of St-12 steel for "Manual Spot" and "Nipper Spot" exhibit the same failure mode, but in different life spans because of different spot types. The typical failure mode for MTS specimens of both "Manual Spot" and "Nipper Spot" is shown in Figure 4.1. The first crack that propagates through the thickness of the sheet is defined as the primary crack and the corresponding weld is defined as the primary weld [3]. Primary cracks were always seen on the flanged pieces of the MTS specimens in these experimental studies. The crack on the opposite side of the primary weld, again on the flanged piece, is identified as the secondary crack on the primary weld as shown in Figures 4.1 and 4.2. The other weld is called the secondary weld, which also has its own primary and secondary cracks. It is not uncommon to see that the primary crack on the primary weld has similar size to the primary crack on the secondary weld. However the secondary crack on a weld is generally smaller than the primary crack on the same weld.

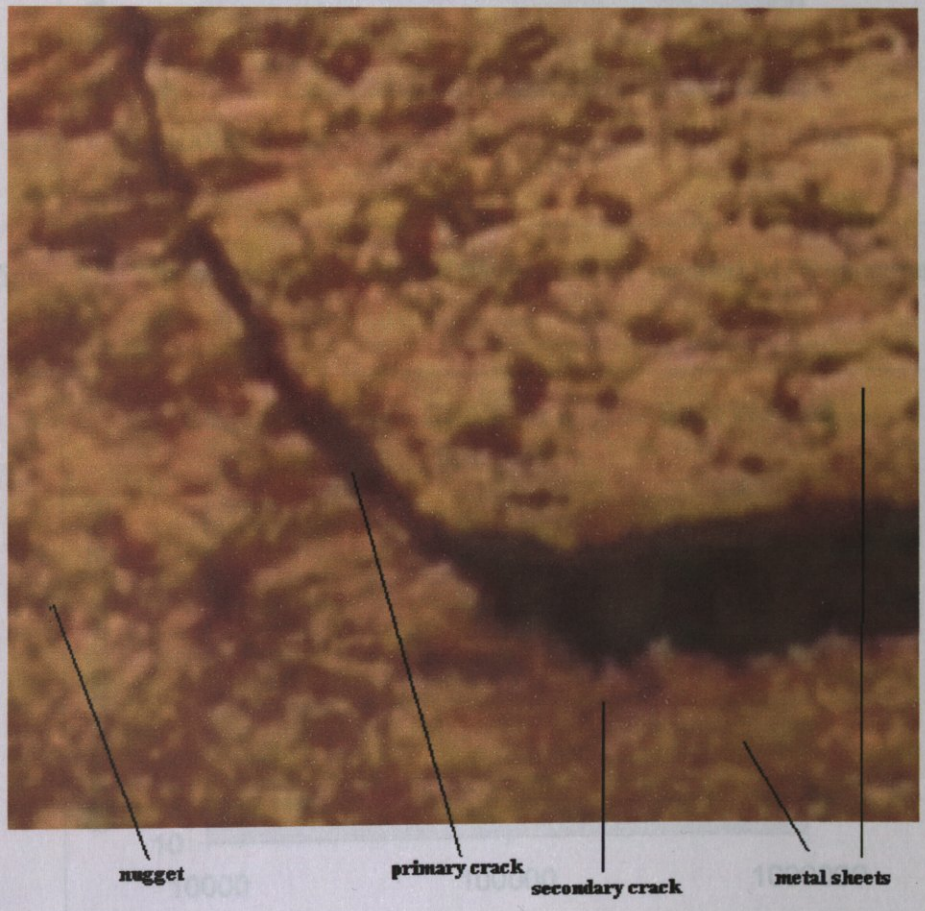

Figure 4.2. Fatigue crack of MTS specimens

4.3. Load versus Life Results

The fatigue life data of the MTS specimens under constant amplitude loading conditions are given in Figures 4.3, 4.4, and 4.5. These figures show the stress vs. life data under R-ratios of changing between 0.050 and 0.075 for both "Manual Spot" and "Nipper Spot" of St-12 steel.

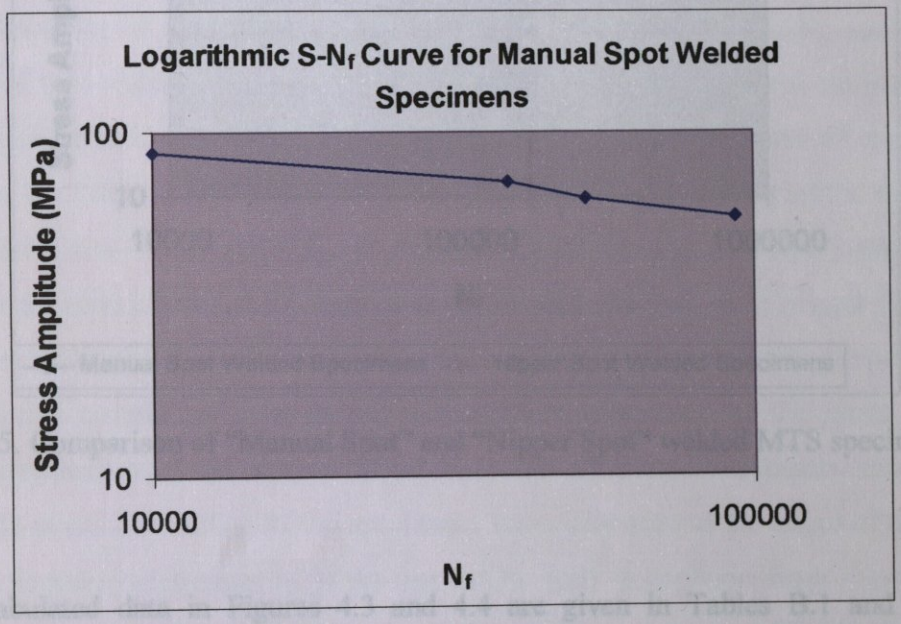

Figure 4.3. The stress vs. life data for "Manual Spot" welded MTS specimen

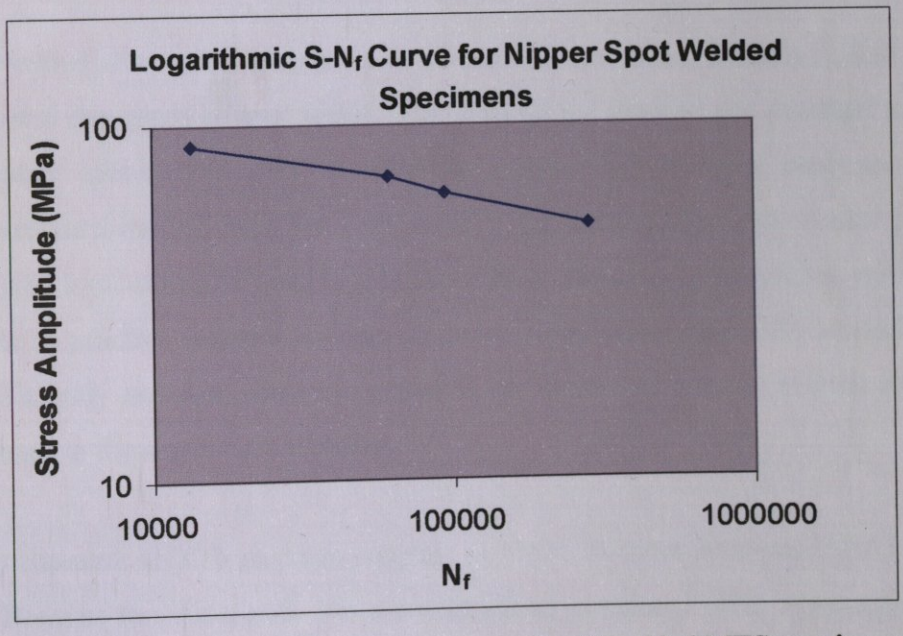

Figure 4.4. The stress vs. life data for "Nipper Spot" welded MTS specimen

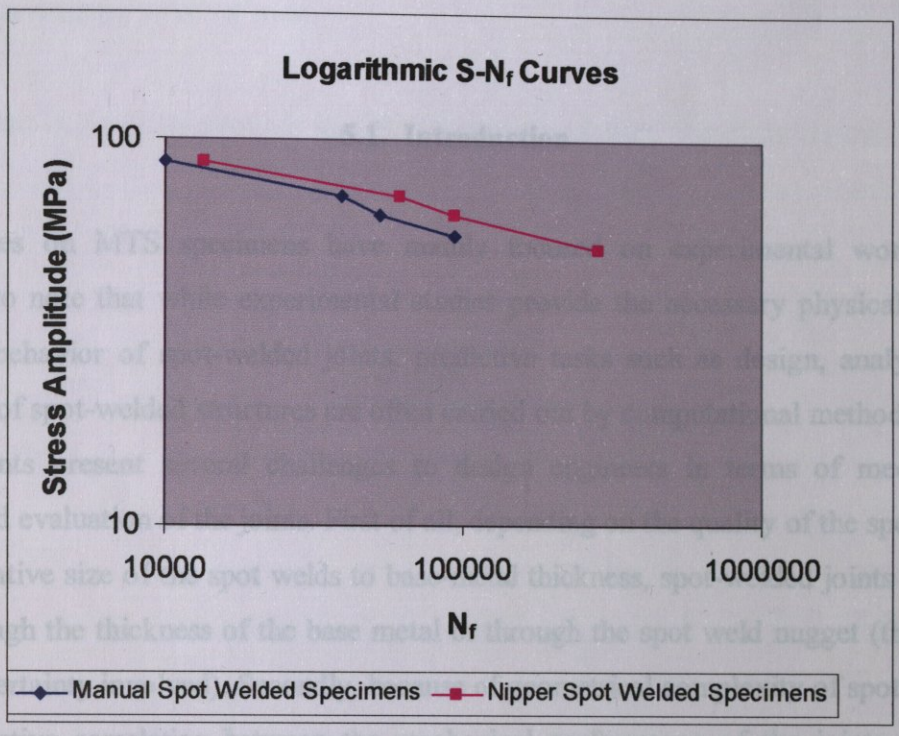

Figure 4.5. Comparison of "Manual Spot" and "Nipper Spot" welded MTS specimens

The tabulated data in Figures 4.3 and 4.4 are given in Tables B.1 and B.2 in Appendix B.

5. FINITE ELEMENT RESULTS

5.1. Introduction

Studies on MTS specimens have mainly focused on experimental work. It is important to note that while experimental studies provide the necessary physical insight about the behavior of spot-welded joints, predictive tasks such as design, analysis and evaluation of spot-welded structures are often carried out by computational methods. Spot-welded joints present several challenges to design engineers in terms of mechanical analysis and evaluation of the joints. First of all, depending on the quality of the spot welds and the relative size of the spot welds to base-metal thickness, spot-welded joints can fail either through the thickness of the base metal or through the spot weld nugget (there is a certain uncertainty involved). Secondly, because of geometrical complexity of spot welded joints, effective correlation between the mechanical performance of the joints and the stress and deformation fields around the joints is difficult from experimental results. For example, the stress distribution in the specimens, especially around the edges of the joints and hence fracture mechanism of joints can not be fully understood from experimental results. Hence numerical methods have advantages over experimental methods in terms of especially stress distribution and fracture mechanism of specimen.

Spot-welded joints are widely used in automobile structures. Since a typical vehicle contains several thousands of spot welds, it is often (if not always) not practical to model each and every spot-welded joint in detail in a full-scale structural analysis. Hence, simplified structural models have been proposed in the literature for spot welded joints in large-scale structural computations [43]. In order to be adequate, a simplified joint model must be able to produce relevant loading, stress or deformation quantities around a joint that are sufficiently accurate when compared to the results of a more refined model or when compared to the experimental studies.

It was choosed ANSYS package program as Finite Element Analysis (FEA) tool for this study. Because this FEA code has a strong solver compared with other commercial FEA software. In other words, ANSYS is one of the most suitable software in order to

model the specimen and do analysis in this study. As a result, actually, finite element analysis was done by ANSYS code.

In general, a typical analysis in ANSYS consists of three phases as shown in Figure 5.1.

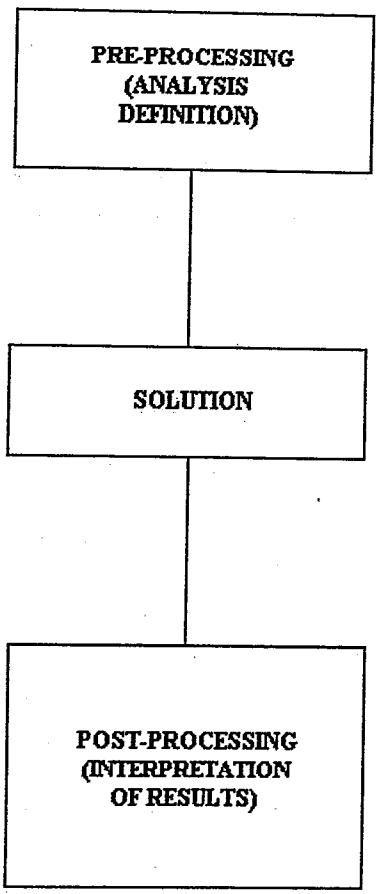

Figure 5.1. Steps of a typical analysis in ANSYS

Input data is prepared in the analysis phase. In this study, data included the following things;

- Model Description;
  - geometry,
  - selections from the element library,

- geometric real constants describing properties of elements (i.e., area, depth, volume, etc.)
- material properties

- Boundary Conditions;
  - constraints,
  - loads-forces, pressures
- Analysis Types and Options;

The analysis is performed in the solution phase.

Solution results are evaluated in the third phase, that is "interpretation of results". Hence using results, we can determine if the objective of the analysis was met. Tools in order to use in making this decision in this study included:

- Graphics
  - deformed or distorted shape plots,
  - contour maps,
  - graphs of one variable vs. another
- Scans of Results
- Combination of Results

5.2. Model Description

The spot-welded joint is composed of the nugget and base metal as shown in Figures 3.4 and 3.5. The material properties, which again obtained from Mercedes-Benz Türk A.Ş., are listed as shown in Table 5.1.

Table 5.1. Material properties

	Base Material	Nugget
Young's Modulus (MPa)	1.9E5	2.0E5
Poisson's Ratio	0.25	0.20

The geometric dimensions of the MTS specimen are shown in Figure 3.6 as being the following data;

- The two end pieces of MTS specimen are 70 mm in length, 40 mm in width and 1 mm in thickness.
- The center piece of MTS specimen 90 mm in length, again 40 mm in width and 1 mm in thickness but at the same time has two flanges which are 9 mm in height and 1 mm in thickness.
- The diameter of the two nuggets is 8 mm.
- The two end pieces and center piece of MTS specimen were connected with the spot weld so as to the overlap length of the two pieces is 35 mm.
- The space between the overlap portions of pieces was assumed as 0.02 mm because in previous studies, generally this value has been choosed as 0.02 mm.

In normal conditions, only half of the specimen could be modeled in order to make most use of its symmetry, but this thought is valid especially for linear static analysis. For dynamic analysis and nonlinear static analysis (in this study, due to the contact elements that were situated between the overlap portions of specimens in order to overcome the penetration in the overlap portions, nonlinearity was present) etc., it is not reasonable to apply symmetry conditions arbitrarily, including both geometry symmetry wherever possible to decrease model size and loading symmetry. Because if it is tried to use symmetry conditions in nonlinear analysis or dynamic analysis, some modes might be missing and it could not be predicted what mode might be missed due to the application of symmetry conditions. However, if it is thought that superficial results are enough for a study, then it can be applied symmetry boundary conditions in nonlinear analysis as static analysis. In addition, in this study, the specimen model was not huge at all, hence its elements number and node number etc. was pretty small compared with the general finite element model. So model size and computer time for analysis were not problem in this study.

In conclusion, it can be said that it was used full shape (not symmetric model) of the MTS specimen in numerical analysis, that is in ANSYS package program, for accuracy of

the obtained results via the ANSYS package program and for the most detailed practical model.

Solid 45 was adopted as the element type in order to mesh the parts (two end pieces and one centerpiece) of the MTS specimen in this study. When the model of spot or nugget was obtained, volume sweep meshing technique was used in order to create regular element pattern in the spot areas.

In addition, the specimen materials were assumed to be homogeneous, isotropic and linearly elastic; large deformation and nugget indentation were not considered. Detailed three-dimensional stress variations within and around spot welds were obtained using the ANSYS finite element code for MTS specimen. These stress variations can be used to provide a rationale for observed failures that were seen in experimental studies. It can be also examined how the stress fields in the two joined base-metal sheets in MTS specimen vary relative to each other when the two sheets (that is the end pieces and centerpiece) have different configurations, that is different shapes, especially from TS specimen. In other words, the flanges' effects could be analyzed easily looking the finite element results that were obtained via the ANSYS finite element code.

Several finite element models have been proposed in the literature for spot-welded joints. In general, according to Xu and Deng [43], there are four types of spot-welded models which are single-bar model, spoke-bar model, multiple rigid-bar model and solid nugget model as shown in Figure 5.2.

According to Xu and Deng [43], the rigid bar model is usually used in optimization analyses and other spot weld models are mostly used in fatigue and fracture failure analysis, hence in this study solid nugget model was choosed as the description of the spot-weld of MTS specimens.

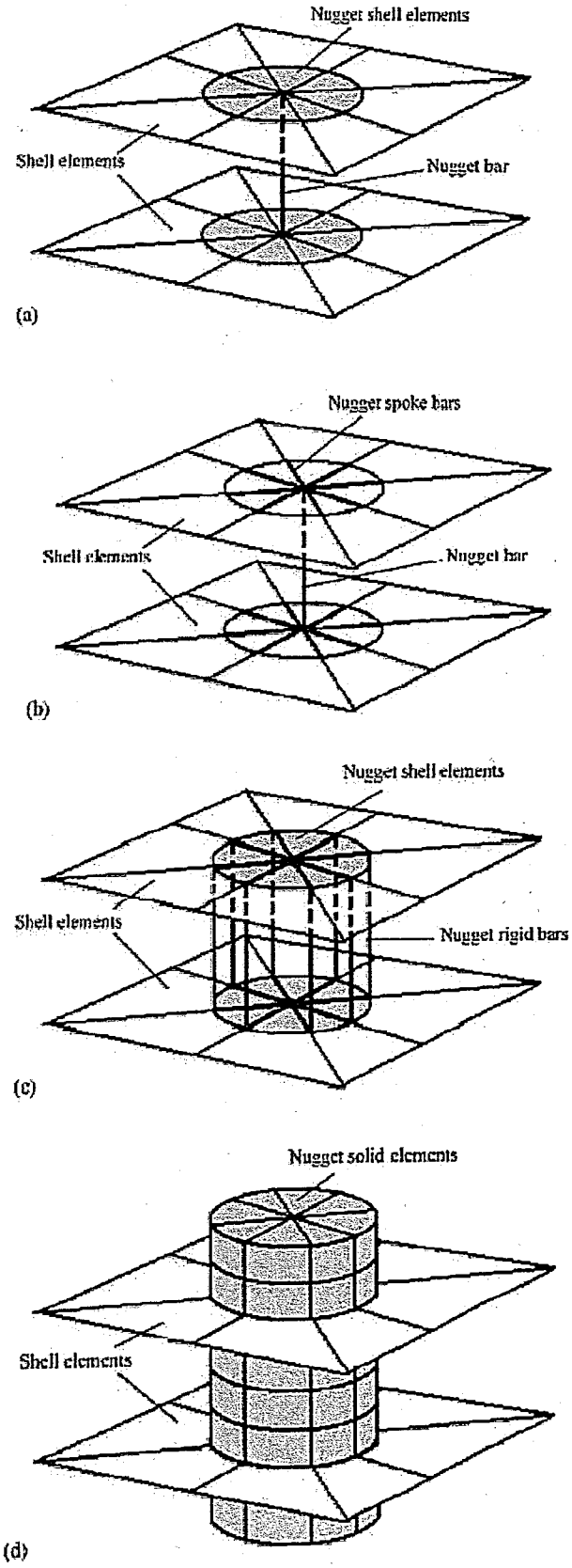

Figure 5.2. A schematic description of four types of spot-weld models: (a) single-bar model, (b) spoke-bar model, (c) multiple rigid-bar model, and (d) solid nugget model [43].

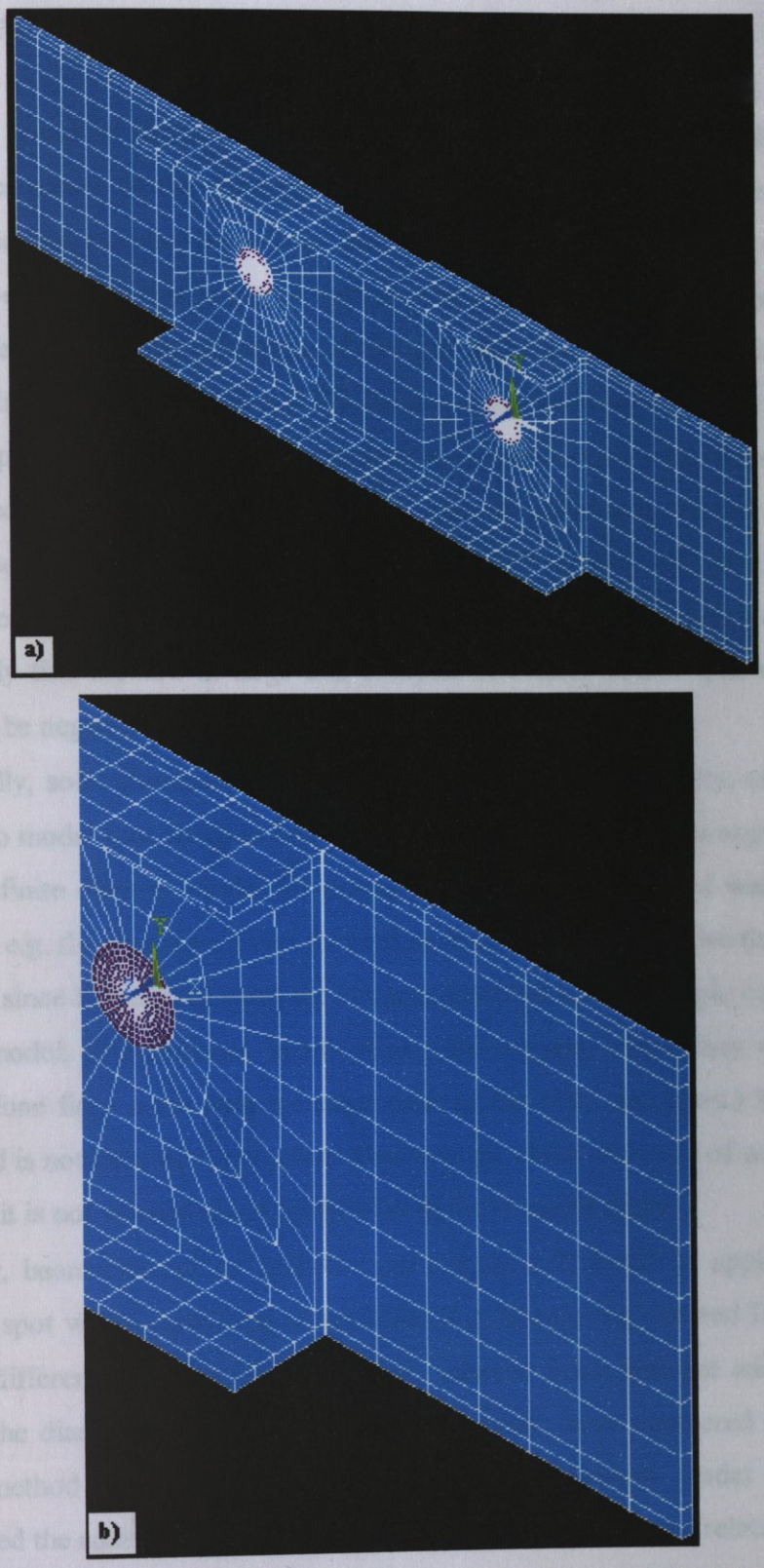

Figure 5.3. Finite element mesh of MTS specimen; a) Full shape of MTS specimen, b) Focused shape on right spot of MTS specimen

On the other hand, there are usually three ways in order to model spot weld in Finite element analysis using ANSYS package program.

- First it could be merged the nodes where the spot welds were applied after whole volumes pieces of the specimen, that is two end pieces and one centerpiece, were obtained and modeled separately. But this method could not capture weld properties well. Because the whole pieces were modeled using same material properties, but in real life, the material properties of the spot and base metal are different from each other. In addition, again in real life there is a gap between the overlap pieces of the MTS specimen and if it had been merged to obtain the spot weld areas after modeling the pieces of the specimen separately, this so called gap would not have been obtained at all. Hence, this method was not logical to use in this type specimens that spot welds are play important roles in working conditions. In other words, it is better to apply this method in large and complex structures where spot welds' role can almost be neglected.
- Secondly, solid elements, such as Solid 45 as being in this study, could be used in order to model spot welds as being the base metal. Of course, this approach leads to a heavy finite element model for practical structures with lots of welds. But simple model, e.g. the specimen it was focused on in this study, it provides the most accurate results since it is easy to catch the stress concentration, for example on the nugget, by solid model. (Furthermore, in this study, the nuggets, where they were interested, were done finer mesh than the other parts of the MTS specimen.) Meanwhile, this method is not choosed on practical structures on which hundreds of welds are applied unless it is not worried about application of the so called study.
- Finally, beam element or rigid element (Figure 5.2) could be applied in order to model spot welds. According to scientists, e.g. Shengyong, Xu and Deng [43], there is no difference or very little difference between beam element and rigid element since the diameter of spot welds are usually pretty large compared with its length. This method is most common in practical finite element model because it has balanced the accuracy and model size. It is noted that the kinetic relations at two ends of weld from this method is different for that obtained from first two methods.

Using the above explanations, the finite element meshes of MTS specimen were created as shown in Figure 5.3. (The dimensions of the specimen were given in Figure 3.6.) The total number of elements is 9328 and the total number of nodes is 9387 in the MTS model in Figure 5.3.

The specimen sheets were not divided into layers in the thickness direction, but small elements were used within and around the spot-weld nugget because the most critical parts of the MTS specimens under finite element analysis are spot-welded portions and because it was aimed to obtain exact results. In addition, because of the three-dimensional nature of the stress state in the spot-weld nugget and because of the anticipated stress concentration or singularity at the nugget boundary on the faying surface of the plates, small finite elements were used within and around the nugget and larger elements were used in the outer regions of MTS specimens. In other words, finer meshes are introduced near to the edges of the lap joints and also the spot weld, the minimum dimension in the meshes being 0.0005 mm. A gap of 0.02 mm was assumed in the spot-welded specimen in the lap zones, with exception of the spot-weld zone, so that no mesh is needed here in the spot-welded specimen.

5.3. Boundary Conditions

In Figure 5.4, a modified tensile-shear specimen is shown, where the cylindrical regions denote the spot-weld nugget and the flanged parts of MTS were used to align the tensile loads and to minimize nugget rotation.

The coordinate axes, which are shown in Figures 5.3 and 5.4, are for a right-hand system, with the "z" axis pointing outwards and the origin sitting at the center of one weld nugget.

As it was mentioned previously, because of simplicity of MTS specimen and also accuracy of the results that was obtained using ANSYS package program, it was not used boundary symmetry conditions for 3-D finite element model of MTS specimen in terms of both geometric symmetry and loading conditions. Figure 5.4 shows the boundary conditions of the MTS finite element model.

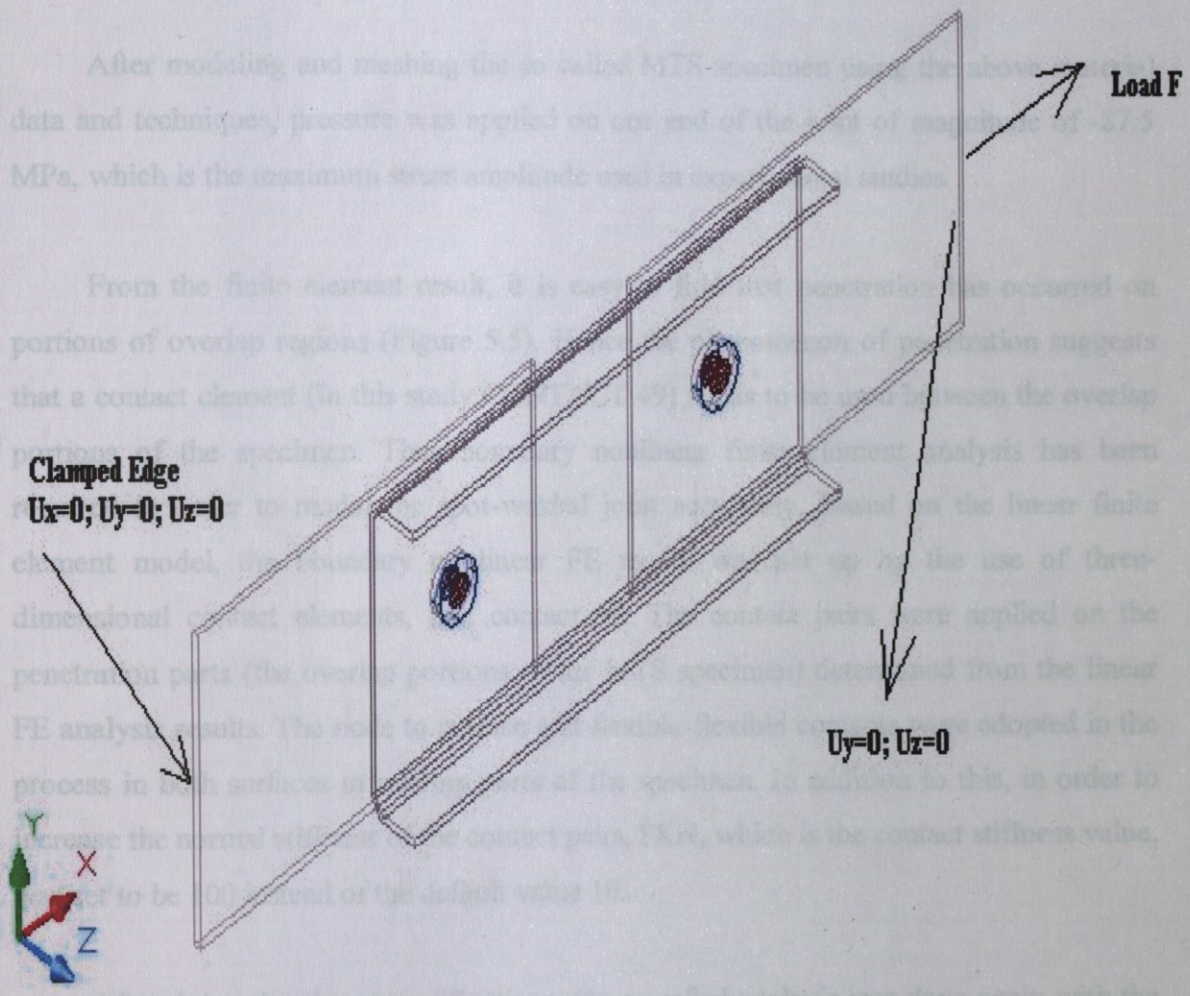

Figure 5.4. Boundary conditions of the finite element model for MTS specimens

As it can be seen in Figure 5.4., one end of the MTS specimen was clamped, that is displacements and rotations were set to zero. Besides this, the other end of the MTS specimen was constrained on "y" and "z" directions but not on "x" direction, that is on the force direction. These constraints were applied because it was aimed to obtain a similar situation to the conditions of experimental study.

As load, it was used negative pressure (in order to obtain tension effect) on the area of one end's surface. It was used pressure instead of load directly, because the distribution of nodes on so called surface was not homogeneous because of the modeling of the specimen (Figure 5.3).

5.4. Analysis

After modeling and meshing the so called MTS specimen using the above material data and techniques, pressure was applied on one end of the joint of magnitude of -87.5 MPa, which is the maximum stress amplitude used in experimental studies.

From the finite element result, it is easy to find that penetration has occurred on portions of overlap regions (Figure 5.5). Hence the phenomenon of penetration suggests that a contact element (in this study CONTACT 49) needs to be used between the overlap portions of the specimen. Thus boundary nonlinear finite element analysis has been required in order to model the spot-welded joint accurately. Based on the linear finite element model, the boundary nonlinear FE model was set up by the use of three-dimensional contact elements, i.e., contact 49. The contact pairs were applied on the penetration parts (the overlap portions of the MTS specimen) determined from the linear FE analysis results. The node to surface and flexible-flexible contacts were adopted in the process in both surfaces in overlap parts of the specimen. In addition to this, in order to increase the normal stiffness of the contact pairs, FKN, which is the contact stiffness value, was set to be 100 instead of the default value 10.

After doing the above modifications, the so called analysis was done again with the same constraint and load conditions in the linear finite analysis.

From the deformation result shown in Figure 5.6, it was found that the penetration problem disappeared because of the application of contact elements.

All figures showing stress distributions (Figures 5.5 through 5.28) are obtained using axial loading of magnitude 87.5 MPa.

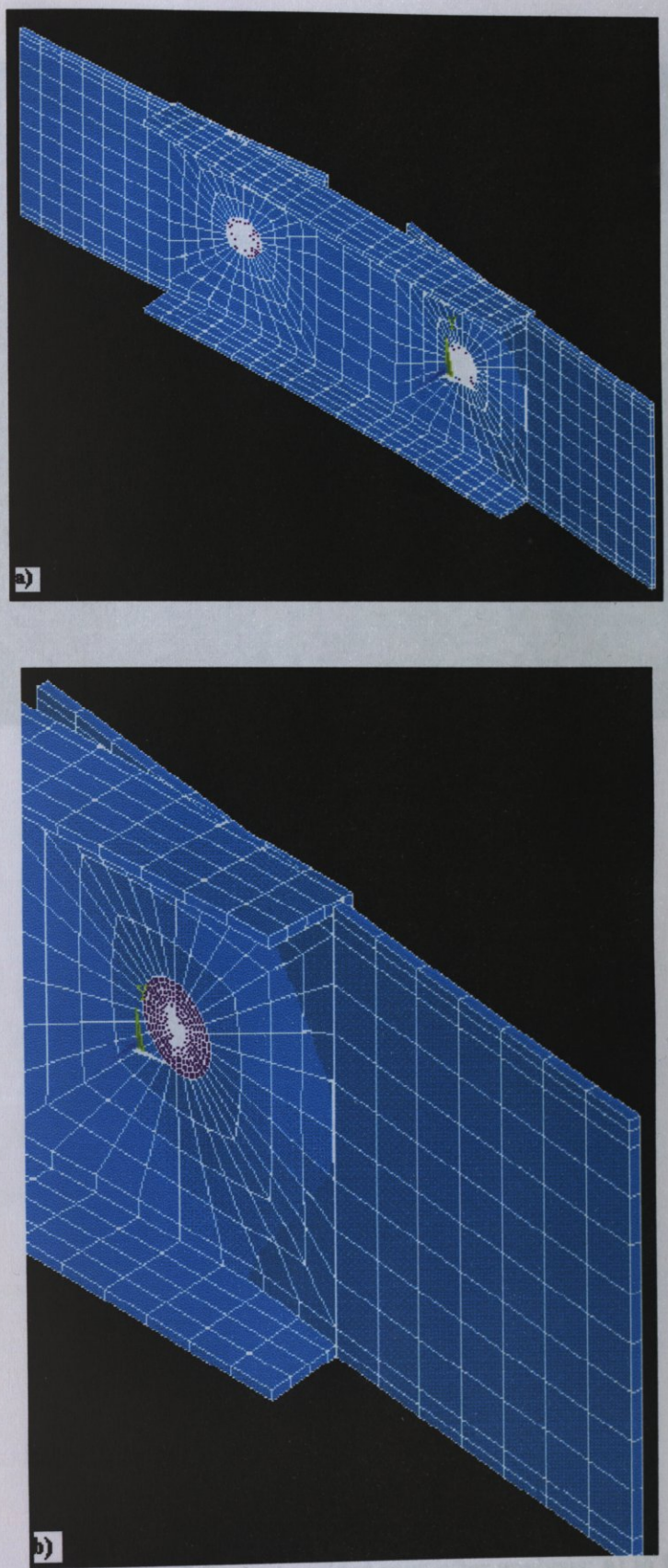

Figure 5.5. Penetrations of the spot-welded joint after analysis; a) in full shape b) in focused (on right spot) shape

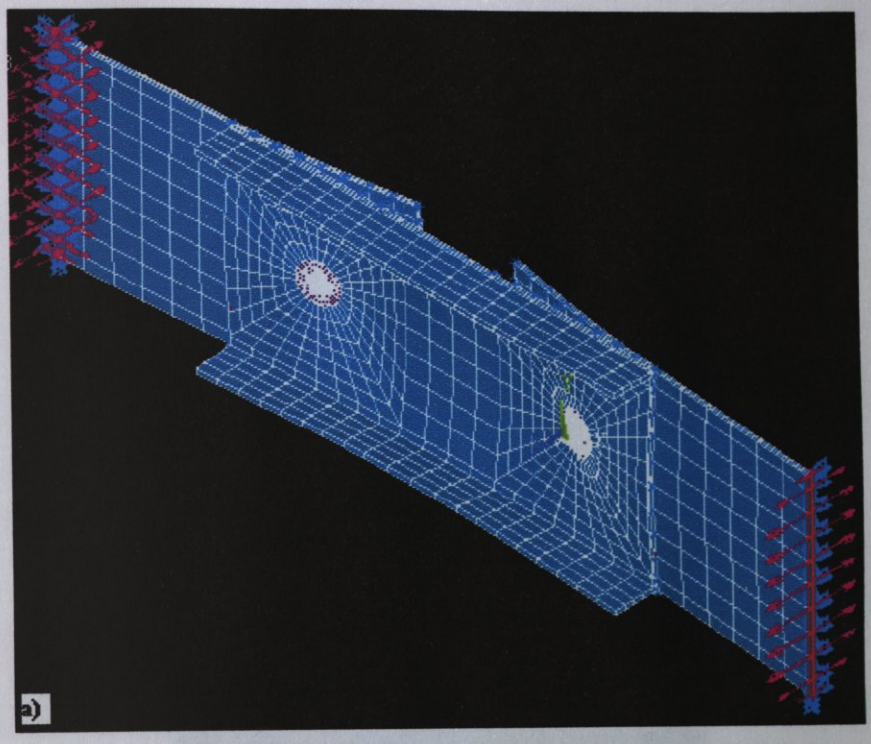

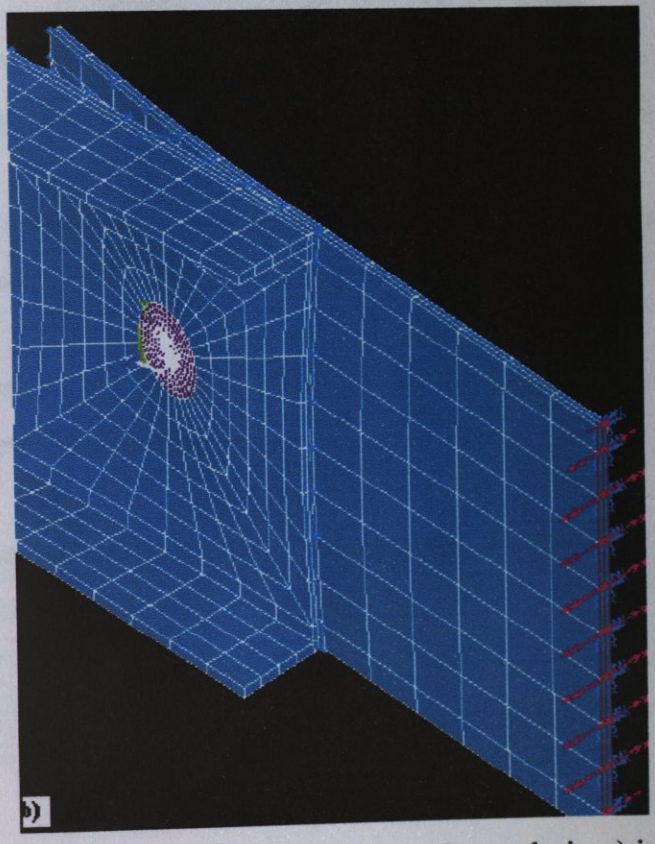

Figure 5.6. Deformation of the spot-welded joint after analysis; a) in full shape b) in focused (on right spot) shape c) in more focused (on right spot) shape

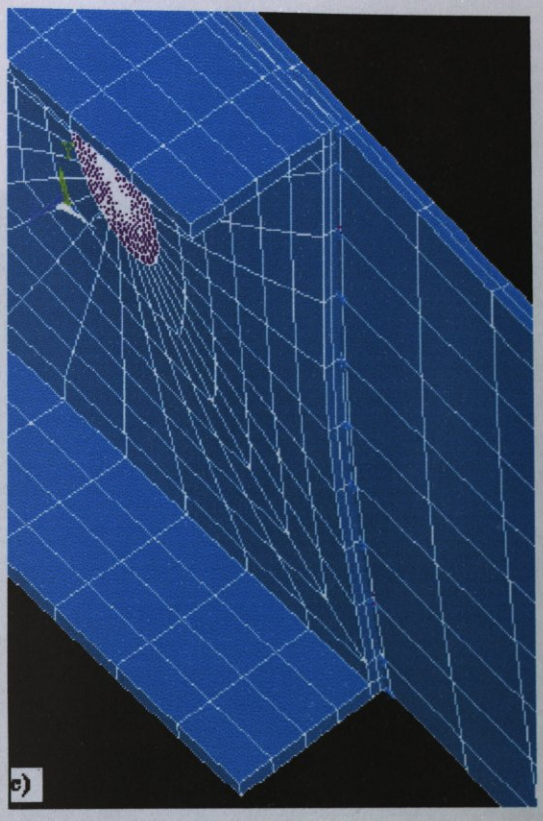

Figure 5.6. Deformation of the spot-welded joint after analysis; a) in full shape b) in focused (on right spot) shape c) in more focused (on right spot) shape [continued]

The stress distributions considering the full shape are obtained after finite element analysis as shown in Figures 5.7 through 5.10.

The stress distributions on the inner surface of the flanged piece of MTS specimen are shown in Figures 5.11 through 5.14.

The stress distributions on the inner surface of the end pieces of MTS specimen are shown in Figures 5.15 through 5.18.

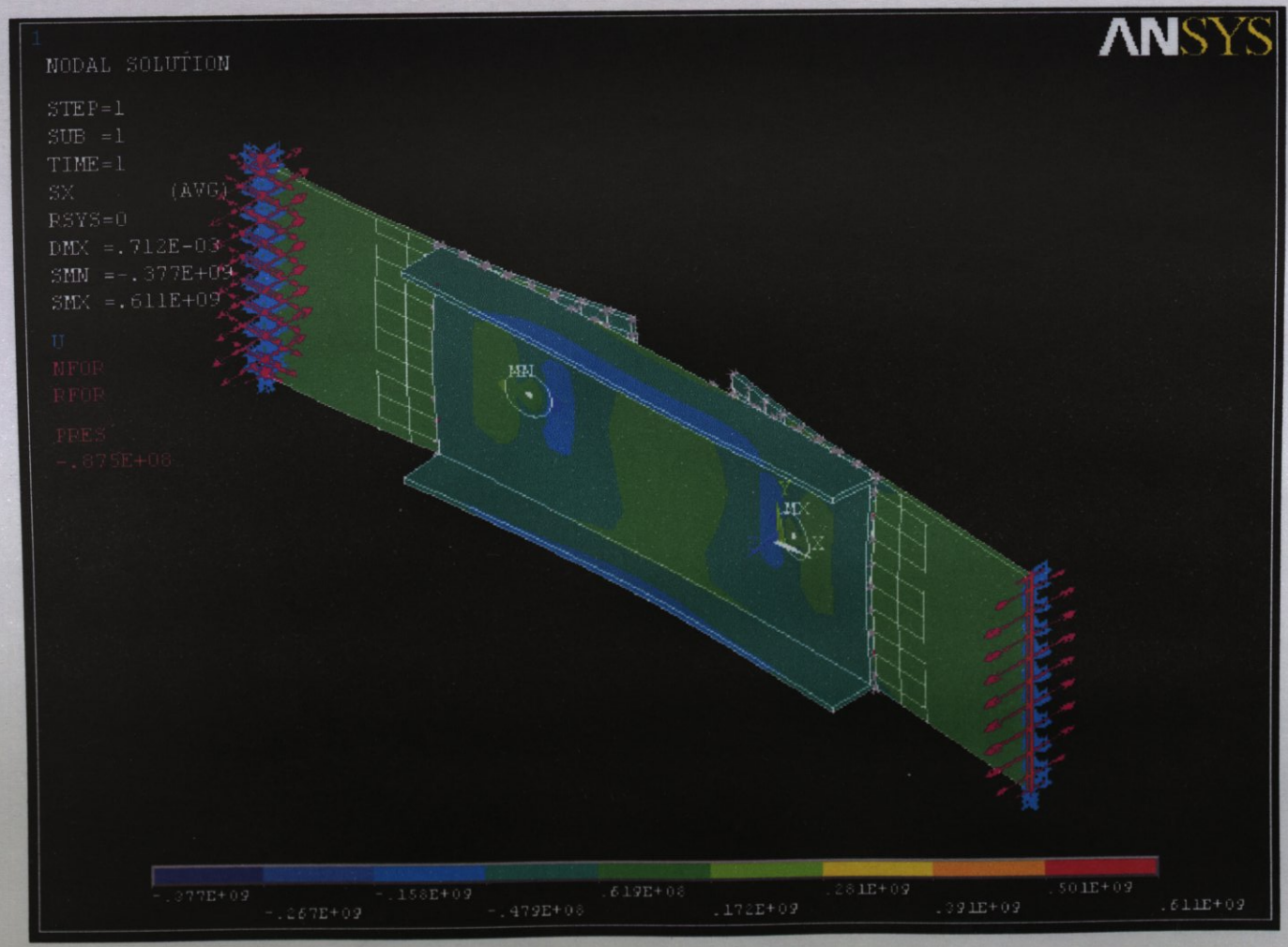

Figure 5.7 The stress distribution in terms of SX (tensile stress) for isometric full shape

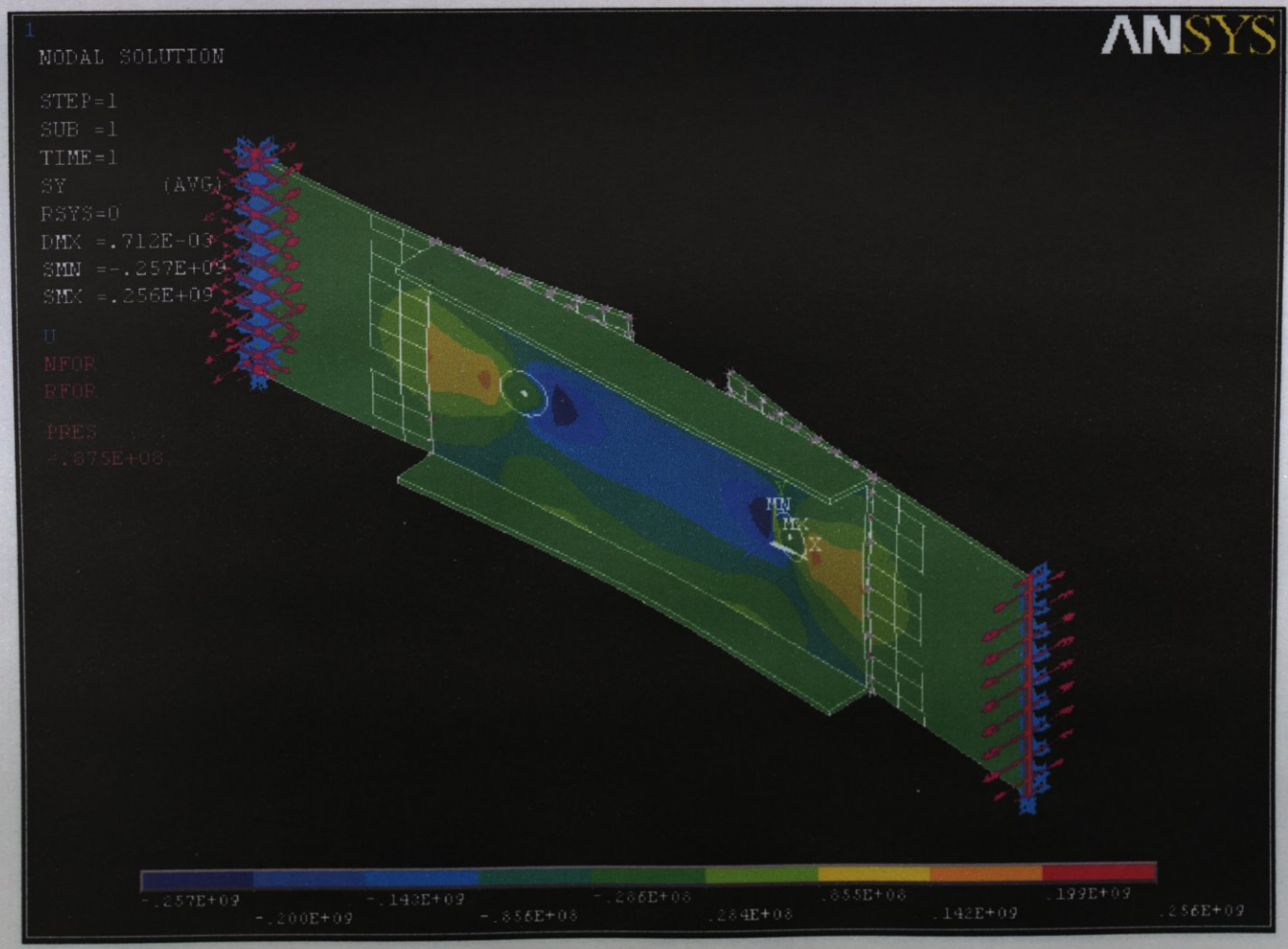

Figure 5.8 The stress distribution in terms of SY for isometric full shape

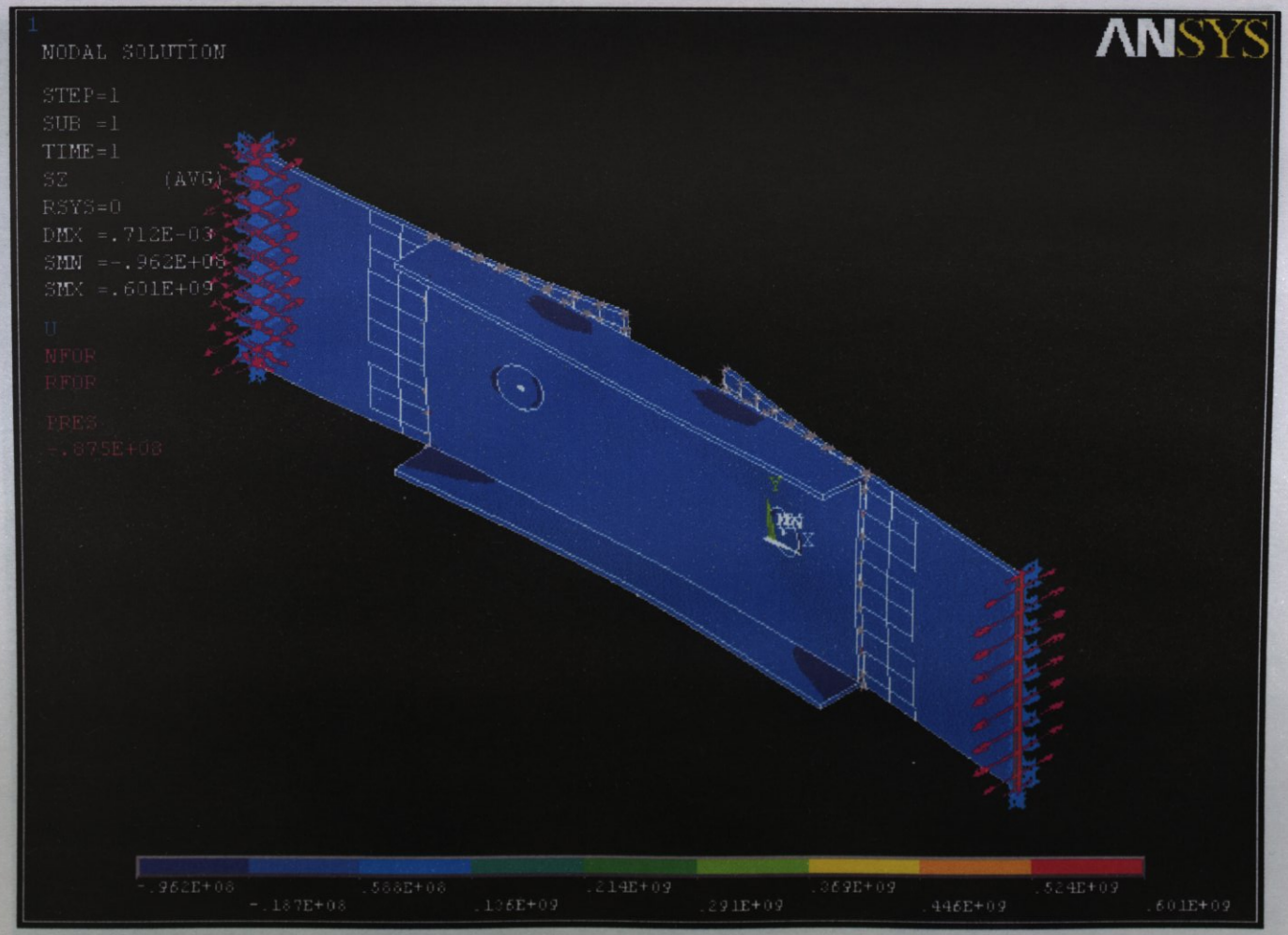

Figure 5.9 The stress distribution in terms of SZ (bending stress) for isometric full shape

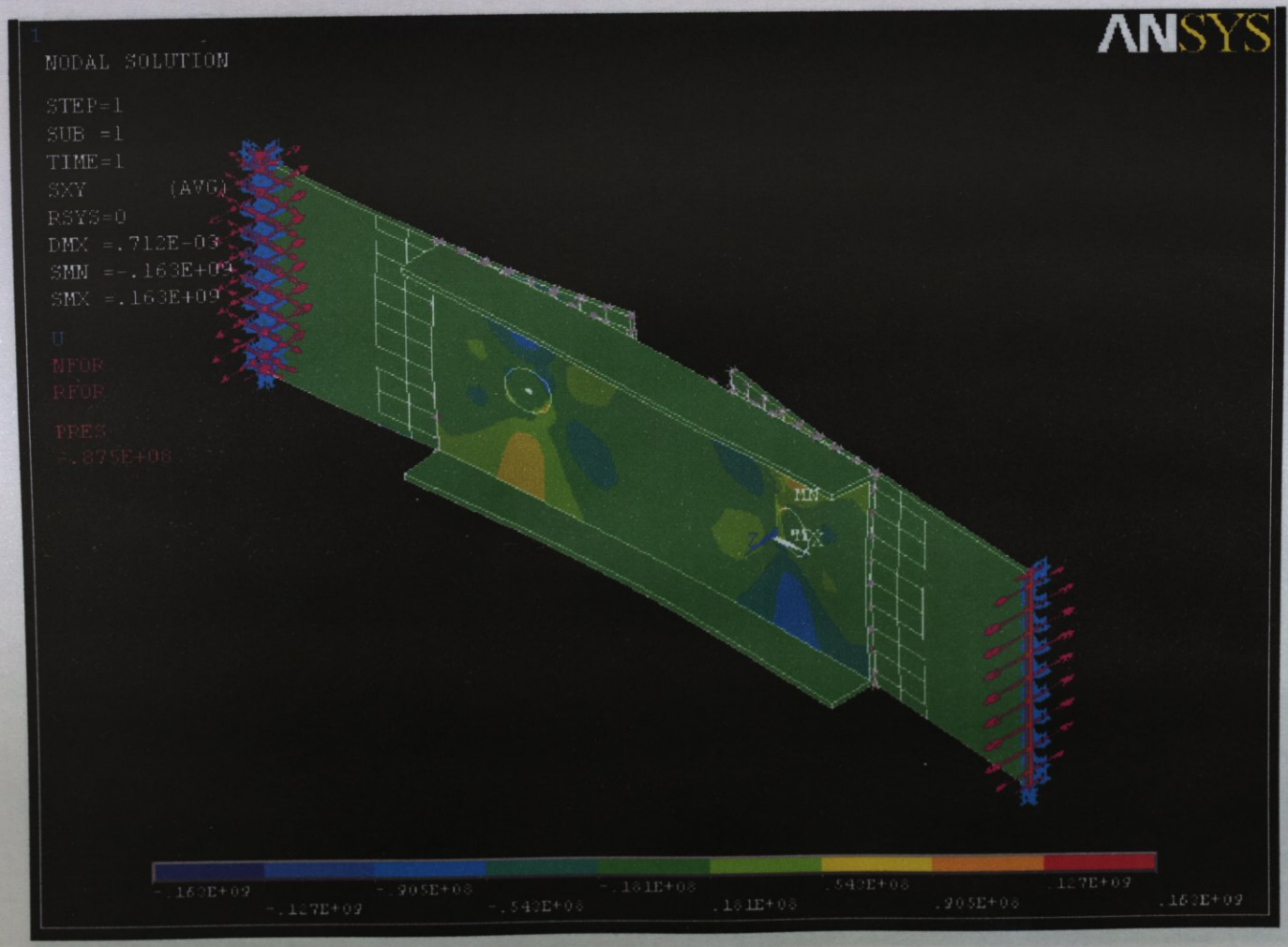

Figure 5.10 The stress distribution in terms of SXY for isometric full shape

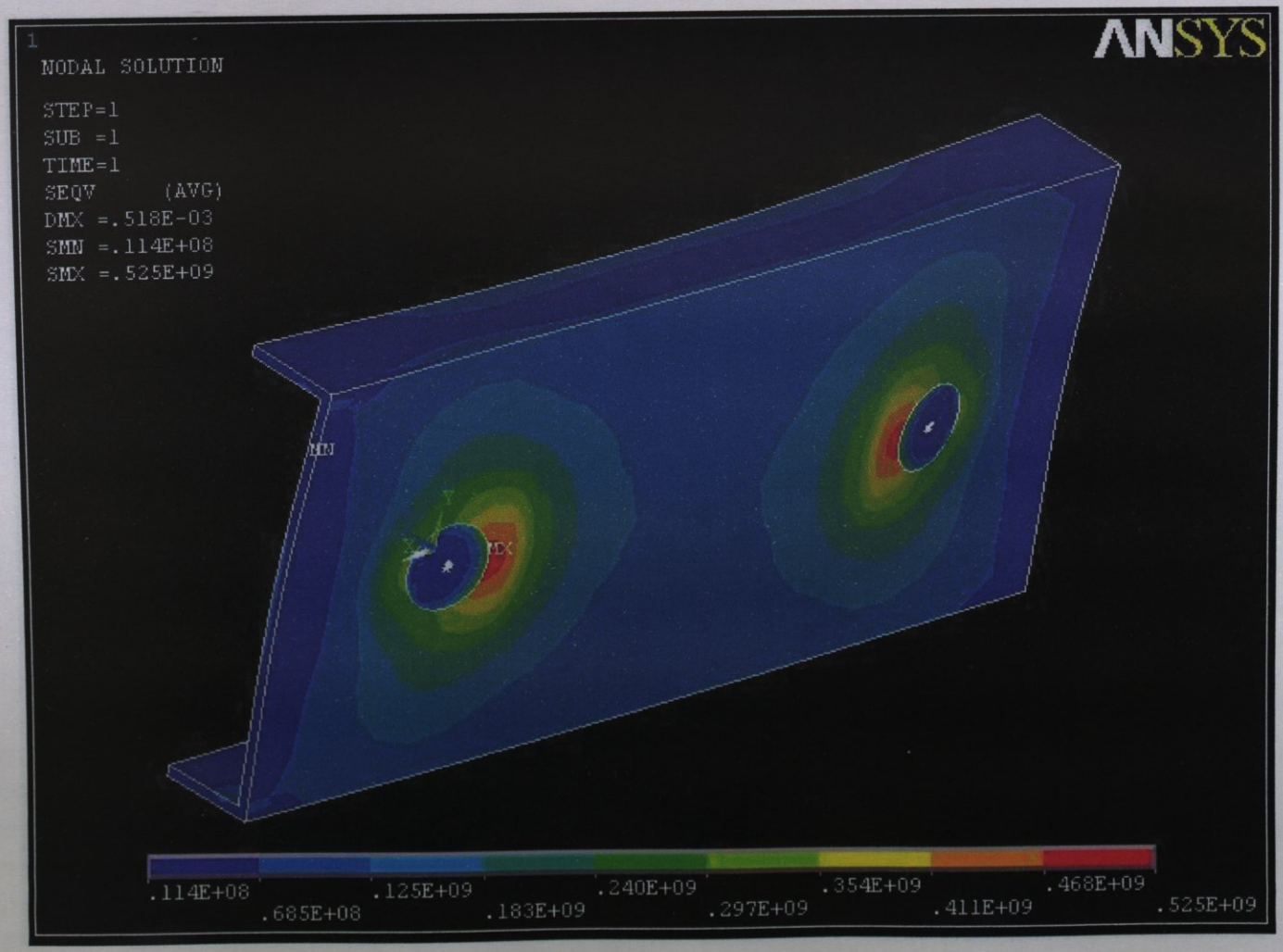

Figure 5.11 Von Mises stress distribution on the inner surface of the flanged part of MTS

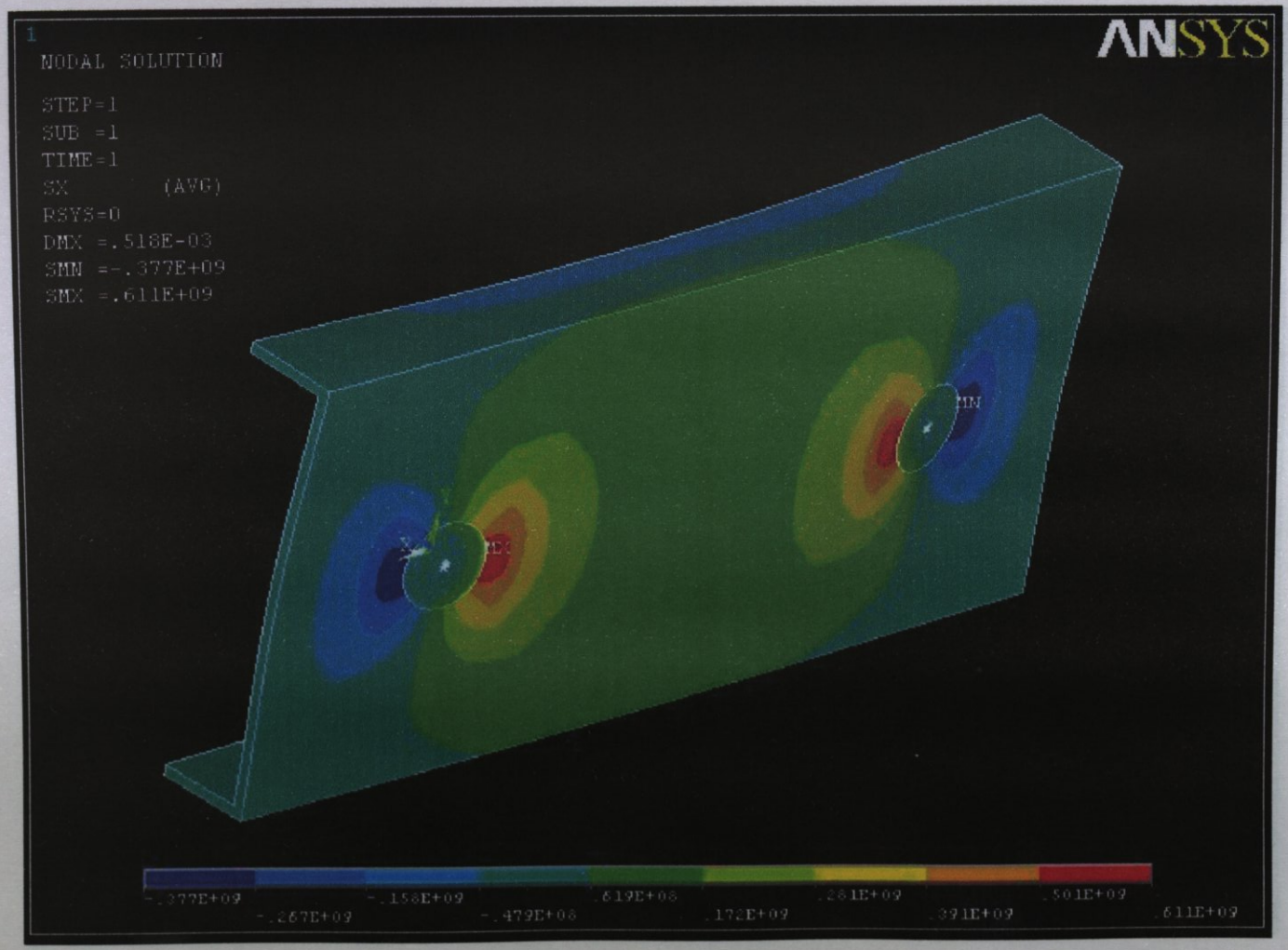

Figure 5.12 Tensile (SX) stress distribution on the inner surface of the flanged part of MTS

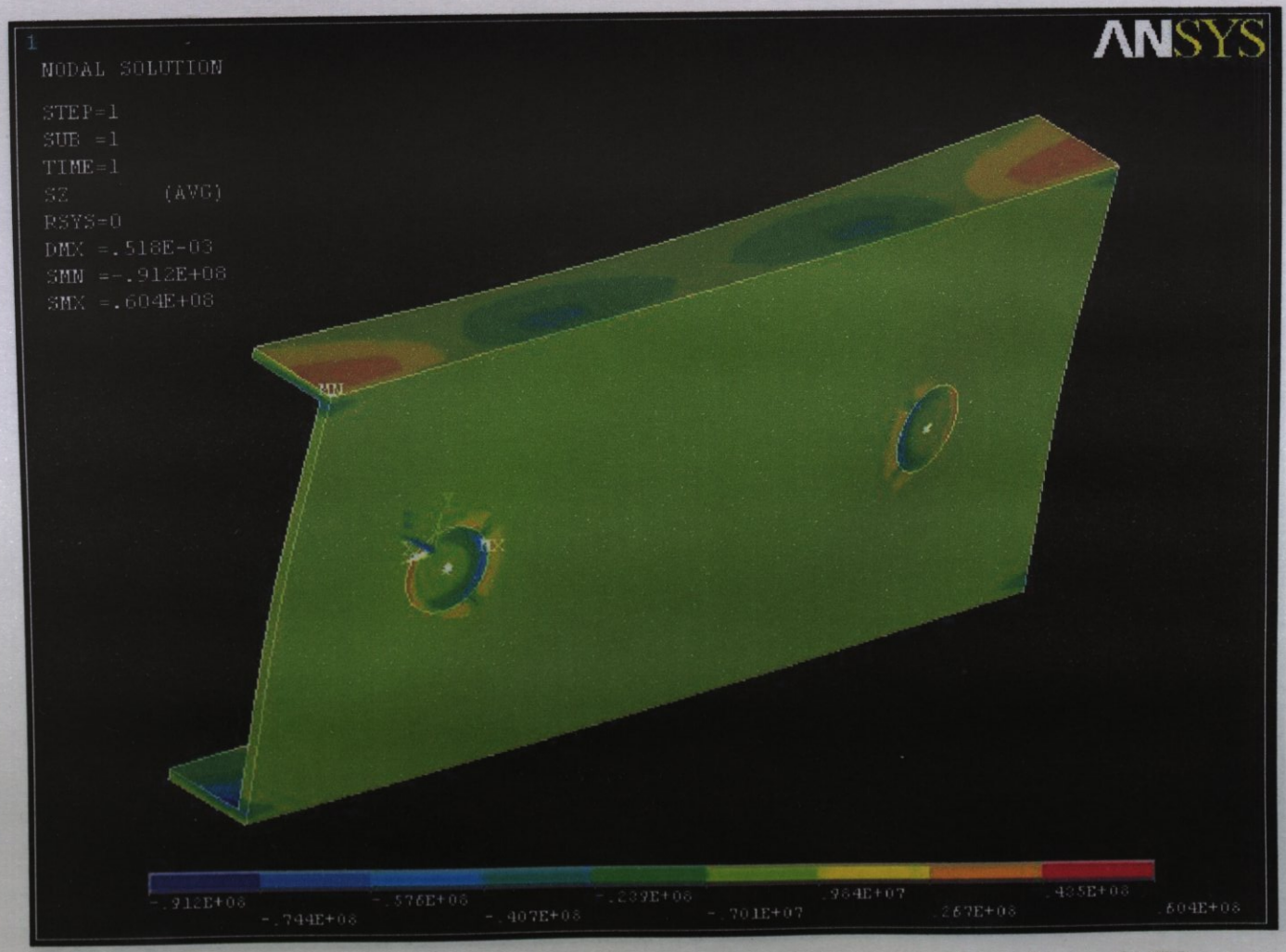

Figure 5.13 Bending (SZ) stress distribution on the inner surface of the flanged part of MTS

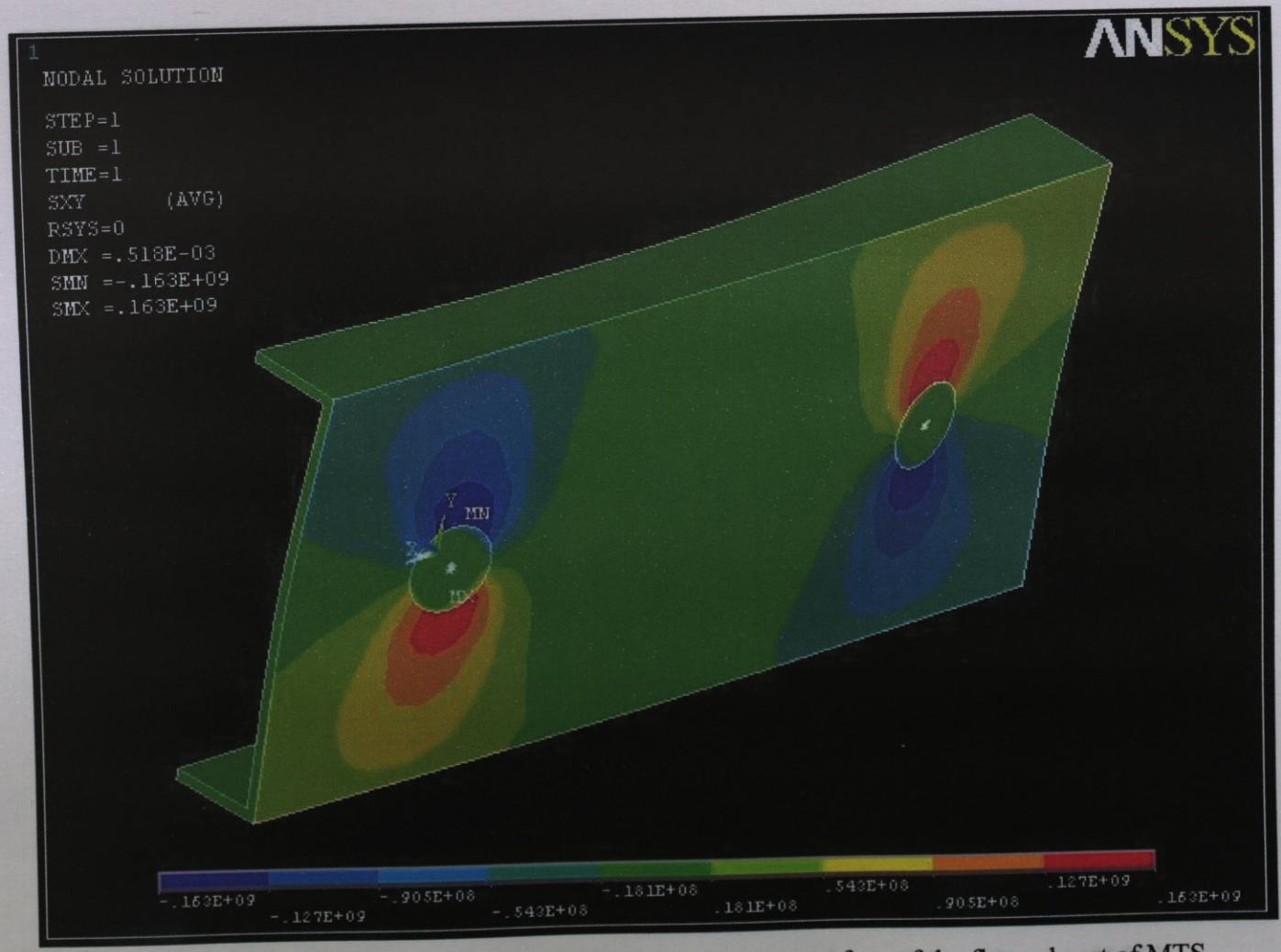

Figure 5.14 Shearing (SXY) stress distribution on the inner surface of the flanged part of MTS

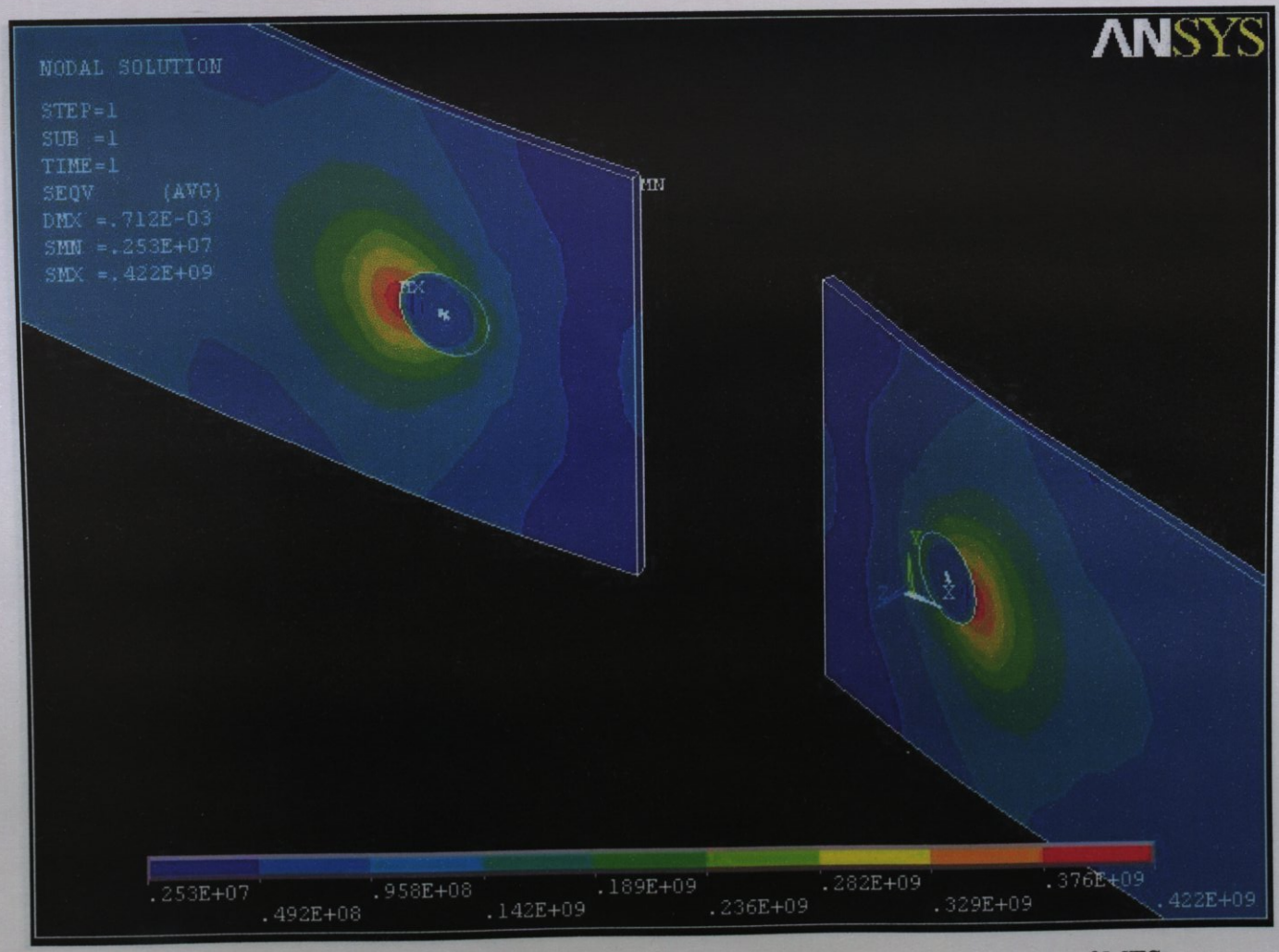

Figure 5.15 Von Mises stress distribution on the inner surfaces of the end parts of MTS

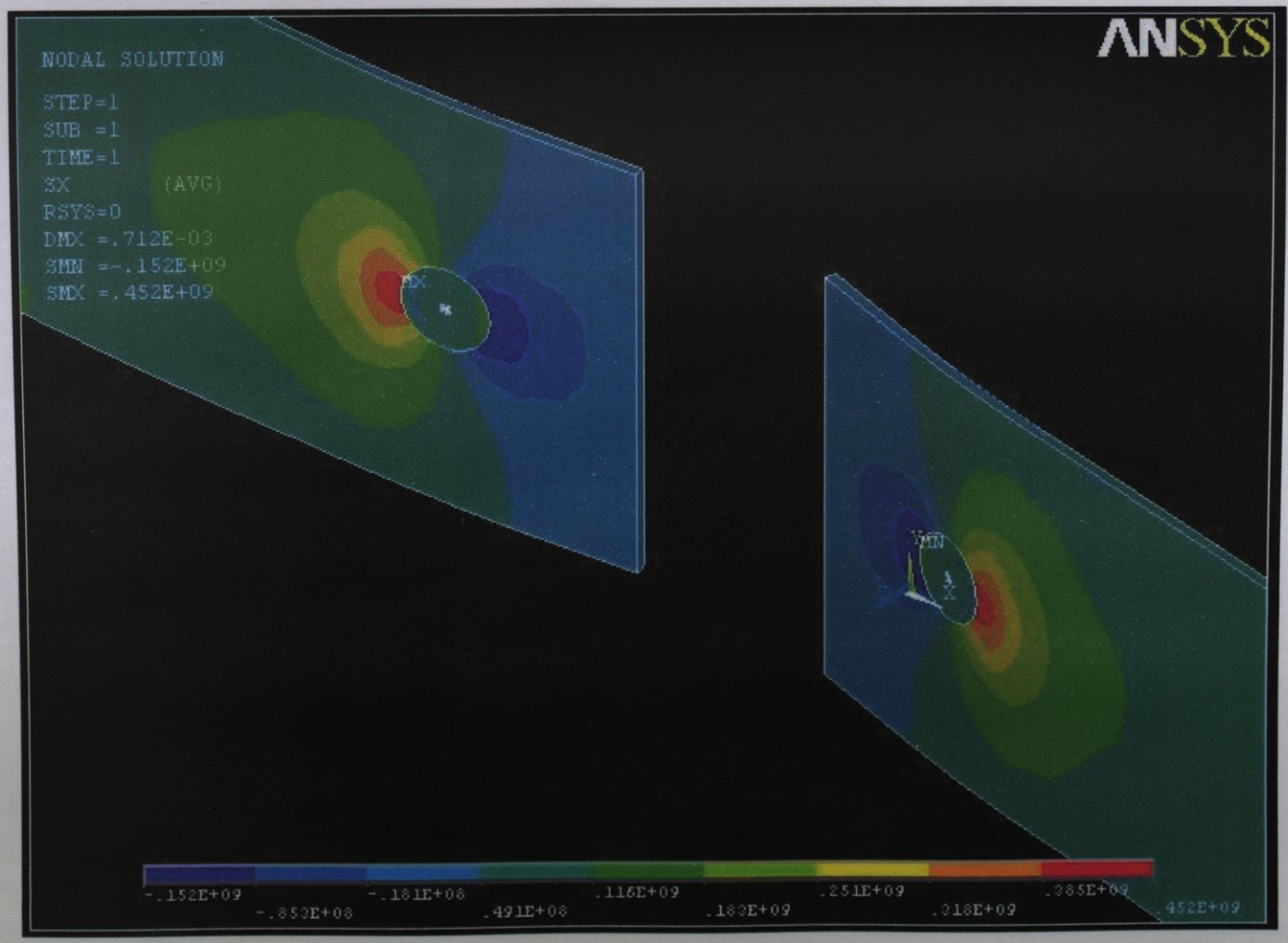

Figure 5.16 Tensile (SX) stress distribution on the inner surfaces of the end parts of MTS

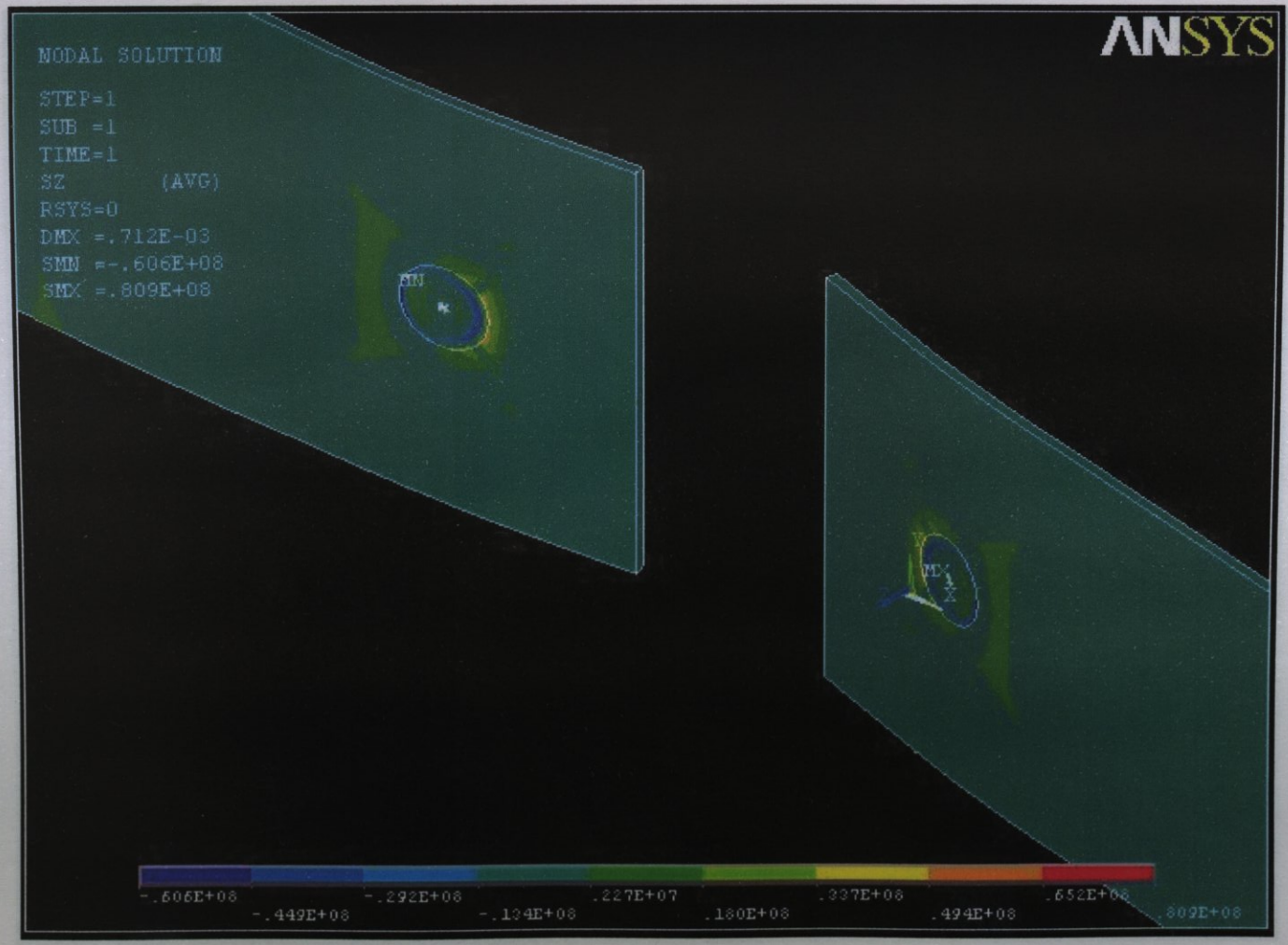

Figure 5.17 Bending (SZ) stress distribution on the inner surfaces of the end parts of MTS

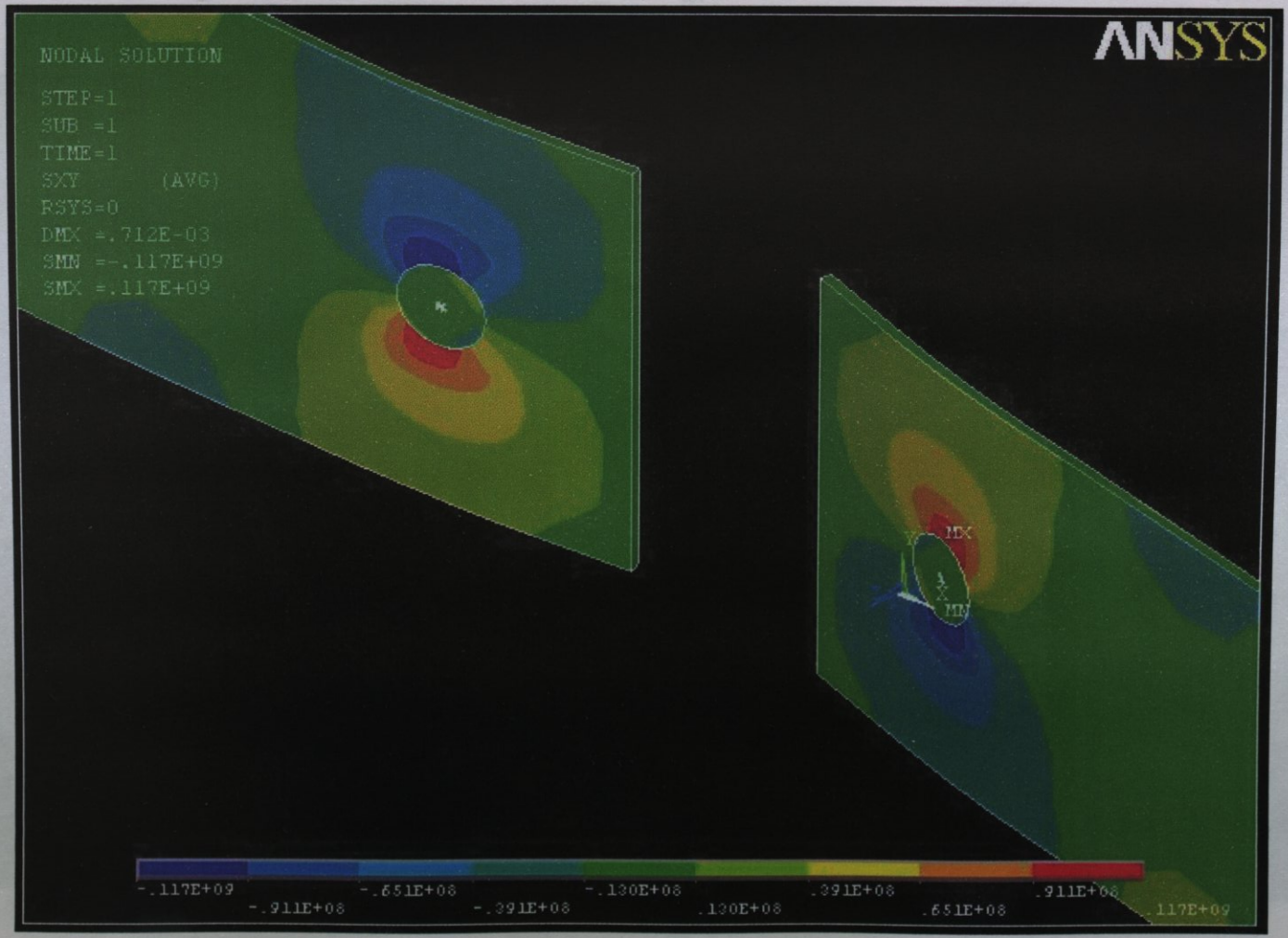

Figure 5.18 Shearing (SXY) stress distribution on the inner surfaces of the end parts of MTS

The stress distributions for again flanged piece and end pieces in terms of path plots are shown in Figures 5.19 through 5.28.

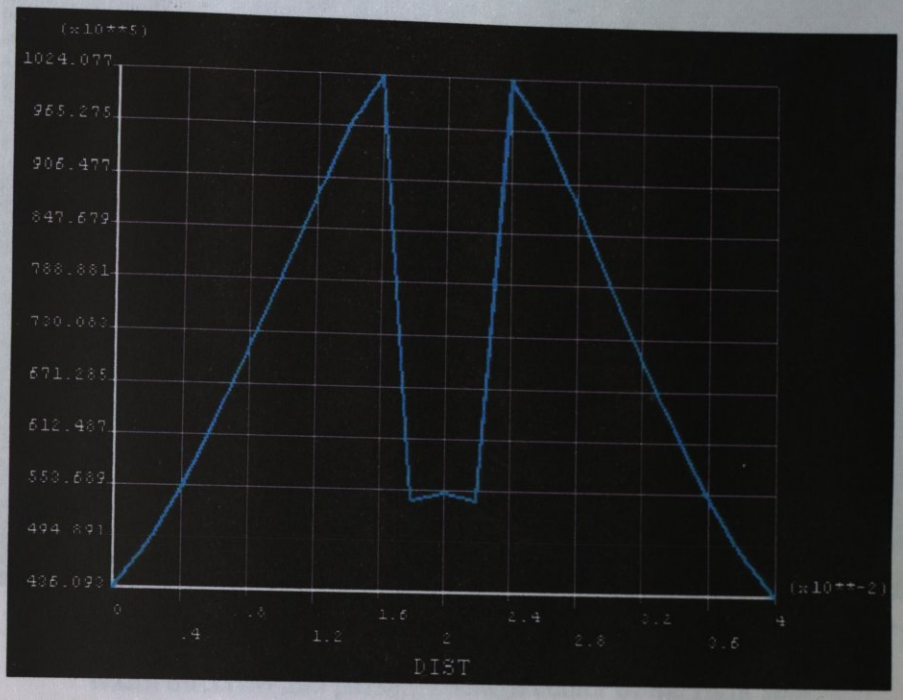

Figure 5.19 Stress distributions (on the inner surface of flanged piece) in terms of SX in the width direction and passing through center of the right spot

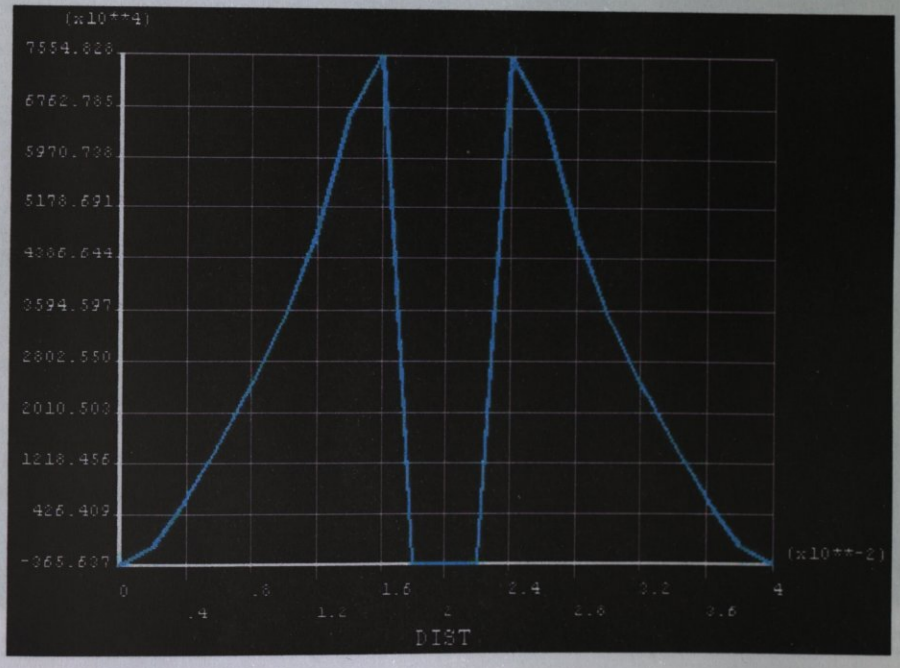

Figure 5.20 Stress distributions (on the inner surface of flanged piece) in terms of SY in the width direction and passing through center of the right spot

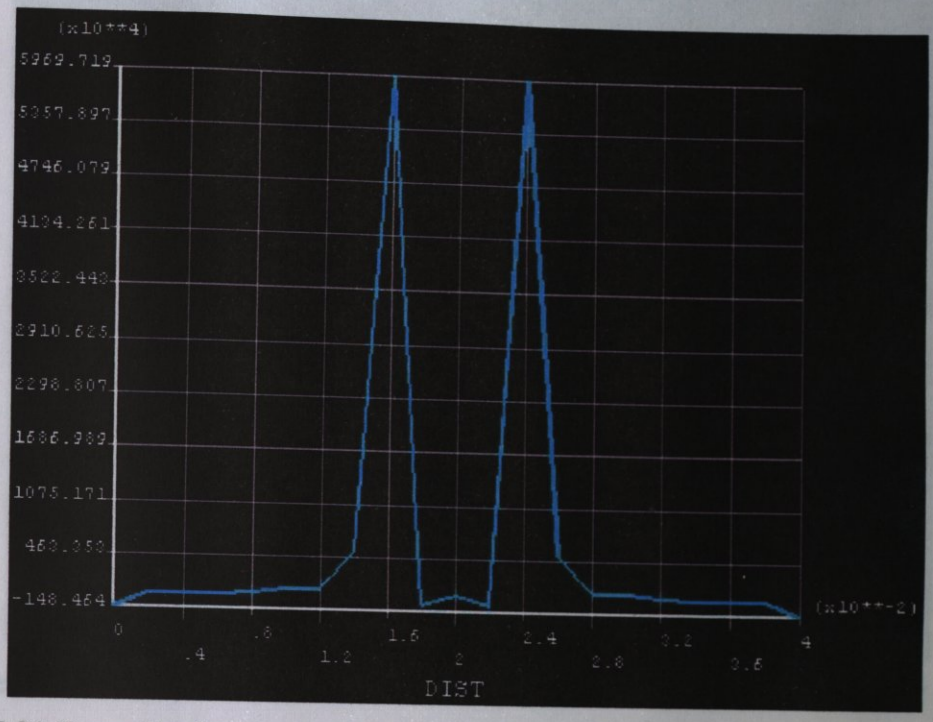

Figure 5.21 Stress distributions (on the inner surface of flanged piece) in terms of SZ in the width direction and passing through center of the right spot

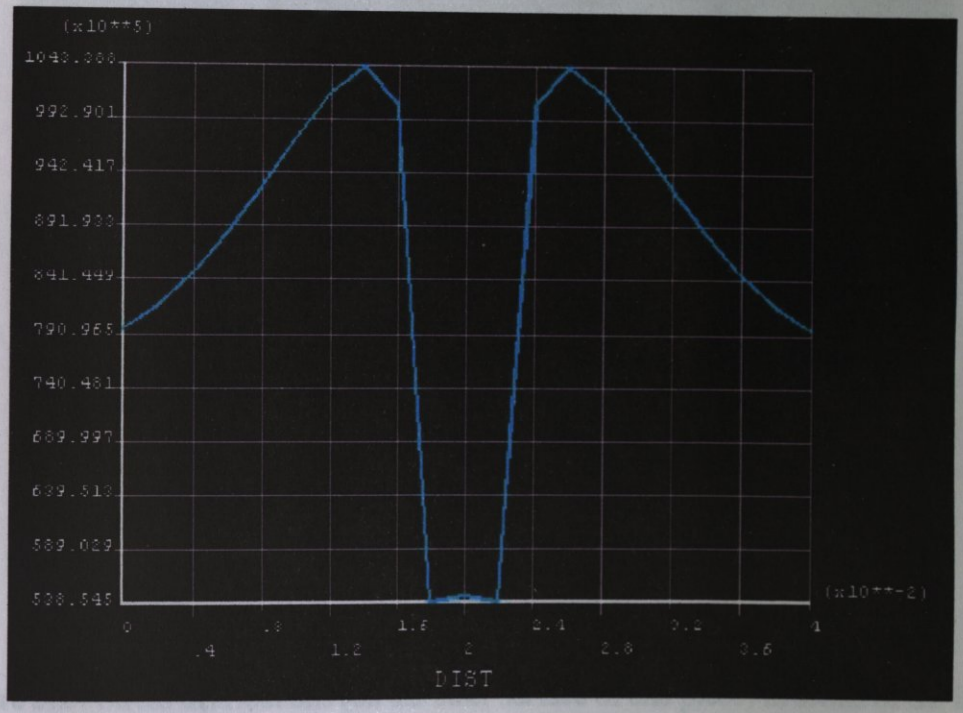

Figure 5.22 Stress distributions (on the inner surface of end piece) in terms of SX in the width direction and passing through center of the right spot

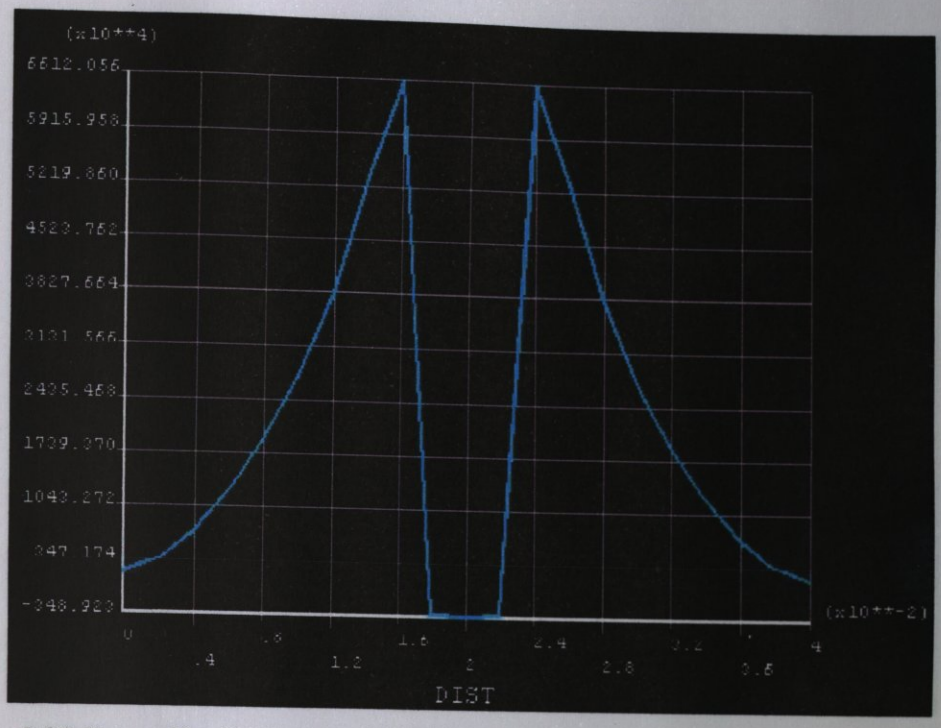

Figure 5.23 Stress distributions (on the inner surface of end piece) in terms of SY in the width direction and passing through center of the right spot

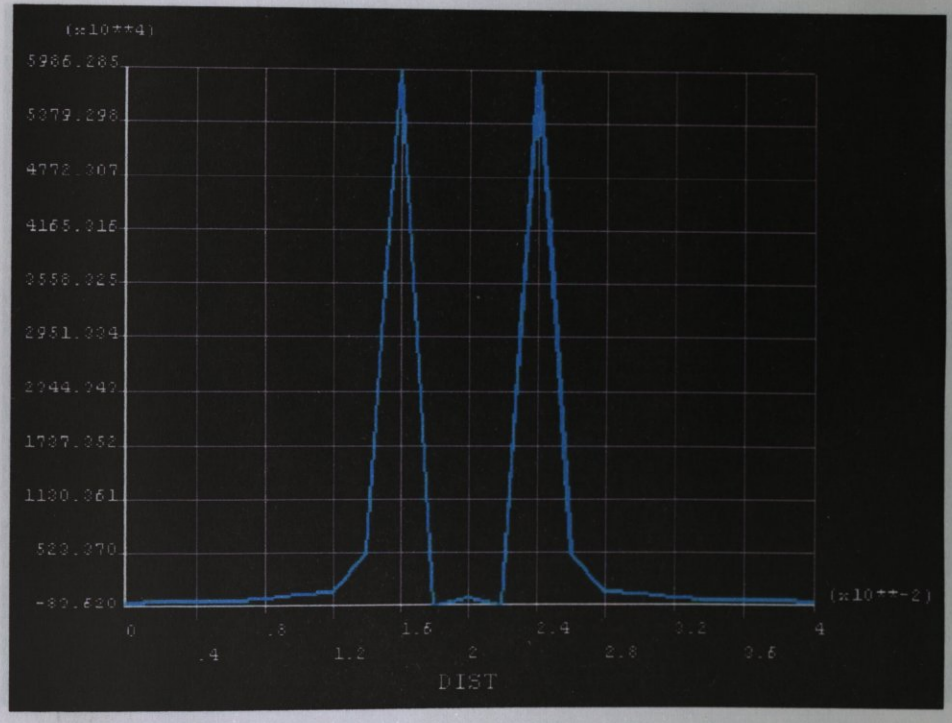

Figure 5.24 Stress distributions (on the inner surface of end piece) in terms of SZ in the width direction and passing through center of the right spot

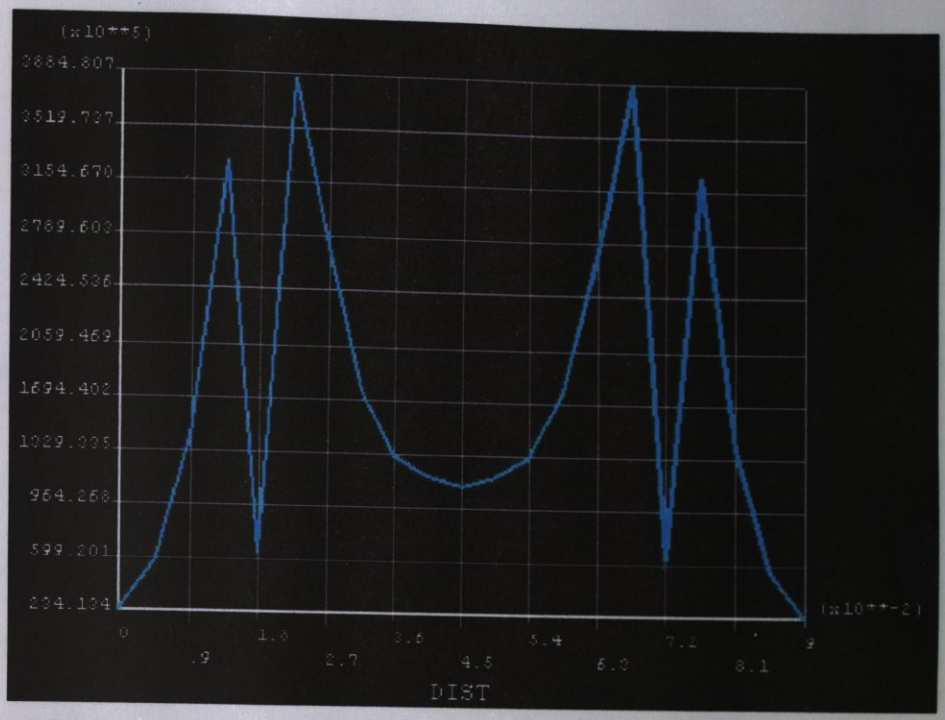

Figure 5.25 Von Mises stress distribution on the inner surface and length direction of flanged piece of specimen

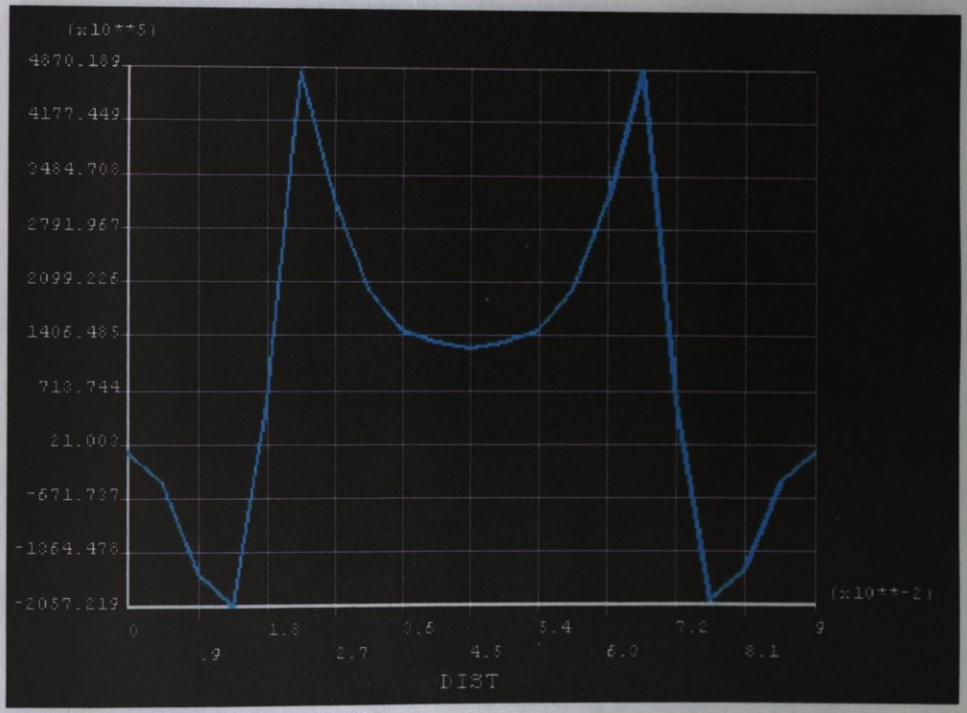

Figure 5.26 Stress distributions (on the inner surface of flanged piece) in terms of SX in the force direction and passing through the centers of the spots

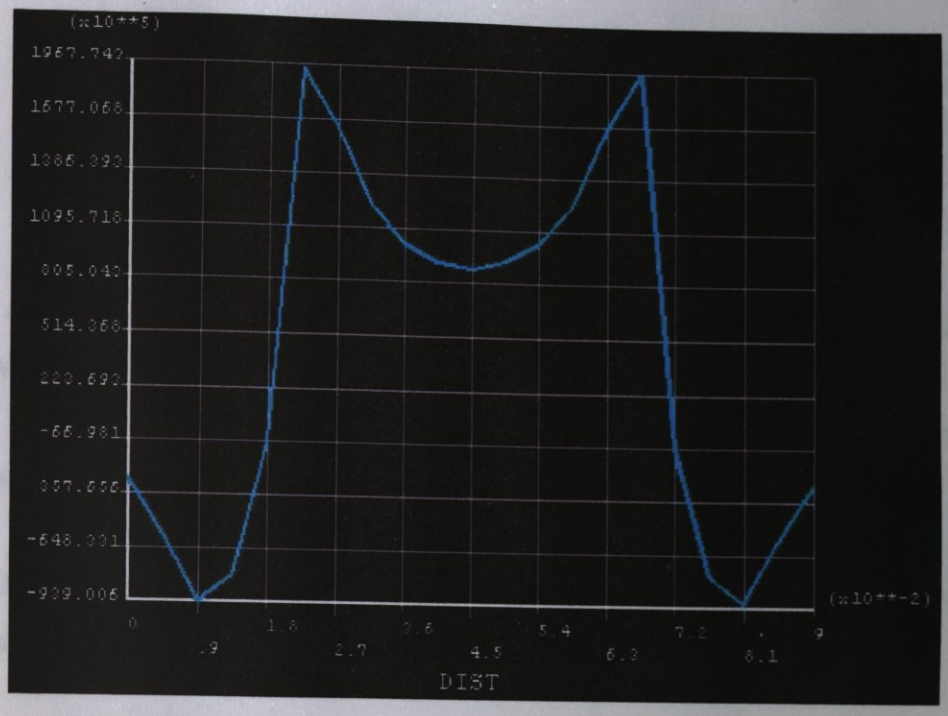

Figure 5.27 Stress distributions (on the inner surface of flanged piece) in terms of SY in the force direction and passing through the centers of the spots

Figure 5.28 Stress distributions (on the inner surface of flanged piece) in terms of SZ in the force direction and passing through the centers of the spots

6. DISCUSSION

6.1. Assessment of Experimental Study

As we explained in Chapter 4, the first crack that propagates through the thickness of the sheet is defined as the primary crack and corresponding weld is defined as the primary weld. The other weld is called the secondary weld, which also has its own primary and secondary cracks.

I was observed that the primary cracks always occurred on the flanged piece (that is the centerpiece) of the modified tensile shear (MTS) specimens.

Evaluating the previous experimental studies and their results, it was thought that the primary cracks always occur on the inner surface of flanged piece (centerpiece) of modified tensile shear specimens at the periphery of one spot. These so called primary cracks first propagated through the periphery of the spot and then propagated through the sheet thickness like a thumbnail and finally the deformation grew separating the sheets from each others.

In all these experimental studies, it was seen that (except one case) the deformation occurs on the spots that lies closer to the piston displacement.

After experimental study, we examined some deformed and undeformed parts, especially spots, of specimens under microscope (Figures 6.1. through 6.6.). After examining, we saw that the failures of specimens were due to cracks that occurred at the peripheries of spots under loading. In this point, it can be added that after cracks occurred and grew, localized necking in the base metal somewhat away from the nugget boundary (in other words in the HAZ) occurred and finally specimens torn completely.

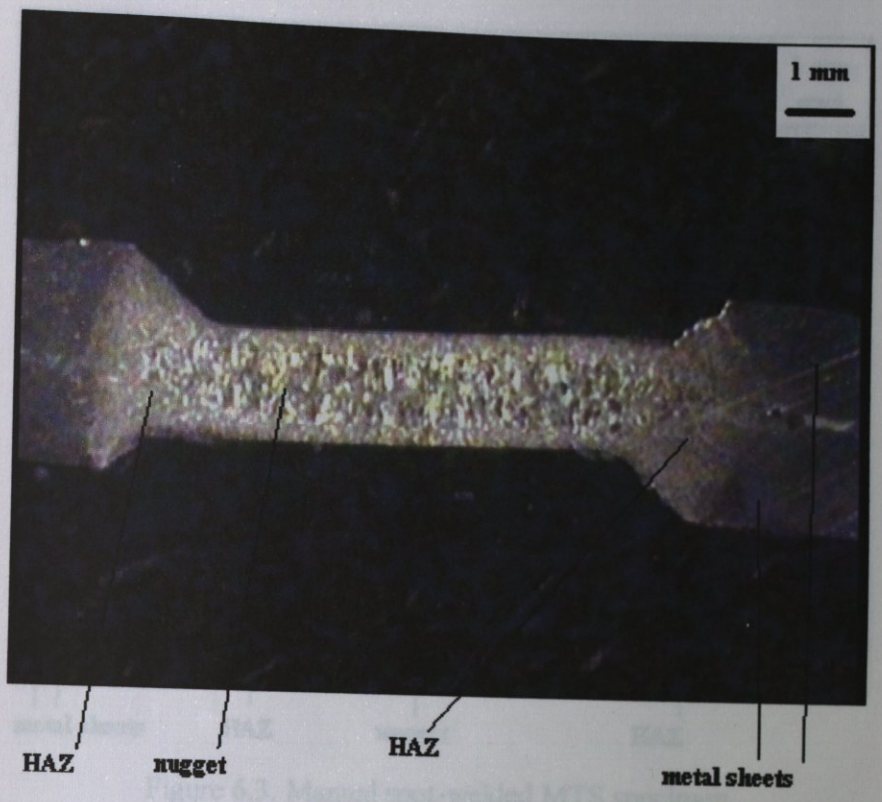

Figure 6.1. Nipper spot-welded MTS specimen

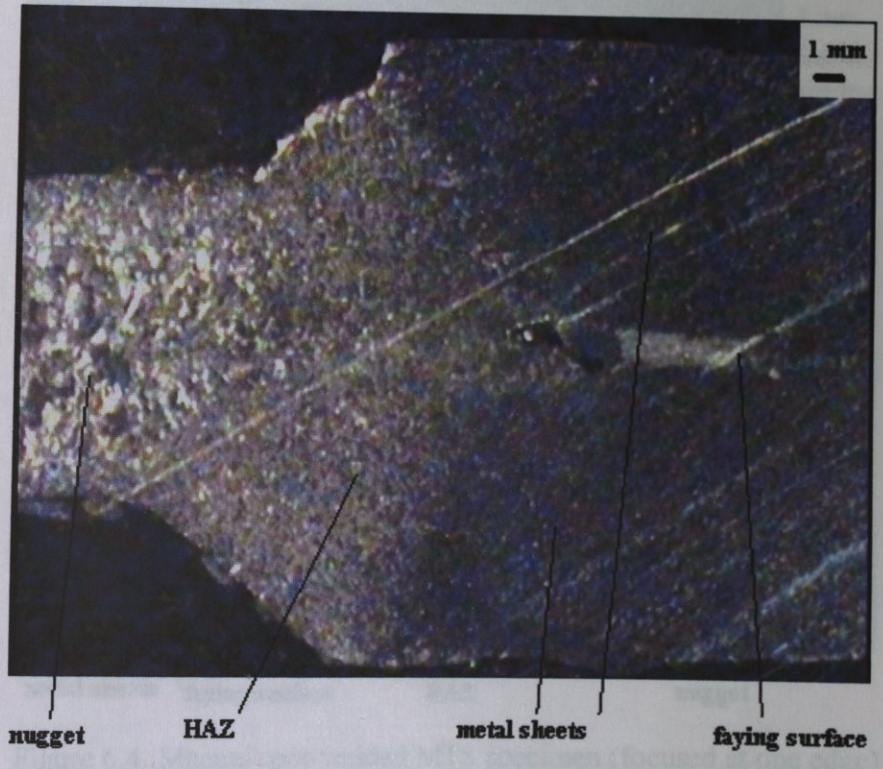

Figure 6.2. Nipper spot-welded MTS specimen (focused at one edge)

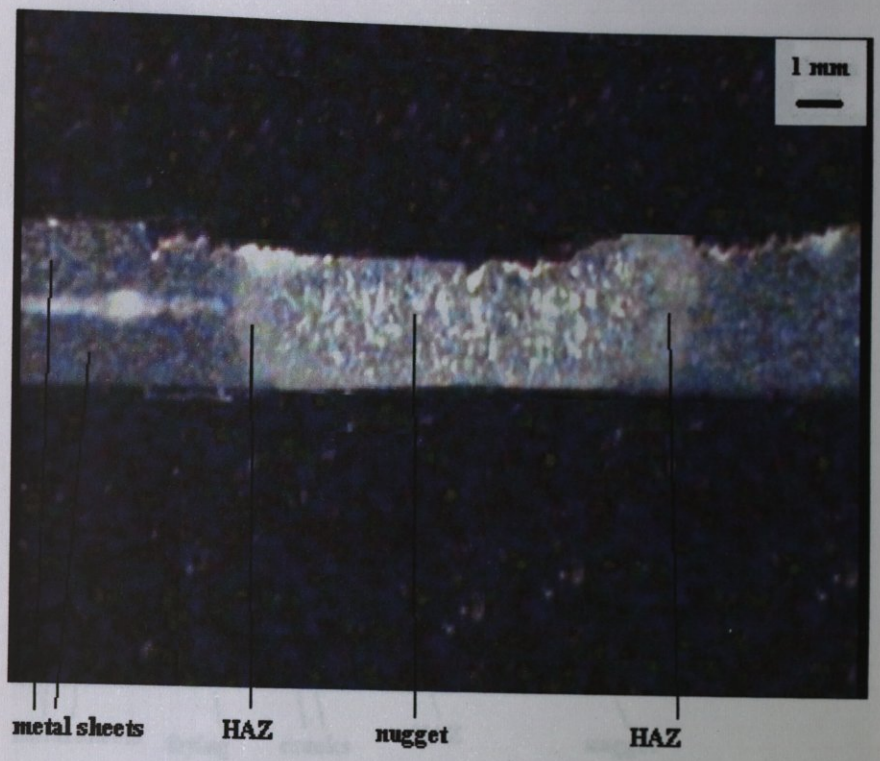

Figure 6.3. Manual spot-welded MTS specimen

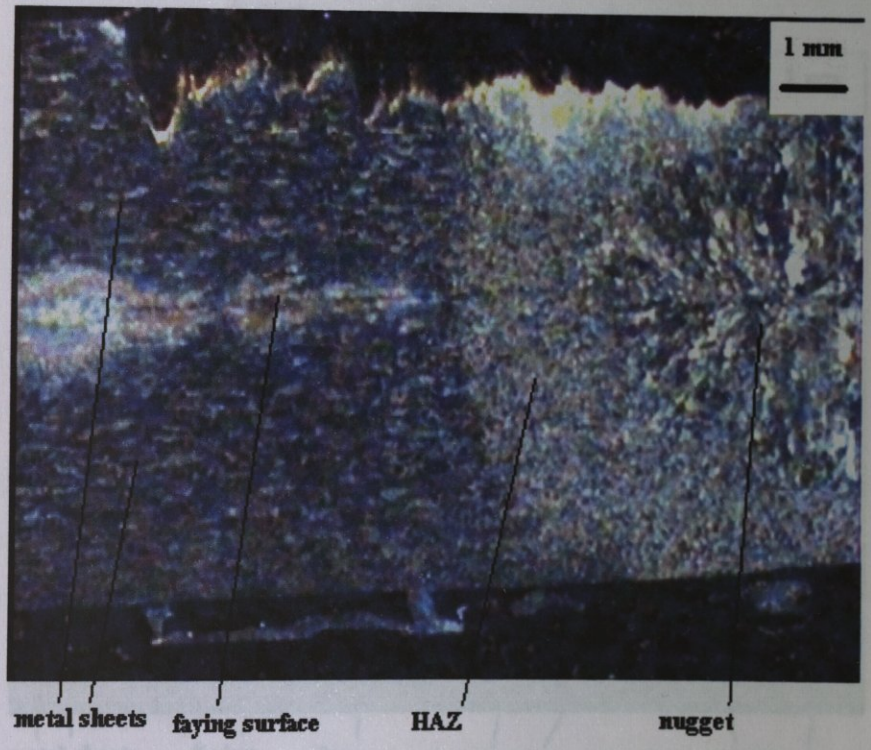

Figure 6.4. Manual spot-welded MTS specimen (focused at one edge)

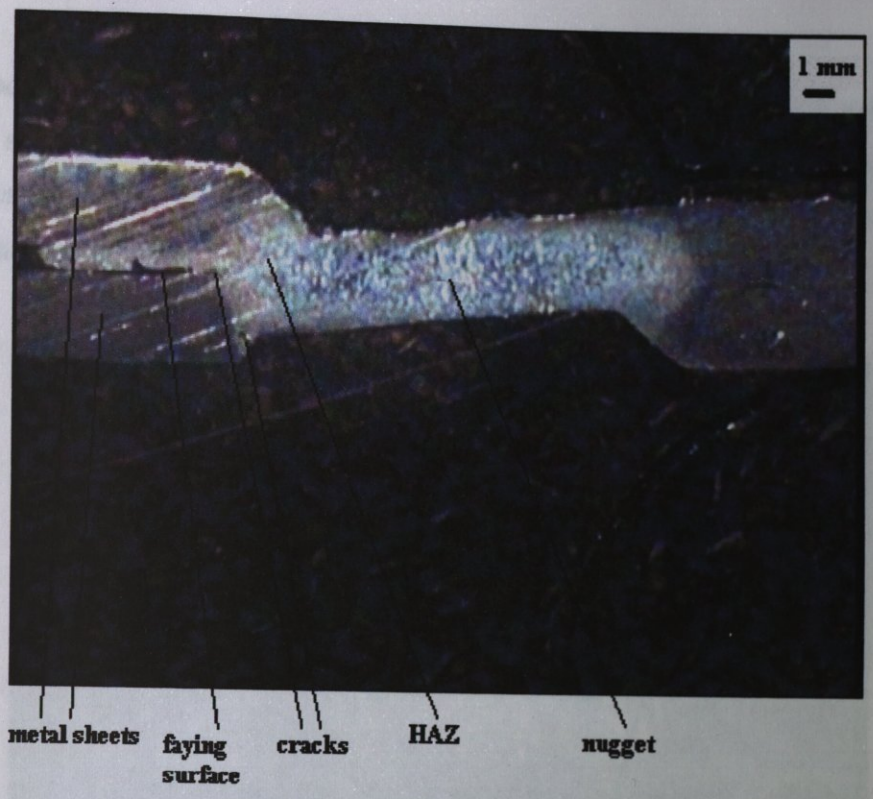

Figure 6.5. Cracks in nipper spot-welded MTS specimen

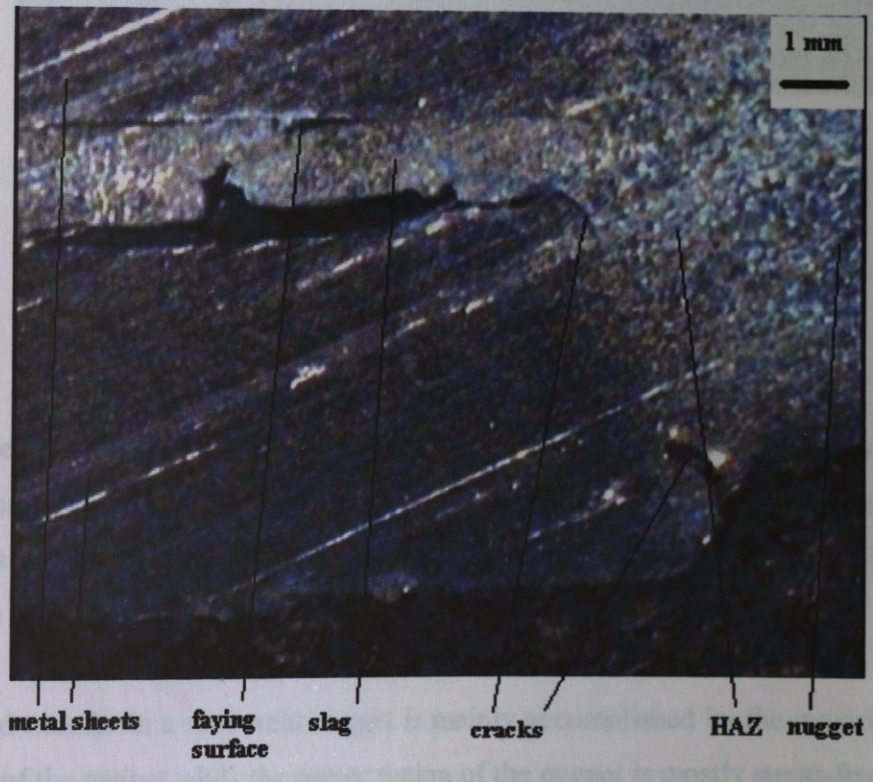

Figure 6.6. Cracks in nipper spot-welded MTS specimen (focused at one edge)

In addition, when examining the deformed and undeformed parts of specimens, it was also seen that even if there are sometimes some gaps or porosities (Figure 6.7) in spots, always cracks occurred on the peripheries of the spots and the specimens deformed through the thickness (not through the spots because of porosities or gaps).

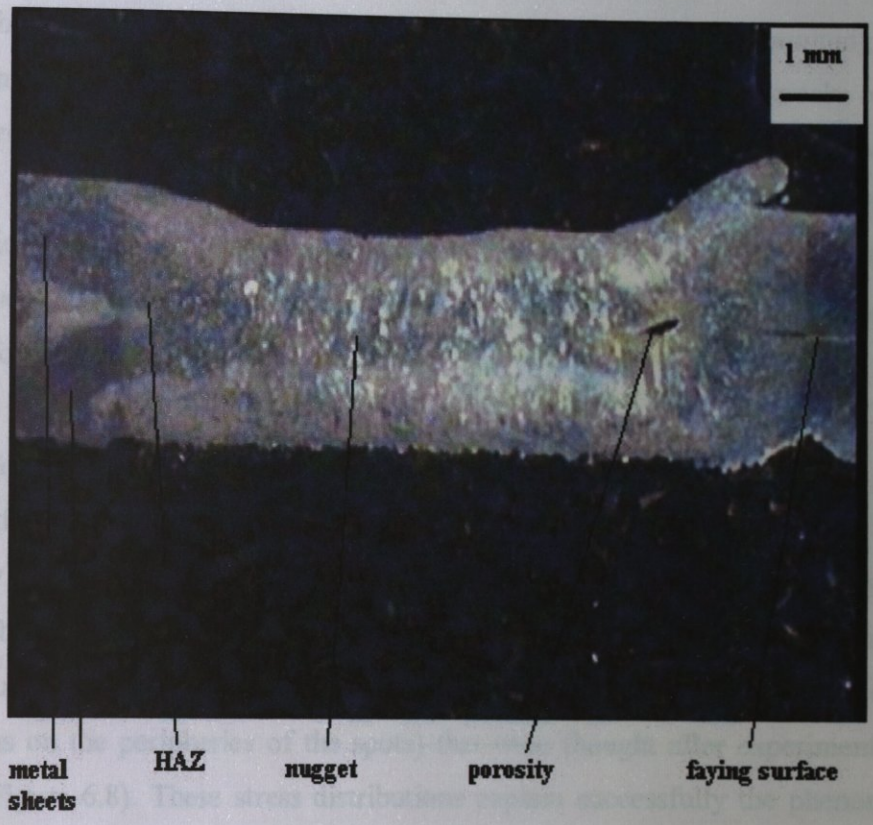

Figure 6.7. Porosity in a manual spot-welded MTS specimen

6.2. Assessment of Finite Element Analysis Study

A detailed study of the three-dimensional mechanical behavior of spot-welded joint has been carried out in terms of modified tensile shear specimens and under linearly elastic conditions. Finite element solutions of the stress fields in the base metal and the nugget have been obtained for the modified tensile shear specimens.

Load transfer in a spot-weld nugget is mainly accomplished by the material near the boundary of the nugget while the center region of the nugget is mostly stress-free. As such,

the load bearing capability of a spot-welded joint may not be significantly reduced by the existence voids in the center region of a nugget as seen in Figure 6.7.

A global view of the stress distributions in the modified tensile-shear specimen are seen in Figures 5.7. through 5.28.

When it was conducted the experimental studies, with examining deformed specimens, actually the cracks of spots, it was thought that the primary cracks occur on the inner surface of flanged piece (or centerpiece) of MTS in one spot's periphery (generally the spot that near the piston displacement). Then these cracks grow firstly through the peripheries of spots up to several millimeters and then the cracks propagate through the thicknesses of the specimen this time. Finally, of course the spots could not bear the applied force and fracture occurs.

When it was conducted the finite element analysis using ANSYS package program, it is clear that a stress concentration or singularity exists at the interception of the nugget boundary with the interface of joined sheets because all Von Mises stresses, tensile stresses, bending stresses etc. (Figures 5.7. through 5.28.) have their maximum magnitudes near the nugget boundary (that is the inner surfaces of flanged or center pieces of MTS specimens on the peripheries of the spots) that were thought after experimental studies' results (Figure 6.8). These stress distributions explain successfully the phenomenon that why the fractures are generally first created around the nugget for the spot-welded joints.

For example, from Figures 5.7 and 5.12, it was found that the maximum tensile stress' value is 611 MPa and occurs in the boundaries of spots (shown in Figure 6.8), which is much higher than the average stress of 87.5 MPa, the stress concentration factor thus being 6.98. The effective stresses at the internal edges of spots are greater than at the external edges of spots (Figures 5.11. through 5.14.).

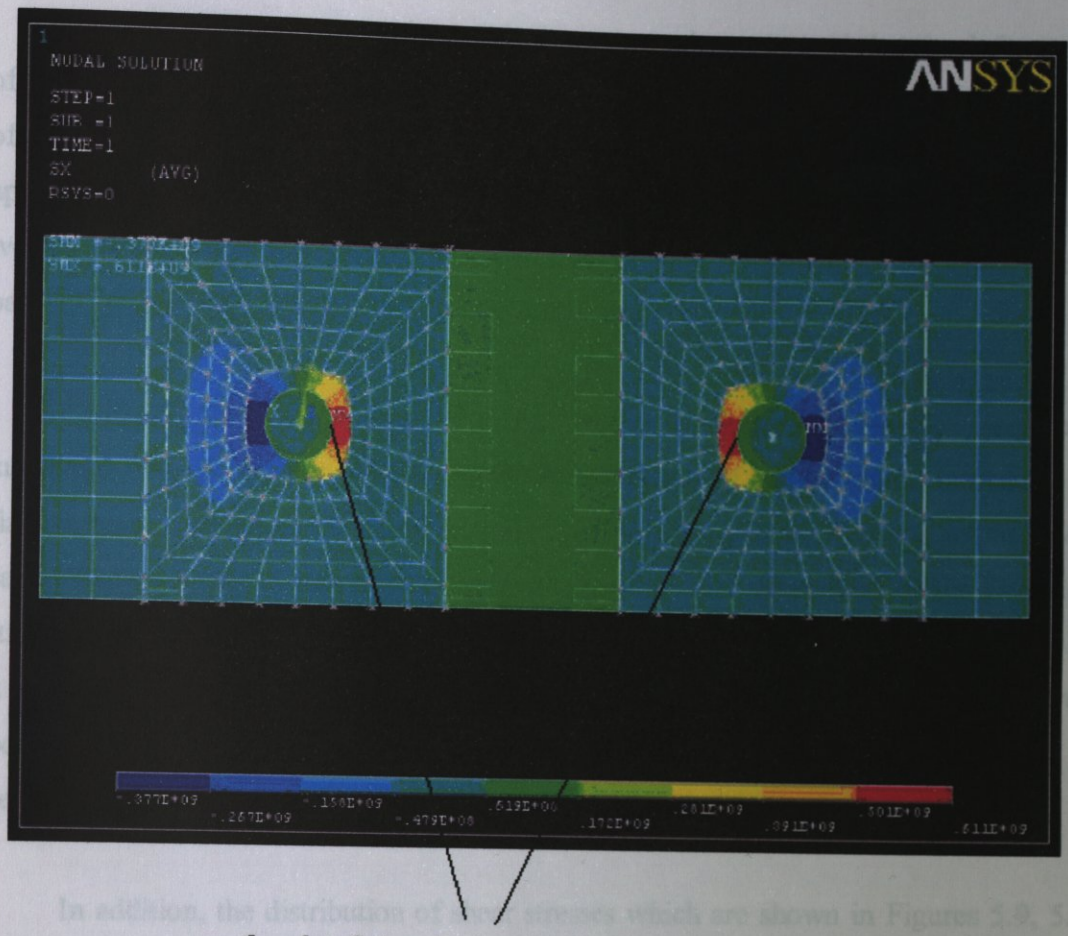

Figure 6.8. Tensile stress distribution on the inner surface of flanged piece (centerpiece) of MTS specimen

Peak tensile-stress values on x, y, and z directions were found at the internal edges of the spot welds, while peak compression-stress values were at the external edges of the spot welds.

It can be said that the high tensile stresses together with the high tearing stresses are all located at the edges of the spot welds in the spot-welded joints, and will cause bending of the lap zones of the specimens even if this bending values in tensile shear specimens are not so critical and important as for modified tensile shear specimens (MTS) because of flanged pieces or centerpieces of MTS specimens. The deformation of the spot-welded specimens in general is shown in Figure 5.6.

Examining the deformed shape of MTS specimen, it can be said that the deformation of lap zones of the spot-welded joint in the middle part is more serious than the other zones of the specimen. The reason for the phenomena may be as follows. The loads which are applied to the spot-welded specimens are borne completely by the spot welds in spot-welded joints. Hence the stresses flow with concentrating to the spot welds in the middle parts of the lap zones, so that high stresses arise there.

Obviously, the greater values of normal stresses in the spot-welded specimens result in a much greater bending deformation in the end pieces of the lap zones, but not in the flanged pieces (centerpieces) of the lap zones. In modified tensile shear specimens, the so called flanges on the centerpieces of MTS prevent the more separations of the two plates (that connected with the spot welds) from each others under applied loads. In other words, it can be concluded that the modified tensile shear specimens behave as partly weld-bonded tensile shear specimens under applied force because of the flanges of the centerpieces.

In addition, the distribution of shear stresses which are shown in Figures 5.9, 5.13, 5.17, 5.21, and 5.24 indicate that the shear stresses in the spot welded zones are much greater than those in other parts of the lap zones, hence there are also shear stress concentrations at the edges of the spot welds in spot-welded joints.

Beside all these findings, it is interesting to find that the inner areas of the nuggets are almost stress free, although peak stress values appear on the outer area of the spot welds. This explains why observed porosity inside the nugget (Figure 6.7) have not effected the fracture mechanisms in the experimental study (As we mentioned in the assessment of experimental study, even if sometimes porosities were seen inside the spot welds under microscope, the fracture always were observed around the nugget.).

7. CONCLUSIONS AND RECOMMENDATIONS

The following conclusions were drawn from this study:

- Numerical FEA stress distribution realistic and shows various characteristic features. It provides numerical capability to make fatigue analysis since all stress and strain values at critical locations are available.
- Results from Finite Element Analysis calculation give a reasonable interpretation for existing experimental results and these experimental results verify the correctness of the numerical method.
- Microscopic examination capability and technique has been developed. Although limited specimens have been sectioned along the study, similar work can be extended when more data is needed.
- Fatigue behavior of various load ranges has been studied. Expected S-N curve trends with typical values of life were determined. Deformation patterns during cycling, and crack development at the spots has been followed, identified and investigated.
- Some differences between the experimental studies and numerical studies have been observed. For example, fracture (except one case) have occurred in the spot that near the piston displacement in experimental studies while the stress distributions on spot welds have been observed as symmetric on these two spots in Finite Element Analysis solution. (According to FEA result, this means that fracture can occur spots neither separately nor in these two spots together, but this is not the situation in experimental studies) This difference is very normal because there are some differences between these two solutions in real situation. For example, there are residual stresses in specimens (that have been used in experimental study) because of manufacturing processes of specimens. In addition, again the homogeneities of specimens in experimental studies are not as formal as ones in numerical studies for example in terms of material particles.

APPENDIX A: PICTURES OF THE TEST

Figure A.1. Picture of the test machine [Material Testing System (MTS)]

Figure A.2. Picture of specimen between grips

APPENDIX B: THE TABULATED DATA OF EXPERİMENTS

For the Figures 4.3 through 4.5 (Logarithmic stress versus life curves for manual spot welded and nipper spot welded specimens), the tabulated data were given in the following tables.

Table B.1. Stresses vs. life results of "Manual Spot" welded MTS specimens

Experiment Number	P_{max}(N)	P_{min}(N)	ΔP(N)	ΔS(MPa)	N_f(cycle)
1	3700	200	3500	87.5	9970
2	3000	150	2850	71.25	39000
3	2700	150	2550	63.75	52470
4	2400	150	2250	56.25	93550

Table B.2. Stresses vs. life results of "Nipper Spot" welded MTS specimens

Experiment Number	P_{max}(N)	P_{min}(N)	ΔP(N)	ΔS(MPa)	N_f(cycle)
1	3700	200	3500	87.5	13370
2	3000	150	2850	71.25	61190
3	2700	150	2550	63.75	93480
4	2250	150	2100	52.5	283150

REFERENCES

1. Mitchell, M. R., and R. W. Landgraf, *1122*Lawrence, "Estimating the Effects of Residual stress on the Fatigue Life of Notch Components", *American Society for Testing and Materials,* Philadelphia, pp. 383-401, 1986.

2. Mabuchi, A., J. Nilsawa, and N. Tomioka, "Fatigue Life Prediction of Spot-welded Box-Section Beams under Repeated Torsion", *SAE Paper 860603,* Soc. Auto. Engrs., Warrendale, PA, 1986.

3. Pan, Ning, *Fatigue Life Study of Spot Welds*, Ph. D. Thesis, Stanford University, May 2000.

4. Henrysson, H. F., *Fatigue of Spot Welded Joints: Experiments and Life Predictions,* Chalmers University of Technology, 2001

5. Mansour, T. M., "Ultrasonic Inspection of Spot Welds in Thin-Gage Steel," *Materials Evaluation,* Vol. 46, pp. 650-658, 1988.

6. Gero, B. M., *Acousto-Ultrasonic Evaluation of Cyclic Fatigue of Spot Welded Structures*, Ms. Thesis, Virginia Polytechnic Institute and State University, August 1997.

7. Newman, J. A., *Life Prediction of Spot Weld: A Fatigue Crack Growth Approach,* Ms. Thesis, Virginia Polytechnic Institute and state University, December 1996.

8. Zhang Y., D. Taylor, "Sheet Thickness Effect of Spot Welds Based on Crack Propagation", *Engineering Fracture Mechanics*, Vol. 67, pp. 55-63, 2000.

9. Swellaw, M. H., P. Kurath, and F. V. Lawrence, "Electric-Potential-Drop Studies of Fatigue Crack Development in Tensile-Shear Spot Welds", *Advances in Fatigue Lifetime Predictive Techniques, ASTM STP,* 1986.

10. Cooper, J. F., and R. A. Smith, "The measurement of Fatigue Cracks at Spot Welds", *International Journal of Fatigue*, pp. 137-140, July 1985.

11. Damico, D. J., T. L. Wilkinson, and L.F. Niks, "Predicting Performance of Adhesively Bonded Joints Based on Acousto-Ultrasonic Evaluation", *American Society for Testing and Materials,* Philadelphia, 1994.

12. Sperle, J. O., "Strength of Spot Welds in High Strength Steel Sheets", *Metal Construction*, pp. 200-203, April 1983.

13. Davidson, J. A., and E. J. Imhof, "A Fracture-Mechanics and Sytem-Stiffness Approach to Fatigue Performance of Spot-Welded Sheet Steels", *SAE Paper 830034,* Soc. Auto. Engrs., Warrendale, PA, 1983.

14. Overbeeke, J. L., and J. Draisma, "Influence of Stress Relieving on Fatigue of Heavy Duty Spot welded Lap Joints", *Metal Construction*, pp. 433-434, September 1978.

15. Overbeeke, J. L., and J. Draisma, "Fatigue Characteristics of Heavy-Duty Spot Welded Lap Joints", *Metal Construction and British Welding Journal*, pp. 213-219, July 1974.

16. Davidson, J. A., and E. J. Imhof, "The Effect of Tensile Strength on the Fatigue Life of Spot-Welded Sheet Steels", *SAE Paper 840110,* Soc. Auto. Engrs., Warrendale, PA, 1984.

17. Pook, L. P., Fracture Mechanics Analysis of the Fatigue Behavior of Spot Welds, *International Journal of Fracture,* Vol. 11, pp. 173-176, 1975.

18. Kan, Y., Fatigue Resistance of Spot-Welds—An Analytic Study, *Metals Engineering,* pp. 26-36, November 1976.

19. Kitagawa, H., and T. Satoh, "Fatigue Strength of Single Spot-Welded Joints of Rephosphorized High-Strength and Low-Carbon Steel Sheets", *SAE Paper 850371,* Soc. Auto. Engrs., Warrendale, PA, 1985.

20. Lawrence, F. V., Predicting the Fatigue Resistance of Welds, *Annual Review of Material Science,* Vol. 11, pp. 401-425, 1981.

21. Mchenry, H. I., and J. M. Potter, "Fatigue Crack Initiation and Growth in Tensile-Shear Spot Weldments", *American Society of Testing and Materials,* pp. 47-77, Philadelphia, 1990.

22. Weixing, Y. *et al.*, "On the Fatigue Notch Factor, K_f", *International Journal of Fatigue*, Vol. 17, No. 4, pp. 245-251, 1995.

23. Peterson, R. E., G. Sines, and J. L. Waisman, "Notch-Sensitivity", *Metal Fatigue*, 1959.

24. Wang, P. C., H. T. Corten, and F. V. Lawrence, "A Fatigue Life Prediction Method for Tensile-Shear Spot Welds", *SAE Paper 850370,* Soc. Auto. Engrs., Warrendale, PA, 1985.

25. Sheppard, S. D., and M. Strange, "Fatigue Life Estimations in Resistance Spot Welds: Initiation and Early Growth Phase", *Fatigue and Fracture Engineering Materials and Structures*, Vol. 15, No. 6, pp. 531-549, 1992.

26. Sheppard, S. D., "Estimation of Fatigue Propagation Life in Resistance Spot Welds", *Advances in Fatigue Lifetime Predictive Techniques: Second Volume, ASTM STP 1211,* M. R. Mitchell, and R. W. Langraf, eds., *American Society for Testing and Materials,* Philadelphia, PA, 1993.

27. Cooper, J. F., and R. A. Smith, "Fatigue Crack Propagation at Spot Welds", *Metal Construction*, pp. 383-386, 1986.

28. Barsom, J. M., J. A. Davidson, and E. J. Imhof, "Fatigue Behavior of Spot Welds under Variable-Amplitude Loading", *SAE Paper 850369,* Soc. Auto. Engrs., Warrendale, PA, 1985.

29. Matsoukas, G., P. Steven, and Y. W. Mai, "Fatigue of Spot-Welded Lap Joints", *International Journal of Fatigue*, Vol. 6, No. 1, pp. 55-57, January 1984.

30. Shinozaki, M. T., T. Kato, I. Takahaski, and T. Irie, "Fatigue of Automobile High Strength Steel Sheets and Their Welded Joints", *SAE Paper 830032,* Soc. Auto. Engrs., Warrendale, PA, 1983.

31. Pollard, B., "Fatigue Strength of Spot Welds in Titanium-Bearing HSLA Steels", *SAE Paper 820284,* Soc. Auto. Engrs., Warrendale, PA, 1982.

32. Paris P. C., and F. Erdogan, "A Critical Analysis of Crack Propagation Laws", *Transactions of the ASME, Journal of Basic Engineering,* Series D, Vol. 85, No. 3, 1963.

33. Newman, J. A., and N. E. Dowling, "A Crack Growth Approach to Life Prediction of Spot-Welded Lap Joints", *Fatigue & Fracture of Engineering Materials & Structures,* No. 21, pp. 1123-1132, 1998.

34. VandenBossche, D. J., "Ultimate Strength and Failure Mode of Spot Welds in High Strength Steels", *SAE Paper 770214,* Soc. Auto. Engrs., Warrendale, PA, 1977.

35. Anderson, T. L., *Fracture Mechanics Fundamentals and Applications*, Texas A & M University, Texas, 1991.

36. Davidson, J. A., and E. J. Imhof, "A Review of the Fatigue Properties of Spot-Welded Sheet Steels", *SAE Paper 830033,* Soc. Auto. Engrs., Warrendale, PA, 1983.

37. Walker, K., "The Effect of Stress Ratio During Crack Propagation and Fatigue for 2024-T3 and 7075-T6 Aluminum", *Effects of Environment and Complex Load History on Fatigue Life, ASTM STP 462, ASTM,* Philadelphia, PA, pp. 1-14, 1970.

38. El-Sayed, M. E. M., T. Stawiarski, and R. Frutiger, "Fatigue Analysis of Spot-Welded Joints under Variable Amplitude Load History", *Engineering Fracture Mechanics,* Vol. 55, No. 3, pp. 363-369, 1996.

39. Fricke, W., "Fatigue Analysis of Welded Joints: State of Development", *Marine Structures,* Vol. 16, pp. 185-200, 2002.

40. Shigley, J. E., *Mechanical Engineering Design*, Vol. 2,1963.

41. Juvinall, R. C., and K. M. Marshek, *Fundamentals of Machine Component Design (Third Edition)*, 2000.

42. Schijve, J., *Fatigue of Structures and Materials*, 2001.

43. Xu, S., and X. Deng, "An Evaluation of Simplified Finite Element Models for Spot-Welded Joints", *Finite Elements in Analysis and Design*, Article in press.